Center for Numerical and Computational Methods in Engineering
Faculty for Exact Sciences & Technology
Universidad Nacional de Tucumán

GRADIENT-BASED POROPLASTIC THEORY

by

Javier Luis Mroginski

Advisor: Prof. Dr. Ing. Guillermo Etse

Thesis submitted in partial fulfillment
of the requirements for the degree of
Doctor in Exact Science and Engineering

October, 2012

Edited with LaTeX

March 8, 2013

Abstract

In this work, a thermodynamically consistent gradient-based formulation for partially saturated cohesive-frictional porous media is proposed. The constitutive model includes a classical or local hardening law and a softening formulation with state parameters of non-local character based on gradient theory. Internal characteristic length in softening regime accounts for the strong shear band width sensitivity of partially saturated porous media regarding both governing stress state and hydraulic conditions. In this way the variation of the transition point of brittle-ductile failure mode can be realistically described depending on current confinement condition and saturation level.

On the other hand, the strain localization problem is study by the spectral analysis of discontinuous bifurcation condition in gradient-based poroplastic media. To evaluate the dependence of the transition point between ductile and brittle failure regime in terms of the hydraulic and stress conditions, the localization acoustic tensor for discontinuous bifurcation is formulated for both drained and undrained conditions, based on wave propagation criterion. On the other hand, the analytical expression for the critical hardening/softening module is obtained by exploring the spectral properties of the acoustic tensor for drained and undrained conditions.

In this work, two materials models are used in order to describe the inelastic mechanical behavior of both clay and young concrete, within the framework of the theory of porous media. First of all, the material model employed to describe the plastic evolution of porous media is the Modified Cam Clay, which is widely used for saturated and partially saturated soils. Then, the gradient-dependent Parabolic Drucker-Prager material model originally proposed by Vrech and Etse (2005) [127] for concrete is extended by means

of the constitutive theory in this thesis to account for gradient poroplastic behaviour. This enriched material model is considered to simulate the behaviour of young concrete whereby the hydraulic condition plays a very important role. Then, localization analysis of both gradient poroplastic material proposed in this thesis is performed, showing the influence of the pore pressure and of the non-associativity degree on the location of the transition point between ductile and brittle failure regime and on the critical bifurcation directions.

A relevant novel aspect in this thesis is the consideration of the porous phase influence on the non-locality degree of the material model. This is done by the definition of an additional characteristic length for the porous phase to take into account its microstruture.

To solve the boundary value problems in this thesis, a new finite element formulation for non-local and inelastic saturated and partially saturated gradient poroplastic materials is proposed. The novel finite element includes interpolation functions of first order (C_1) for the internal variables field, while classical C_0 interpolation functions for the kinematic and pore pressure fields. The proposed finite element formulation is compatible with the thermodynamically consistent gradient poroplastic theory developed in the framework of this thesis see, Mroginski, et al. (2011) [76].

To verify the numerical efficiency of the proposed finite element formulation, the non-local gradient poroplastic constitutive theory is combined with the Modified Cam Clay model for partially saturated continua. Thereby, the volumetric strain of the solid skeleton and the plastic porosity are the internal variables of the constitutive theory. The numerical results in this work demonstrate the capabilities of the proposed finite element formulation to capture diffuse and localized failure modes of boundary value problems of porous media, depending on the acting confining pressure and on the material saturation degree.

Contents

List of Tables

List of Figures

CHAPTER 1

Introduction

The mechanic of porous media constitutes a discipline of great relevance in several knowledge areas like Geophysics, Biomechanics and Materials Science. Its main aim is the description of the kinematic and pore pressure of porous continua when subjected to arbitrary mechanical and/or physical actions. The definitive advantages of porous mechanics to macroscopically describe or predict complex response behavior of cohesive-frictional materials based on fundamental aspects of their microstructure while accounting for the hydraulic properties and their influence in the resulting failure mechanism were recognized by several authors in the scientific community [10, 14, 55]. Consequently, a tendency to replace the theoretical framework of classical continuum mechanics with that of non-linear porous mechanics was observed. Firstly this process took place in case of soil mechanics, see a.o. [31, 21], but subsequently in the field of concrete, see a.o. [122, 92, 70] and, furthermore, of biomaterials, see a.o. [79, 94].

1.1 Main topics

1.1.1 Material instability

Quasi-brittle materials like soil and concrete show a very brittle failure behavior when their kinematic field exhibit localization bands and, moreover, jumps.

In the realm of classical non-porous smeared crack-based continua, the concept of discontinuous bifurcation by means of the so-called localization indicator see a.o. [38, 56] provided the mathematically foundation to distinguish between diffuse and localized or brittle failure modes. Many proposals of constitutive theories for non-porous continua used the discontinuous bifurcation approach to accurately evaluate failure modes under different stress conditions, [90]. A critical situation may arise when discontinuous bifurcation occurs in pre-peak regime before peak stress. This situation may occur in cohesive-frictional materials when subjected to monotonic compressive loading in the low confinement regime due to excessive dilatation that leads to sudden brittle failure [39].

Regarding to non-porous continuous, many authors performed studies about the post peak behavior and the discontinuous bifurcation conditions through the analytical determination of the critical hardening modulus [137, 83, 102, 103, 91]. In some cases they considered anisotropic behavior [137] and enhanced non-local constitutive theories [131] applied to different type of materials such as fiber reinforced concrete [34, 91].

The extension of smeared-crack concept to porous media allows accounting for the influence of the saturation level (or pore pressure) as well as the confinement pressure in the location of the transition point in the stress space. However, the extension of discontinuous bifurcation theory to porous media is not straightforward due to the difficulties related to the additional fields, basically gas and liquid, and their eventual jumps. In this works the following contributions were considered [30, 107, 14, 31, 124, 105, 48, 25, 82]. In some of these contributions, see [124, 105], the discontinuous bifurcation theory was used to differentiate brittle from ductile failure modes of porous materials, following previous and similar works related to non-porous continua.

In conclusion, due to the diversity of the variables involved in the plastic degradation process, the discontinuous bifurcation condition of porous media was studied taking into account the influence of different variables such as the Lode angle [139], water content or fluid pressure [68, 105], porosity [138], hydraulic boundary conditions [74], permeability [135], temperature [115], etc.

To avoid the pathological dependence of the numerical solution in the finite element size and orientation, the constitutive equations need to be enriched by some non-local consideration. One possible approach is to include a second order kinematic fields in the constitutive formulation [22, 23, 40, 2], or eventually a simplified gradient formulation whereby the internal variables are only one of non-local character [117, 130, 35]. When porous media are considered the approach based on non-local effect restricted to internal variables allows other ways to define the characteristic length [76, 75] which is explored in this thesis.

Furthermore, when the localization analysis in porous media is study the hydraulic boundary conditions play a fundamental role and should be appropriately considered. Thereby many authors studied the discontinuous bifurcation condition considering drained and undrained hydraulic conditions [135, 45, 138, 136, 103]. These hydraulic conditions are considered in this thesis as well.

1.1.2 Enhanced gradient-based non-local formulation

An important improvement of classical continuum mechanics was the extension to non-local concepts. The main aim was the regularization of post peak response behavior regarding mesh size and element orientation in case of finite element analyses, see a.o. [117, 40, 36, 2, 130].

Gradient-based constitutive formulations are widely used in mechanical modeling of strain softening materials. Since the pioneer work by Vardoulakis and Aifantis (1991) [123], the strain gradient material theory gained relevant echo in the international scientific community. Amount others, proposals [89, 17, 86, 112, 128, 42] demonstrate both the extensive use of gradient theory in solid materials and its effectiveness to limit the severe mesh size dependency of the so-called smeared crack approach.

In recent years significant progresses and relevant contributions were made in non-local gradient formulations for non-porous materials. Thermodynamic frameworks were considered in the proposals of [2, 3, 95, 96, 125, 46, 53, 130]. Phenomenological aspects of the considered materials at the microscopic level of observation were taken into account in non-local gradient formulations by [97, 9, 63]. Objective descriptions of the gradient internal length based on crystal-plasticity concepts were due to [8, 61, 62, 33], while based on actual confining pressure in case of quasi-brittle materials like concrete as proposed by [130]. Considerations of material anisotropy in the formulation of internal variables evolution laws in case of gradient plasticity are due to [4, 126]. Geometrical analysis of the bifurcation condition in case of non-local gradient formulations were proposed by [127]. Formulation of gradient enhanced coupled damage-plasticity material models and related finite element implementations can be found in [117, 67, 27].

From the predictive capabilities stand point, strain gradient-based constitutive models lead to appreciable diffusions of the failure modes. This is due to the intrinsic well-posedness of the governing equations in case of gradient theory that are able to suppress the loss of strong ellipticity in the form of discontinuous bifurcation of the related local constitutive equations. Nevertheless, the strong diffusion of failure modes predicted by gradient-based models is a relevant disadvantage of this non-local material theory in case of failure behavior of cohesive-frictional materials like rocks, concretes and partial saturated soils, when loaded in the low confinement or tensile regimes [104, 60]. In these cases the shortcomings of classical gradient constitutive models to reproduce the localized failure modes of quasi-brittle materials strongly affect the numerical prediction accuracy despite the mesh objective solutions their provide.

Recently, non-local concepts were also extended for the formulation of porous material models, see a.o. [64, 57, 77, 76]. Likewise, the consideration of microscopic aspects in the formulation of non-local constitutive theories for porous materials are due to [140, 81, 134].

1.1.3 Boundary value problem

From the finite element (FE) stand point, strain gradient constitutive formulations require special provisions for the approximation of the Laplacian to the plastic multiplier in the element domains and on their boundaries. Pioneer contributions in FE technology related to gradient formulations in non-porous media are [22, 23] who proposed C_1 continuity FE to approximate the non-local strain gradient fields, and [133], who proposed a four node FE with one integration point for large strain and strain gradients. FE formulations with C_0 continuity based approximation fields for gradient constitutive models of non-porous media were proposed in [24, 98, 110, 132, 119]. The proposal by De Borst and Pamin [24] considers penalty functions to avoid additional iterations in the solution procedure for the non-local gradient strain fields. This FE formulation includes rotation as nodal variable. It should be noted that the overall numerical performance of this FE is not efficient, as can be observed in [84]. In the others C_0-continuous FE for gradient-based continua [118, 128], the non-local effects are considered to be restricted to the internal variables while their numerical approaches for the variable fields involves additional iterative procedures to solve for the plastic multiplier Laplacian. Other proposals related to C_0 continuity FE technologies for gradient-based solids are by [132, 119, 98]. The last formulation is related to porous metals and requires an additional global iteration procedure to solve the equations system.

Regarding the strain localization problem in saturated soils Stankiewicz and Pamin [85, 114, 113] developed a FE formulation for non-local Cam Clay model based on the strain gradient theory by [22]. It considers, on the one hand, a one-phase approach under fully drained and undrained hydraulic conditions [114, 85] while, on the other hand, a two-phase approach to take into account the permeability and, therefore, the stabilizing role of the fluid phase [113]. One shortcoming of this FE approach is that the non-local gradient fields involve the entire kinematic variables which demands special provisions from the numerical point of view to have the same level of accuracy and efficiency of the well known local material models. Although some similarities between this gradient plasticity formulation and those proposed by Stankiewicz and Pamin [114, 85] there is a conceptual difference in the non-local fields hypothesis. In the present proposal the internal variables are the only ones of non-local character while in the classical framework of gradient plasticity [22, 23, 118, 114] the non-local gradient fields involve the entire kinematic field. On the other hand, it should be noted that in those approaches the non-local effects is represented by means of one characteristic length. This is another difference between the FE formulation proposed by Stankiewicz and Pamin [114, 85] and the one in this thesis.

Therefore, despite the considerable progress made in FE formulation for gradient based materials, there is still a need of efficient FE technologies for quasi-brittle, partially saturated porous media, in which the kinematic fields of the skeleton interact with the hydraulic and pressure fields of the porous phase.

1.2 Main objectives

Following the introduction made before about the three main topics treated in this thesis it can be observed that a further discussion for the following aspects is required

- **At constitutive level**: in spite of the increasing development in constitutive formulations for quasi-brittle porous materials it can be noted that remains the need of a general theory which extends the thermodynamically consistent non-local theory of strain gradients for continuous solids to partially saturated porous media. In this work a new gradient-based poroplastic theory is proposed in order to fulfill this theoretical requirement. Likewise, the dependence of the internal characteristic length with the pore pressure is mathematically demonstrated.

- **About the failure prediction**: given the importance involved in the identification of the failure mode of a material to prevent structural collapse, this topic has been rigorously studied previously. However, the influence of the pore pressure in the post peak behavior of quasi-brittle porous media is a question that has not been explained clearly. In this thesis the influence of pore pressure is discussed through spectral analysis of the localized failure indicator, considering both drained and undrained hydraulic conditions.

- **About the numerical solution of the boundary value problem**: the numerical solution of the boundary value problem presented in this thesis requires the definition of some algorithm aspects which have not been adequately treated so far. Although the numerical implementation of the non-local gradient theories of has been sufficiently discussed previously, the inclusion of pore pressure in the boundary value problem induces a new nonlinearity and the development of a new finite element with special features is required. In this work the numerical implementation of a new finite element with C1 continuity of internal variables as well as the corresponding solution algorithm are presented.

Therefore the following objectives are established

1. Deduce a new thermodynamically consistent gradient-based constitutive theory for partially saturated porous media.
2. Identify the porous phase influence on the softening behavior through the internal characteristic length.
3. Deduce the tangent constitutive tensor for gradient plasticity in porous media.
4. Derive the localized failure indicator corresponding to partially saturated porous media using the non-local constitutive theory proposed in this thesis.
5. Study the influence of both the hydraulic boundary conditions and the pore pressure in the failure mode.
6. Analyze different alternatives of the numerical solution procedure to solve the boundary value problem.
7. Propose a new finite element to consider the convergence requirement of the gradient plasticity formulation in porous media.
8. Present several numerical examples to test the performance of proposed finite element and evaluate its ability to simulate both the diffuse and localized failure modes.

1.3 Work organization

This thesis was structured as follows

Chapter 2 In this Chapter the whole theoretical framework is presented, regarding to linear elasticity, flow theory of plasticity in classical and porous media. Two different formulations for porous media are presented. The first one, based on the *Mixture Theory*, is widely used in multiphasic formulations of porous media [93, 66, 73] in spite of it lack of thermodynamic consistency. The second theoretical framework is based on the *Generalized Theory of Porous Media* [18, 30]. The Thermodynamics hypothesis and postulates concerning to porous media are also stated. Also, basic assumption of the flow theory of poroplasticity as well as the Principle of Maximal Plastic Work for porous continua are presented.

Chapter 3 In Chapter 3 a new thermodynamically consistent gradient-based constitutive theory for partially saturated porous media is proposed [76]. It is based on the Generalized Theory of Porous Media [18]. By considering a selective degree of gradient non-locality the proposed material theory is able to reproduce diffuse and localized failure modes of partially saturated porous media. In this enhanced constitutive formulation the non-local effect is restricted to internal variables based on previous work for non-porous media [116, 129]. This fundamental hypothesis introduces a new concept of the internal characteristic length [76, 75] whereby the non-local contribution of the porous phase in the constitutive behavior may be considered through an additional internal length, l_p.

Chapter 4 In this Chapter the thermodynamically consistent gradient poroplastic constitutive theory proposed in this thesis is particularized for the modified Cam Clay plasticity model and the Parabolic Drucker-Prager material model. The aim is to predict failure behavior of both partially saturated soils and young concrete. The mathematical definition of both internal characteristic lengths for solid and porous phases, are presented in both models as well as the thermodynamically consistent plastics potentials functions.

Chapter 5 In this Chapter the discontinuous bifurcation condition for partially saturated porous media considering both drained and undrained hydraulic boundary conditions is presented. Also, the critical hardening module for localization is deduced for both drained and undrained hydraulic boundary conditions. The influence of water content or pore pressure and of the degree of non-associativity is also evaluated.

Chapter 6 This Chapter deals with the numerical solutions of boundary value problems. Therefore a new C_1 continuity based FE formulation is proposed for gradient-based constitutive formulation of saturated and partially saturated porous media with the capacity to reproduce both localized and diffuse failure modes that characterized quasi-brittle materials like concrete and soils [75]. A distinguish aspect of this FE formulation is the inclusion of interpolation functions of first order continuity (C_1) only for the internal variables while the kinematic fields are interpolated with C_0-continuous functions. Similarly to [118, 128] present FE formulation considers gradient material models with internal variables being the only ones of non-local character. This reduces the involved complexity of the FE formulation. The proposed FE technology is particularly appropriated to be used with the thermodynamically consistent non-local gradient theory developed in this thesis.

Chapter 7 In this Chapter numerical predictions of the FE formulation proposed in this thesis are presented. The influence of the gradient characteristic length on the ductility in post-peak regime is evaluated as well as the overall numerical predictions.

Chapter 8 The main conclusions as well as the recommendations for future developments are discussed.

Appendices Seven appendices are included to describe numerical details not included in the main portion of the thesis.

CHAPTER 2

Theoretical framework

In this Chapter two different approaches for lineal elastic porous media formulations are discussed.

The first one is based on the well know Mixture Theory which is used to model multiphase systems considering the continuum mechanics principles generalized to several inmiscible continua. The basic assumption is that, at any instant of time, all phases are present at every material point, and momentum and mass balance equations are postulated within this theoretical assumption. Like other models, mixture theory requires constitutive relations to close the system of equations. Probably, the main disadvantage of this mixture-theory-based formulation is the lack of thermodynamical consistency. The second approach, which is the one adopted in this work, is based on two fundamental concepts to reconcile continuum mechanics with the microscopic discontinuities inherent in porous media constituted by solid and fluid phases. The first concept is to consider that the porous medium is composed by the superposition of several continua that move with different kinematics, while mechanically interacting and exchanging energy and matter. The second concept is the transport of the governing equations of the superposed fluid and solid continua from their common current configuration to an initial reference configuration related to the solid skeleton.

2.1 Mixture theory for porous media formulation

In classical mechanics, a continuum distribution of particles (fluids or solids), for which the balance laws and constitutive relationships are valid, is taken for granted. The phenomena to be studied here, occurs in domains occupied by different phases. There is an omnipresent phase, i.e., the solid skeleton, whose voids are considered to be filled with fluid (gas or liquid) separated by a membrane called interface. The difference between constituents and phases should be emphasised here: the phases are chemically homogeneous portions of the multiphase system, whose mechanical behaviour is assumed to be uniform. On the other hand, the constituents are the individual parts that yield the phases but acting each one independently from the others; the gaseous phase may be constituted by a gas mix, with several constituents.

At least there are three possible levels to describe the intergranular configuration of multiphase porous media: the macroscopic, the mesoscopic and the microscopic level. At the microscopic (and mesoscopic) level, the real porous media structure should be considered.

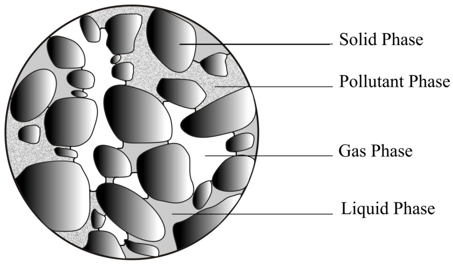

Figure 2.1: Multiphase medium: Representative elemental volume at microscopic level

In Fig. 2.1 a representative volume at microscopic level is presented. In addition to the solid phase it can be observed three different fluid phases, corresponding to a general multiphase porous media [72, 73], the liquid, gaseous and the inmiscible pollutant. The governing equations are established considering each constituent separately, giving rise to a complicated solution. Furthermore, the microscopic properties are usually awkward to assess. However, the mixture approach provides an appropriate theoretical framework for this kind of multiphasic phenomenon [66].

One noteworthy feature of the mixture description is the fact that at each material point all phases are assumed to be simultaneously present. In a volume fraction, the following elements may be found:

- Solid Phase: $\eta^s = 1 - n$, being $n = \left(dv^w + dv^g + dv^\pi\right)/dv$ the porosity and dv^i the differential volume of the i constituent.
- Liquid Phase: $\eta^w = nS_w$, being $S_w = dv^w / \left(dv^w + dv^g + dv^\pi\right)$ the water saturation degree.
- Gaseous Phase: $\eta^g = nS_g$, being $S_g = dv^g / \left(dv^w + dv^g + dv^\pi\right)$ the air saturation degree.
- Pollutant phase: $\eta^\pi = nS_\pi$, being $S_\pi = dv^\pi / \left(dv^w + dv^g + dv^\pi\right)$ the pollutant saturation degree.

The aforesaid equations yield

$$S_w + S_g + S_\pi = 1 \tag{2.1}$$

and the multiphase media density is given by

$$\rho = \rho_s + \rho_w + \rho_g + \rho_\pi = (1-n)\,\rho^s + nS_w\rho^w + nS_g\rho^g + nS_\pi\rho^\pi \tag{2.2}$$

Within this condition, and provided that the medium is constituted by different phases, any of them may be described relatively to any other previously defined, for example the solid phase. Thereby, relative velocities of the liquid, gas and pollutant phases may be addressed as follows

$$\boldsymbol{v}^{ws} = \boldsymbol{v}^{w} - \boldsymbol{v}^{s} \quad , \quad \boldsymbol{v}^{gs} = \boldsymbol{v}^{g} - \boldsymbol{v}^{s} \quad , \quad \boldsymbol{v}^{\pi s} = \boldsymbol{v}^{\pi} - \boldsymbol{v}^{s} \tag{2.3}$$

2.1.1 Governing equations

The classical continuum mechanic balance equations will be taken into account to obtain the microscopic behaviour of an individual phase. For any thermodynamic attribute ψ, the general conservation equation for a single phase may be written as follows [69]

$$\frac{\partial \rho \psi}{\partial t} + \mathrm{div}\,(\rho \psi \dot{\boldsymbol{r}}) - \mathrm{div}\,\boldsymbol{i} - \rho\,\boldsymbol{b} = \rho\,\boldsymbol{G} \tag{2.4}$$

where $\dot{\boldsymbol{r}}$ is the phase local velocity in a fixed spatial point, ρ is the density, $\boldsymbol{b}$ is the external supply, $\boldsymbol{i}$ is the associated flux vector and $\boldsymbol{G}$ is the internal net production of ψ.

Macroscopic balance equations

The macroscopic balance equations are obtained by the systematic application of the pioneer work of [49, 50, 51] to Eq. (2.4), in which for each constituent, the thermodynamic variable is substituted by the appropriated microscopic property [66]. The pollutant behaviour may be depicted in two different forms, depending on its mixing capability with the fluid or with the gaseous phase. In the most general situation, i.e. with immiscible pollutants, the behaviour may be described as another fluid phase, whereas with a soluble pollutant, three possible transport processes must be considered: advection, diffusion and dispersion.

Solid Phase From Eq. (2.4) and recalling the material time derivative of any differentiable function f^α, given in its spatial description and referring to a moving particle of the α phase,

$$\frac{\partial^{v} f^{\alpha}}{\partial t} = \frac{\partial^{\alpha} f^{\alpha}}{\partial t} + \mathrm{grad} f^{\alpha} \cdot \boldsymbol{v}^{v\alpha} \tag{2.5}$$

the mass balance expression for the solid phase is obtained

$$\frac{\partial^{s} \rho_s}{\partial t} + \rho_s \mathrm{div}\,\boldsymbol{v}^{s} = 0 \tag{2.6}$$

where $\boldsymbol{v}^s$ is the solid skeleton velocity and

$$\text{div}\,(\rho_s \boldsymbol{v}^s) = \rho_s \text{div}\ \boldsymbol{v}^s + grad\ \rho_s \cdot \boldsymbol{v}^s \tag{2.7}$$

Taking into account Eq. (2.2) and Eq. (2.7), it is obtained

$$\frac{(1-n)}{\rho^s}\frac{\partial^s \rho^s}{\partial t} - \frac{\partial^s n}{\partial t} + (1-n)\,\text{div}\ \boldsymbol{v}^s = 0 \tag{2.8}$$

Liquid Phase The microscopic mass balance equation for the liquid phase is tantamount to the corresponding one for the solid phase being $\boldsymbol{G} \neq 0$ due to the possible water transformation into vapour and conversely.

Then, taking into account Eq. (2.4), with $\rho \boldsymbol{G} = -\dot{\boldsymbol{m}}$ the following expression is obtained

$$\frac{\partial^w \rho_w}{\partial t} + \rho_w \text{div}\ \boldsymbol{v}^w = -\dot{\boldsymbol{m}} \tag{2.9}$$

where $\boldsymbol{v}^w$ is the liquid phase mass velocity and $-\dot{\boldsymbol{m}}$ is the amount of water per unit volume transformed into vapor. From Eq. (2.2) results

$$\frac{(1-n)}{\rho^s}\frac{\partial^s \rho^s}{\partial t} + \text{div}\ \boldsymbol{v}^s + \frac{n}{\rho^w}\frac{\partial^s \rho^w}{\partial t} + \frac{n}{S_w}\frac{\partial^s S_w}{\partial t} + \frac{1}{S_w \rho^w}\text{div}\,(n S_w \rho^w \cdot \boldsymbol{v}^{ws}) = -\frac{\dot{\boldsymbol{m}}}{S_w \rho^w} \tag{2.10}$$

Gaseous Phase The gaseous phase is considered to be composed by two constituents: dry air (ga) and water vapour (gw). Since both elements are miscible and their physical behaviour are similar, they may be treated as a single phase occupying the same differential volume, nS_g. Regardless of the internal mass production due to self-chemical reactions, the microscopic balance equation for this phase is also given by Eq. (2.4). Thus, As well as previous section, the mass balance equation for the dry air and water vapour mixture will be

$$\frac{\partial}{\partial t}(n S_g \rho^g) + \text{div}\,(n S_g \rho^g \boldsymbol{v}^g) = \dot{\boldsymbol{m}} \tag{2.11}$$

with $\rho^g = \rho^{ga} + \rho^{gw}$ and $\boldsymbol{v}^g = 1/\rho^g\,(\rho^{ga}\boldsymbol{v}^{ga} + \rho^{gw}\boldsymbol{v}^{gw})$

Once again, after some algebraic manipulation of the above expression, taking into account Eqs. (2.3), (2.5) and (2.8) the subsequent relationship is obtained

$$\frac{(1-n)}{\rho^s}\frac{\partial^s \rho^s}{\partial t} + \text{div}\ \boldsymbol{v}^s + \frac{n}{S_g}\frac{\partial^s S_g}{\partial t} + \frac{n}{\rho^g}\frac{\partial^s \rho^g}{\partial t} + \frac{1}{S_g \rho^g}\text{div}\,(n S_g \rho^g \cdot \boldsymbol{v}^{gs}) = \frac{\dot{\boldsymbol{m}}}{S_g \rho^g} \tag{2.12}$$

Constitutive equations and state relationships

To provide a complete description of the mechanical behaviour, constitutive equations are required.

Fluid phase stress tensor From the second law of Thermodynamic [72], the stress tensor for the fluid phase may be written as

$$\boldsymbol{t}^{\gamma} = -\eta^{\gamma} p^{\gamma} \mathbf{I} \tag{2.13}$$

being $\mathbf{I}$ the second-order unit tensor, p^{γ} is pressure of the phase γ and η^{γ} is the phase volume fraction of the same phase. It may be clearly noticed that no deviatoric stresses are present in the fluid phase stress tensor.

Cauchy stress tensor for solid phase The stress tensor for the solid phase is given by

$$\boldsymbol{t}^{s} = (1-n)\left(\boldsymbol{t}_{e}^{s} - \boldsymbol{I} p^{s}\right) \tag{2.14}$$

being the solid phase pressure

$$p^{s} = S_{w} p^{w} + S_{g} p^{g} \tag{2.15}$$

The volume fraction $(1-n)$ points out that $\boldsymbol{t}^{s}$ is the stress exerted over the solid phase. In order to obtain the total Cauchy stress, $\boldsymbol{\sigma}$, the expressions derived for the liquid and the gaseous phases in Eq. (2.13) must be added to Eq. (2.14)

$$\boldsymbol{\sigma} = \boldsymbol{t}^{s} + \boldsymbol{t}^{w} + \boldsymbol{t}^{g} = \boldsymbol{\sigma}' + \mathbf{I}\left(p^{w} S_{w} + p^{g} S_{g}\right) \tag{2.16}$$

Solid mass density Considering a compressible solid mass, an expression for the time derivative of the solid mass density may be obtained from the mass conservation differential equation assuming that the solid mass density is a function of p^{s} and $\mathrm{tr}\boldsymbol{\sigma}'$ [108],

$$\frac{1}{\rho^{s}} \frac{\partial^{s} \rho^{s}}{\partial t} = \frac{1}{K_{s}} \frac{\partial^{s} p^{s}}{\partial t} - \frac{1}{3(n-1) K_{s}} \frac{\partial^{s}\left(\mathrm{tr}\boldsymbol{\sigma}'\right)}{\partial t} \tag{2.17}$$

where the following expressions were considered

$$\frac{1}{\rho^{s}} \frac{\partial^{s} \rho^{s}}{\partial p^{s}} = \frac{1}{K_{s}} \qquad , \qquad \frac{1}{\rho^{s}} \frac{\partial^{s} \rho^{s}}{\partial\left(\mathrm{tr}\boldsymbol{\sigma}'\right)} = -\frac{1}{3(n-1) K_{s}} \tag{2.18}$$

being, K_s the grain compressibility coefficient and $\mathrm{tr}\boldsymbol{\sigma}'$ the first invariant of the stress tensor. Having in mind the constitutive relationship for the first invariant of the effective stress tensor, the following expression is valid

$$\frac{\partial^s \mathrm{tr}\boldsymbol{\sigma}'}{\partial t} = 3K_T \left(\mathrm{div}\boldsymbol{v}^s + \frac{1}{K_s}\frac{\partial^s p^s}{\partial t} - \beta_s \frac{\partial^s T}{\partial t} \right) \tag{2.19}$$

where, K_T, is the skeleton bulk modulus. Combining Eq. (2.17) and Eq. (2.19), results

$$\frac{1}{\rho^s}\frac{\partial^s \rho^s}{\partial t} = \frac{1}{1-n}\left[(\alpha - n)\frac{1}{K_s}\frac{\partial^s p^s}{\partial t} - \beta_s (\alpha - n)\frac{\partial^s T}{\partial t} - (1-\alpha)\,\mathrm{div}\ \boldsymbol{v}^s \right] \tag{2.20}$$

The incompressible grain condition, i.e. $1/K_s = 0$ and $\alpha = 1$, do not indicate whatsoever a rigid or incompressible skeleton, since under load application, an interstitial voids re-arrangements is undertaken.

State equation for the liquid phase Considering isothermal conditions the water solid state equation was developed by Murty, et al (1994) [78]

$$\rho^w = \rho^{wo}\exp\left[C_w\left(p^w - p^{wo}\right)\right] \tag{2.21}$$

where the superscript o stands for the initial state, β_w is the thermal expansion coefficient and C_w is the compressibility coefficient. Being the time derivative

$$\frac{1}{\rho^{wo}}\frac{\partial^w \rho^w}{\partial t} = \frac{1}{K_w}\frac{\partial^w p^w}{\partial t} \tag{2.22}$$

where $K_w = 1/C_w$ is the water bulk modulus. Equation (2.22) may be also obtained from the mass balance differential equation [66].

State equation for the gaseous phase The gaseous phase may be considered as a mixture of perfect ideal gases, dry air and water vapour. Therefore, it is possible to apply the ideal gas laws by relating the constituent partial pressure (p^{ga} or p^{gw}), the constituent mass concentration in the gaseous phase (ρ^{ga} or ρ^{gw}) and the absolute temperature, θ. The perfect gas state equations applied to dry air (ga), to water vapour (qw) and to the air (g), are [66]

$$p^g = p^{ga} + p^{gw} = \rho^{ga}\theta\mathrm{R}/M_a + \rho^{gw}\theta\mathrm{R}/M_w \tag{2.23}$$

where R is the universal gas constant and M_w and M_g are the molar masses of the water vapour and dry air constituent, respectively, being the gas mixture

$$\rho^g = \rho^{ga} + \rho^{gw} \qquad , \qquad M_g = \left(\frac{\rho^{gw}}{\rho^g}\frac{1}{M_w} + \frac{\rho^{ga}}{\rho^g}\frac{1}{M_a} \right)^{-1} \tag{2.24}$$

2.1.2 General field equations for elastic modeling of porous media

Macroscopic balance laws are transformed by the introduction of the constitutive relationships previously defined.

Solid phase The solid phase behaviour may be conveniently depicted using the lineal momentum balance equation, which is obtained from Eq. (2.4) by appropriately setting the state variables $\boldsymbol{i}$, $\boldsymbol{b}$ and $\boldsymbol{G}$.

$$\mathbf{L}^T\boldsymbol{\sigma} + \rho\boldsymbol{g} = 0 \tag{2.25}$$

where $\boldsymbol{g}$ is the gravity acceleration and

$$\mathbf{L}^T = \begin{vmatrix} \partial/\partial x & 0 & 0 & \partial/\partial y & 0 & \partial/\partial z \\ 0 & \partial/\partial y & 0 & \partial/\partial x & \partial/\partial z & 0 \\ 0 & 0 & \partial/\partial z & 0 & \partial/\partial y & \partial/\partial x \end{vmatrix} \tag{2.26}$$

Liquid phase Considering the rate the saturation degree for the gaseous phase from Eq. (2.2) without presence of pollutants immiscible,

$$\frac{\partial S_g}{\partial t} = -\frac{\partial S_w}{\partial t} \tag{2.27}$$

Introducing the liquid phase state Eq. (2.22), the solid phase pressure Eq. (2.15), and the solid phase density Eq. (2.20), in the macroscopic balance of the liquid phase Eq. (2.10), the following expression is obtained

$$\begin{aligned} &\left[\frac{(\alpha - n)}{K_s} S_w \left(S_w + \frac{C_w}{n}\left(p^g - p^w\right)\right) + \frac{nS_w}{K_w} - C_w\right]\frac{\partial p^w}{\partial t} \\ &\qquad\qquad \left[\frac{(\alpha - n)}{K_s} S_w \left(S_g - \frac{C_w}{n}\left(p^g - p^w\right)\right) + C_w\right]\frac{\partial p^w}{\partial t} \\ &\qquad\qquad\qquad + \alpha\, S_w m^T \mathbf{L}\frac{\partial u}{\partial t} + \frac{1}{\rho^w}\nabla^T\left[\frac{kk^{rw}}{\mu^w}\left(-\nabla p^w + \rho^w g\right)\right] = 0 \end{aligned} \tag{2.28}$$

where $C_w = n\partial S_w/\partial p^{gw}$ is the derivative of the water saturation with respect to the suction, which may be obtained with the aid of the soil characteristic curve $(S_w - p^{gw})$ [72, 25, 41].

Gaseous phase From the gaseous phase balance equation for isothermal processes Eq. (2.12), and considering the state equation for the gaseous phase Eq. (2.23), the relative velocity definition Eq. (2.3), the solid phase density Eq. (2.20), the following mathematical statement is obtained

$$\begin{aligned}
&\left[\frac{(\alpha-n)}{K_s}S_g\left(S_w-\frac{C_w}{n}\left(p^w-p^g\right)\right)+C_w\right]\frac{\partial p^w}{\partial t}\\
&\qquad+\left[\frac{(\alpha-n)}{K_s}S_g\left(S_g+\frac{C_w}{n}\left(p^w-p^g\right)\right)-C_w+\frac{nS_gM_g}{\rho^g\theta\mathrm{R}}\right]\frac{\partial p^g}{\partial t}\\
&\qquad\qquad+\alpha S_g\, m^T\mathbf{L}\frac{\partial u}{\partial t}+\frac{1}{\rho^g}\nabla^T\left[\frac{kk^{rg}}{\mu^g}\left(-\nabla p^g+\rho^g g\right)\right]=0 \qquad (2.29)
\end{aligned}$$

Finally, the boundary value problem may be solved by the differential equation system of Eqs. (2.25), (2.28) and (2.29).

2.2 Generalized theory of porous media

The main aim of this Section is to describe the deformation and the kinematics of a porous medium composed by a deformable skeleton and fluids saturating the porous space.

The underlying idea consists in approaching the porous medium as the superimposition of two continua, the skeleton and the fluid ones. The description of the kinematics of each continuum separately is very similar to that of monophasic continua.

The laws of physics governing the evolution of a porous continuum involve the time rate of the physical quantities attached either to the skeleton or to the fluid.

2.2.1 Description of porous media

Key argument to reconcile continuum mechanics with the intrinsic microscopic discontinuities of porous like materials composed by several interacting phases, is to consider them as thermodynamically open continuum systems. Thus, their kinematics and deformations are referred to those of the skeleton. Contrarily to mixture theories based upon an averaging process [66, 20, 54, 73], the representation of porous media is made by a superposition, in time and space, of two or more continuum phases. In case of non-saturated porous continua we recognize three phases, the skeleton, the liquid and the gaseous phases.

Porous media are multiphase systems with interstitial voids in the grain matrix filled with water (liquid phase), water vapor and dry air (gas phase) at microscopic level, see Fig. 2.2a. The connected porous space is a continuous space where the fluid flows as a homogeneous continuous medium. The matrix is composed of both a solid part and a possible occluded porosity, whether saturated or not, but through which no filtration occurs, see Fig. 2.2b. The connected porosity is the ratio of the volume of the connected

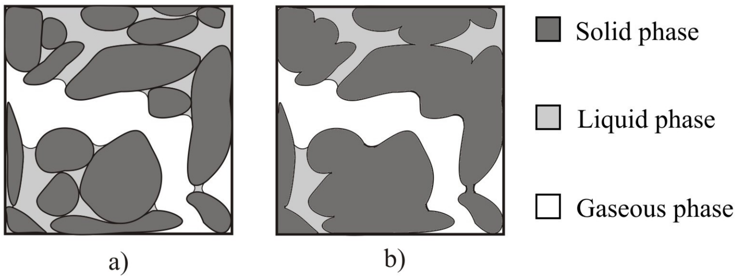

Figure 2.2: Porous media description. a) Microscopic level ; b) study level

porous space to the total volume. In what follows the term *porosity*, used without further specification, refers to the entire connected porosity.

This hypothesis of continuity assumes the existence of a representative elementary volume which is relevant at the macroscopic scale for all the physical phenomena involved in the intended application. The physics is supposed to vary continuously from one to another of those juxtaposed infinitesimal volumes whose junction constitutes the porous medium.

2.2.2 Mass balance

Continuity equation

Let ρ^f and ρ^s be the intrinsic fluid and matrix mass densities so that $\rho^f n \mathrm{d}\Omega$ and $\rho^s (1-n)\,\mathrm{d}\Omega$ are the fluid and the skeleton mass currently contained in the material volume $\mathrm{d}\Omega$, respectively. Accordingly, the macroscopic or apparent skeleton and fluid mass densities are $\rho^f n$ and $\rho^s (1-n)$, respectively. When no mass change occurs, neither for the skeleton nor the fluid contained in the volume $\mathrm{d}\Omega$, the mass balance can be expressed in the form

$$\frac{\mathrm{d}^s}{\mathrm{d}t}\int_\Omega \rho^s (1-n)\ \mathrm{d}\Omega = 0 \tag{2.30}$$

$$\frac{\mathrm{d}^f}{\mathrm{d}t}\int_\Omega \rho^f n\,\mathrm{d}\Omega = 0 \tag{2.31}$$

The particle derivative of a volume integral $\mathrm{d}^\pi \mathcal{F}/\mathrm{d}t$ with respect to the π phase of field $\mathcal{F}$ is defined by

$$\frac{\mathrm{d}^\pi}{\mathrm{d}t}\int_\Omega \mathcal{F}\,\mathrm{d}\Omega = \int_\Omega \left(\frac{\partial \mathcal{F}}{\partial t} + \left(\mathcal{F}V_i^\pi\right)_{,i}\right)\mathrm{d}\Omega \tag{2.32}$$

Then, applying Eq. (2.32) to Eq. (2.30) and Eq. (2.31)

$$\frac{\partial\left(\rho^{s}\left(1-n\right)\right)}{\partial t}+\left(\rho^{s}\left(1-n\right)V_{i}^{s}\right)_{,i}=0 \tag{2.33}$$

$$\frac{\partial\left(\rho^{f}n\right)}{\partial t}+\left(\rho^{f}nV_{i}^{f}\right)_{,i}=0 \tag{2.34}$$

The fluid mass content. The relative flow vector.

The appropriate formulation of the constitutive equations considering the skeletonfluid coupling will be required, referring the motion of the fluid to the initial configuration of the skeleton. With that purpose, let $J^{f}\mathrm{d}a$ be the fluid mass flowing between time t and t + dt through the infinitesimal skeleton material surface da oriented by the unit normal $\boldsymbol{n}$.

$$J^{f}\mathrm{d}a=\boldsymbol{w}\cdot\boldsymbol{n}\,\mathrm{d}a \tag{2.35}$$

where $\boldsymbol{w}\left(\boldsymbol{x},t\right)$ is the Eulerian relative flow vector of fluid mass.

Given that $n\left(\boldsymbol{V}^{f}-\boldsymbol{V}^{s}\right)\cdot n\mathrm{d}a\mathrm{d}t$ is the infinitesimal fluid volume flowing through the skeleton surface da during the infinitesimal time dt, the relative vector of fluid mass $\boldsymbol{w}$ is defined by

$$\boldsymbol{w}=\rho^{f}n\left(\boldsymbol{V}^{f}-\boldsymbol{V}^{s}\right) \tag{2.36}$$

Then, replacing the definition of Eq. (2.36) allows to refer the fluid mass balance to the skeleton motion by rearranging the fluid continuity equation Eq. (2.34) in the form

$$\frac{\mathrm{d}^{s}\left(\rho^{f}n\right)}{\mathrm{d}t}+\rho^{f}nV_{i,i}^{f}+w_{i,i}=0 \tag{2.37}$$

The Lagrangian approach to the fluid mass balance can be carried out by introducing the Lagrangian fluid mass content m per unit of initial volume $\mathrm{d}\Omega_0$. The amount m is related to the Eulerian fluid mass content $n\rho^{f}$ per unit volume according to

$$n\rho^{f}\,\mathrm{d}\Omega=m\,\mathrm{d}\Omega_{0} \tag{2.38}$$

From the Lagrangian relation between the current $\mathrm{d}\Omega$ and initial volume $\mathrm{d}\Omega_0$

$$\phi\,\mathrm{d}\Omega_{0}=n\,\mathrm{d}\Omega\quad;\quad\phi=nJ \tag{2.39}$$

follows

$$m=\rho^{f}\phi \tag{2.40}$$

where ϕ is the Lagrangian porosity. Furthermore, considering the Lagrangian vector $\boldsymbol{M}(\boldsymbol{X}, t)$ related to $\boldsymbol{w}$ through

$$\boldsymbol{w} \cdot \boldsymbol{n}\, \mathrm{d}a = \boldsymbol{M} \cdot \boldsymbol{N} \mathrm{d}A \tag{2.41}$$

$$\nabla \boldsymbol{w}\, \mathrm{d}\Omega = \nabla \boldsymbol{M} \mathrm{d}\Omega_0 \tag{2.42}$$

Finally, replacing Eq. (2.40), Eq. (2.41) and Eq. (2.42) in Eq. (2.37) the Lagrangian approach of the fluid mass continuity equation is derived

$$\frac{\mathrm{d}m}{\mathrm{d}t} + M_{i,i} = 0 \tag{2.43}$$

2.2.3 Thermodynamics of Porous Continua

Postulate of Local State

The postulate of local state stipulates that the internal energy of a homogeneous system is independent of the evolution rate and can be characterized by the same state variables as the ones characterizing equilibrium states.

Regarding continuous mediums, the postulate of local state also establishes that the thermodynamic states of any material volume Ω follows from the thermodynamics of the material elementary volumes $\mathrm{d}\Omega$ forming the domain Ω, and exchanging heat and mechanical work between them. As a consequence, the thermodynamic laws can be applied in an integral form to additive quantities such as the energy and the entropy.

The postulate of local state is extended to porous continua by considering that their thermodynamics are obtained by adding the thermodynamic contributions of each constituent, that is the solid skeleton and the fluid continua.

First law of the Thermodynamic

The first law of Thermodynamics expresses the conservation of energy in all forms.

At any time, the material derivative of energy $\dot{\mathbb{E}}$ contained in the subdomain Ω is the sum of the work rate $\mathcal{P}_{ext}$ of the external forces and the rate $\mathcal{Q}$ of external heat supply.

On the other hand, the energy $\dot{\mathbb{E}}$ of a system can be expresed as the sum of its kinetic $\dot{\mathcal{K}}$ and internal energy $\dot{\mathcal{E}}$ of each component of this system. Considering a body occupying the volume Ω, with boundary $\partial\Omega$, the first law of the thermodynamic can be expressed as

$$\dot{\mathbb{E}} = \dot{\mathcal{K}} + \dot{\mathcal{E}} = \mathcal{P}_{ext} + \mathcal{Q} \tag{2.44}$$

with

$$\dot{\mathcal{E}} = \frac{\mathrm{d}}{\mathrm{d}t}\int_{\Omega} e \,\mathrm{d}\Omega \tag{2.45}$$

$$\dot{\mathcal{K}} = \frac{1}{2}\int_{\Omega} \rho^s (1-\phi)\,|\dot{u}_i \dot{u}_i| + \rho^f \phi\,|w_i w_i| \;\mathrm{d}\Omega \tag{2.46}$$

$$\mathcal{P}_{ext} = \int_{\Omega} \rho b_i \dot{u}_i \,\mathrm{d}\Omega + \int_{\partial\Omega} \sigma_{ij} n_i \dot{u}_j - \frac{p}{\rho^f} w_i n_i \,\mathrm{d}\partial\Omega \tag{2.47}$$

$$\mathcal{Q} = \int_{\Omega} r \,\mathrm{d}\Omega - \int_{\partial\Omega} h_i n_i \,\mathrm{d}\partial\Omega \tag{2.48}$$

Here, e is the internal energy density (per unit mass), b_i is the body force, σ_{ij} is the stress, r is a heat source density and h_i is the heat flux. The displacement u_i, the unit normal vector on $\partial\Omega$, n_i, and the mass density ρ, were also included.

Considering the equilibrium equation, the explicit form of the internal energy density for local dissipative porous material follows from Eq.(2.44) as

$$\dot{e} = \sigma_{ij}\dot{\varepsilon}_{ij} - h_f M_{i,i} - h_{i,i} + r \tag{2.49}$$

The Second law of Thermodynamic

While, the first law states the conservation of energy in all of its forms, the second law states that the energy can only deteriorate. The energy which can be transformed into efficient mechanical work can only decrease irreversibly. The second law introduces a new physical quantity, the entropy, which can only increase when an isolate system is considered.

Therefore, the second law of thermodynamics states: *There is an additive thermodynamic function, called entropy $\mathcal{S}$, such that its material derivative attached to any material system Ω is at least equal to the rate of external supplied entropy.*

Let s be an entropy volume density (per unit mass), the total entropy contained in the system Ω is

$$\mathcal{S} = \int_{\Omega} s \,\mathrm{d}\Omega \tag{2.50}$$

According to the second law of thermodynamic (entropy inequality) the entropy $\mathcal{S}$ of a thermodynamic system can not decrease. This can be expressed as

$$\dot{\mathcal{S}} + \mathcal{Q}_\theta \geq 0 \tag{2.51}$$

with

$$\dot{\mathcal{S}} = \frac{\mathrm{d}}{\mathrm{d}t}\int_{\Omega} s \,\mathrm{d}\Omega \;\;;\;\; \mathcal{Q}_\theta = \int_{\Omega} \frac{r}{\theta} \,\mathrm{d}\Omega - \int_{\partial\Omega} \frac{n_i h_i}{\theta} \, d\partial\Omega \tag{2.52}$$

being Q_θ the entropy flux. Transforming the surface integral of Eq. (2.52) into a volume integral, it follows that the volume integral in Eq. (2.51) must be non-negative for any system Ω, which yields

$$\dot{s} + \left(s_f M_i\right)_{,i} + \left(\frac{h_i}{\theta}\right)_{,i} - \frac{r}{\theta} \geq 0 \tag{2.53}$$

Then invoking the first law by Eq. (2.49) in order to eliminate r, the global form of the Clausius-Duhem inequality (CDI) can be obtained as

$$\sigma_{ij}\dot{\varepsilon}_{ij} + \theta\dot{s} - \dot{e} - M_{i,i}\left(h_f - \theta s_f\right) + M_i\left(\theta s_{f,i} - h_{f,i}\right) - \frac{h_i}{\theta}\theta_{,i} \geq 0 \tag{2.54}$$

Introducing the Helmholtz's free energy $\Psi = e - s\theta$ as well as the free enthalpy of fluid per mass unit (or Gibbs potential) $g_f = h_f - s_f\theta$, the following expression is attained

$$\sigma_{ij}\dot{\varepsilon}_{ij} - g_f M_{i,i} - s\dot{\theta} - \dot{\Psi} - M_i\left(s_f\theta_{,i} + g_{f,i}\right) - \frac{h_i}{\theta}\theta_{,i} \geq 0 \tag{2.55}$$

Finally, considering the mass balance equation of Eq. (2.43) the above expression of the CDI can be rewritten in the form

$$\Phi_s + \Phi_f + \Phi_\theta \geq 0 \tag{2.56}$$

with

$$\Phi_s = \sigma_{ij}\dot{\varepsilon}_{ij} + g_f\dot{m} - s\dot{\theta} - \dot{\Psi} \tag{2.57}$$
$$\Phi_f = -M_i\left(s_f\theta_{,i} + g_{f,i}\right) \tag{2.58}$$
$$\Phi_\theta = -\frac{h_i}{\theta}\theta_{,i} \tag{2.59}$$

Skeleton dissipation : The first component of Eq. (2.56) is regarded to the skeleton dissipation, Φ_s. Owing to the additive character of the Helmholtz free energy and entropy, the following expression can be assumed

$$\Psi = \Psi_s + m\Psi_f \tag{2.60}$$
$$s = s_s + m\, s_f \tag{2.61}$$

where Ψ_s and Ψ_f account for skeleton and fluid energy densities, as well as s_s and s_f are referred to the skeleton and the fluid entropy densities, respectively.

The fluid state equations, presented in Section 2.2.2 combined with the above definitions, together with Eq. (2.40) allow to express Φ_s in the form

$$\Phi_s = \sigma_{ij}\dot{\varepsilon}_{ij} + p\dot{\phi} - s_s\dot{\theta} - \dot{\Psi}_s \tag{2.62}$$

This expression of the skeleton dissipation Φ_s matches the standard expression of the dissipation of a solid phase. Indeed, the strain work rate of an ordinary solid would reduce to the term $\sigma_{ij}\dot{\varepsilon}_{ij}$. In the case of a porous continuous, the strain work rate related to the skeleton is obtained by adding $p\dot{\phi}$, to account for the action of the pore pressure on the skeleton through the internal walls of the porous network.

Porous dissipation : The second source of dissipation, Φ_f in Eq. (2.56), accounts for the viscous dissipation due to the relative motion of the fluid with respect to the skeleton.

Thermal dissipation : The third and last source of dissipation, Φ_θ in Eq. (2.56), involves the temperature gradient $\theta_{,i}$ and therefore the thermal state of the elementary contiguous systems. It is related to the dissipation due to heat conduction.

Owing to the very distinct nature of the dissipations identified before, the decoupling hypothesis consists of substituting the unique inequality (2.56) by

$$\Phi_s = \sigma_{ij}\dot{\varepsilon}_{ij} + p\dot{\phi} - s_s\dot{\theta} - \dot{\Psi}_s \geq 0 \tag{2.63}$$

$$\Phi_f = -M_i\left(s_f\theta_{,i} + g_{f,i}\right) \geq 0 \tag{2.64}$$

$$\Phi_\theta = -\frac{h_i}{\theta}\theta_{,i} \geq 0 \tag{2.65}$$

Inequality (2.63) states that only the part Φ_s of the infinitesimal strain work supplied to the skeleton, that is $\sigma_{ij}\dot{\varepsilon}_{ij} + p\dot{\phi}$ minus the corrective thermal term $s_s\dot{\theta}$, can be stored by the skeleton in the form of free energy. That means in a form which is eventually recoverable into efficient mechanical work. Indeed, owing to possible irreversible sliding of the matter forming the matrix, the non-stored part of the strain work is spontaneously transformed into the form of heat. Inequality (2.64) states the same as (2.63) but for the fluid. In addition, inequality (2.65) stipulates that heat spontaneously flows from high to low temperatures.

2.2.4 State Equations of the Skeleton

State variables and state equations for skeleton

Skeleton free energy Ψ_s should admit ε_{ij}, ϕ and θ as natural arguments since its rates appear in Eq. (2.63) for the skeleton dissipation Φ_s. In addition, accounting for the postulate of local state, the free energy of the skeleton is rate independent and can be expressed in the form

$$\Psi_s = \Psi_s \left(\varepsilon_{ij}, \phi, \theta, q_\alpha \right) \tag{2.66}$$

being q_α the internal variables, with $\alpha = s, p$ for solid or porous phase, which are considered here as scalar variables. This set of variables cannot be externally controlled.

In this Section the study is restricted to linear elastic behaviour, therefore, evolutions of internal variables will not be considered,

$$\frac{\mathrm{d}q_\alpha}{\mathrm{d}t} = \dot{q}_\alpha = 0 \tag{2.67}$$

ε_{ij}, ϕ, θ and q_α form a set of state variables for the skeleton. Indeed, for a given values of this set of variables the state of the skeleton free energy is known irrespectively of its past evolution. Nevertheless, ε_{ij}, ϕ and θ form a subset of external state variables since their variations can be externally controlled.

Considering the rate of Eq. (2.66) and replacing in Eq. (2.63)

$$\left(\sigma_{ij} - \frac{\partial \Psi_s}{\partial \varepsilon_{ij}} \right) \dot{\varepsilon}_{ij} + \left(p - \frac{\partial \Psi_s}{\partial \phi} \right) \dot{\phi} - \left(s_s + \frac{\partial \Psi_s}{\partial \theta} \right) \dot{\theta} \geq 0 \tag{2.68}$$

Inequality (2.68) must hold whatever the signs of $\dot{\varepsilon}_{ij}$, $\dot{\phi}$ and $\dot{\theta}$ are. Therefore, variations of any independent variables are fully independent of the others. Assuming also that ε_{ij}, ϕ and θ are rate independent, we conclude that

$$\sigma_{ij} = \frac{\partial \Psi_s}{\partial \varepsilon_{ij}} \quad ; \quad p = \frac{\partial \Psi_s}{\partial \phi} \quad ; \quad s_s = -\frac{\partial \Psi_s}{\partial \theta} \tag{2.69}$$

These are the state equations relative to the skeleton and relate, the state variables ε_{ij}, ϕ and θ to their conjugated thermodynamic variables σ_{ij}, p and $-s_s$.

By defining the free energy in the form

$$\Pi_s = \Psi_s - p\,\phi \tag{2.70}$$

then, Eqs. (2.69) can be inverted as

$$\sigma_{ij} = \frac{\partial \Pi_s}{\partial \varepsilon_{ij}} \quad ; \quad \phi = -\frac{\partial \Pi_s}{\partial p} \quad ; \quad s_s = -\frac{\partial \Pi_s}{\partial \theta} \tag{2.71}$$

State variables and state equations for porous materials

Considering the expression Eq. (2.57) for skeleton dissipation instead of Eq. (2.63), the free energy density should accordingly be written as

$$\Psi = \Psi\left(\varepsilon_{ij}, m, \theta, q_\alpha\right) \tag{2.72}$$

thus, the following state equations for porous materials are derived

$$\sigma_{ij} = \frac{\partial \Psi}{\partial \varepsilon_{ij}} \quad ; \quad g_f = \frac{\partial \Psi}{\partial m} \quad ; \quad s = -\frac{\partial \Psi}{\partial \theta} \tag{2.73}$$

2.2.5 Thermoporoelastic state equations

The dissipation related to the skeleton when thermoporoelastic behaviors is considered should be neglected as well as internal variables. The constitutive equations reduce to state equations (see Section 2.2.4). Nevertheless their operational formulation needs an explicit expression for the skeleton free energy Ψ_s.

Therefore, the dissipation related to a thermoelastic skeleton considering infinitesimal transformation is

$$\sigma_{ij}\dot{\varepsilon}_{ij} + p\dot{\phi} - s_s\dot{\theta} - \dot{\Psi}_s = 0 \tag{2.74}$$

Alternatively, using of energy Π_s defined in Eq. (2.70),

$$\sigma_{ij}\dot{\varepsilon}_{ij} - \phi\dot{p} - s_s\dot{\theta} - \dot{\Pi}_s = 0 \tag{2.75}$$

Owing to Eq. (2.71) it is worthwhile to note Maxwell's symmetry relations

$$\frac{\partial \sigma_{ij}}{\partial \varepsilon_{kl}} = \frac{\partial \sigma_{kl}}{\partial \varepsilon_{ij}} \quad ; \quad \frac{\partial \sigma_{ij}}{\partial p} = -\frac{\partial \phi}{\partial \varepsilon_{ij}} \quad ; \quad \frac{\partial \sigma_{ij}}{\partial \theta} = -\frac{\partial s_s}{\partial \varepsilon_{ij}} \quad ; \quad \frac{\partial \phi}{\partial \theta} = \frac{\partial s_s}{\partial p} \tag{2.76}$$

From Eq. (2.75) $\dot{\Pi}_s = \sigma_{ij}\dot{\varepsilon}_{ij} - \phi\dot{p} - s_s\dot{\theta}$, then differentiating state equations (2.71)

$$\dot{\sigma}_{ij} = \frac{\partial \dot{\Pi}_s}{\partial \varepsilon_{ij}} = \frac{\partial}{\partial \varepsilon_{ij}}\left(\sigma_{ij}\dot{\varepsilon}_{ij} - \phi\dot{p} - s_s\dot{\theta}\right) \tag{2.77}$$

$$\dot{\phi} = -\frac{\partial \dot{\Pi}_s}{\partial p} = -\frac{\partial}{\partial p}\left(\sigma_{ij}\dot{\varepsilon}_{ij} - \phi\dot{p} - s_s\dot{\theta}\right) \tag{2.78}$$

$$\dot{s}_s = -\frac{\partial \dot{\Pi}_s}{\partial \theta} = -\frac{\partial}{\partial \theta}\left(\sigma_{ij}\dot{\varepsilon}_{ij} - \phi\dot{p} - s_s\dot{\theta}\right) \tag{2.79}$$

and taking into account Maxwell's symmetry relations Eq. (2.76) follows

$$\dot{\sigma}_{ij} = C^s_{ijkl}\dot{\varepsilon}_{ij} - B_{ij}\dot{p} - \alpha^s_{ij}\dot{\theta} \tag{2.80}$$

$$\dot{\phi} = B_{ij}\dot{\varepsilon}_{ij} + \frac{\dot{p}}{\mathrm{M}} - 3\alpha_\phi\dot{\theta} \tag{2.81}$$

$$\dot{s}_s = \alpha^s_{ij}\dot{\varepsilon}_{ij} - 3\alpha_\phi\dot{p} + C_v\dot{\theta} \tag{2.82}$$

In Eqs. (2.80)-(2.82) the coefficients C^s_{ijkl}, B_{ij}, α^s_{ij}, $1/\mathrm{M}$, $3\alpha_\phi$ and C_v are the thermoporoelastic properties. They are functions of state variables ε_{ij}, p and θ which must satisfy such relations expressing the integrability of Eqs. (2.80)-(2.82). For instance, the relation expressing the integrability of Eq. (2.80) is

$$\frac{\partial C^s_{ijkl}}{\partial \varepsilon_{mn}} = \frac{\partial C^s_{ijmn}}{\partial \varepsilon_{kl}} \quad ; \quad \frac{\partial C^s_{ijkl}}{\partial p} = -\frac{\partial B_{ij}}{\partial \varepsilon_{kl}} \quad ; \quad \frac{\partial C^s_{ijkl}}{\partial \theta} = -\frac{\partial \alpha^s_{ij}}{\partial \varepsilon_{kl}} \tag{2.83}$$

The standard equations of incremental thermoelasticity for non-porous media are recovered by letting $\dot{p} = 0$ in Eq. (2.80) and Eq. (2.82):

- $C^s_{ijkl} = \partial^2\Pi_s/\partial\varepsilon_{ij}\partial\varepsilon_{kl}$ is the tangent elastic stiffness module. Owing to Maxwell's relations and to symmetry conditions $\sigma_{ij} = \sigma_{ji}$ and $\varepsilon_{ij} = \varepsilon_{ji}$, the following symmetries relations are admitted:

$$C^s_{ijkl} = C^s_{klij} \quad ; \quad C^s_{ijkl} = C^s_{ijlk} \quad ; \quad C^s_{ijkl} = C^s_{jikl} \tag{2.84}$$

- α^s_{ij} is the skeleton tangent thermal dilation tensor, with symmetry $\alpha^s_{ij} = \alpha^s_{ji}$. Again, owing to Maxwell's relations, the term $\alpha^s_{ij} = -\partial^2\Pi_s/\partial\theta\partial\varepsilon_{ij}$ also represents the skeleton tangent strain latent heat. That is the heat per unit of strain that the skeleton exchanges with the outside in an evolution when both temperature and pressure are held constant ($\dot{\theta} = \dot{p} = 0$)
- $C_v = -\partial^2\Pi_s/\partial\theta^2$ is the skeleton tangent volumetric heat capacity, when strain ε_{ij} and pressure p are held constant ($\dot{\varepsilon}_{ij} = \dot{p} = 0$)

With regard to thermoporoelasticity, the incremental state equation (2.81) related to the change in porosity involves new thermoporoelastic properties:

- $B_{ij} = -\partial^2\Pi_s/\partial\varepsilon_{ij}\partial p$ component of Biot's tangent tensor with symmetry $B_{ij} = B_{ji}$. It linearly relates the change in porosity to the strain variation when both pressure and temperature are held constant ($\dot{\theta} = \dot{p} = 0$).
- $1/\mathrm{M} = -\partial^2\Pi_s/\partial p^2$ is the inverse of Biot's tangent modulus linking the pressure variation $\dot{p}$ and the porosity variation $\dot{\phi}$ in an evolution when both strain and temperature are held constant ($\dot{\varepsilon}_{ij} = \dot{p} = 0$).
- $3\alpha_\phi = \partial^2\Pi_s/\partial\theta\partial p$ stands for a volumetric thermal dilation coefficient related to the porosity.

Linearization of porous medium

The thermoporoelastic behavior is obtained when the intrinsic dissipation equals zero for any possible evolution, and thus no internal variable is required. Then the constitutive equations of thermoporoelastic elementary systems reduce to only the state equations of Eq. (2.73) where the free energy Ψ is a function of the external variables ε_{ij}, m and θ.

In order to deduce the formal expression of the free energy a physical linearization approach is carried out. This process consists in assuming small deformation of skeleton, small temperature variations, as well as small variations of fluid mas content. Under this hypothesis of *small transformation* the free energy $\Psi = \Psi\left(\varepsilon_{ij}, m, \theta\right)$ should be considered as a second-order expansion with regard to arguments ε_{ij}, m and θ [18]. Thus, the following expression of the free energy is obtained

$$\Psi = \sigma^0_{ij}\varepsilon_{ij} + g^0_f m - s^0\theta + \frac{1}{2}\varepsilon_{ij}C_{ijkl}\varepsilon_{kl} + \frac{1}{2}\mathrm{M}\left(\frac{m}{\rho^f}\right)^2 - \frac{1}{2}C_v\theta^2 - \mathrm{M}B_{ij}\varepsilon_{ij}\left(\frac{m}{\rho^f}\right) - A_{ij}\varepsilon_{ij}\theta - 3\alpha_\phi m\theta \quad (2.85)$$

The accuracy of the above expression related to Ψ and its arguments ε_{ij}, m and θ can actually be estimated only if the exact expression of the function Ψ is known. Thus, small deformations do not necessarily mean infinitesimal deformations, i.e. $\|\varepsilon_{ij}\| <<< 1$.

Some coefficients of Eq. (2.85) were introduced before in Eqs. (2.80)-(2.82). However, the superscript ^{0} is referred to the initial value of the corresponding variable, i.e. g^0_f is the initial free enthalpy of the fluid phase and s^0 is the initial entropy density.

Effective stress and stiffness tensor in thermoporoelasticity

Equation (2.80) can be rewritten in the following form

$$\dot{\sigma}_{ij} = \dot{\sigma}'_{ij} - \mathrm{M}B_{ij}\dot{p} \quad (2.86)$$

with

$$\dot{\sigma}'_{ij} = C^s_{ijkl}\dot{\varepsilon}_{ij} - \alpha^s_{ij}\dot{\theta} \quad (2.87)$$

The tensor σ'_{ij} is usually called the elastic effective stress tensor. Equation (2.87) linearly relates the stress tensor σ'_{ij}, the strain tensor ε_{ij} and the temperature θ in case of thermoelastic solid. Thus, the effective stress tensor may be interpreted as the stress tensor that produces (elastic) strain in the solid skeleton.

On the other hand, combining Eq. (2.80) and Eq. (2.81) the following expression is obtained

$$\dot{\sigma}_{ij} = C_{ijkl}\dot{\varepsilon}_{ij} - \mathrm{M}B_{ij}\dot{\phi} - \alpha_{ij}\dot{\theta} \tag{2.88}$$

being

$$C_{ijkl} = C^{s}_{ijkl} + \mathrm{M}B_{ij}B_{kl} \quad ; \quad \alpha_{ij} = \alpha^{s}_{ij} + 3\alpha_{\phi}\mathrm{M}B_{ij} \tag{2.89}$$

Owing to the symmetry of B_{ij}, α^{s}_{ij} and C^{s}_{ijkl}, the second order tensor α_{ij} preserves symmetry as well as the fourth order tensor C_{ijkl} satisfy the same symmetry relations of C^{s}_{ijkl}, Eq. (2.84). The tensor C^{s}_{ijkl} introduced in Eq. (2.80), can be interpreted as the elastic effective stiffness tensor for isothermal conditions. It is usually called drained elastic constitutive tensor for isothermic process, while the fourth order tensor C_{ijkl} is identified as undrained elastic constitutive tensor for isothermic condition, as well.

Stress tensor for partially saturated porous media

Partially saturated porous media are continuous media with voids filled by two fluid continuous phases, the liquid phase and the gaseous phase. The mechanical behavior of partially saturated porous media is usually described by the effective stress tensor σ'_{ij}, defined previously in Eq. (2.87) for biphasic porous media.

The extension of the present generalized theory of porous media to partially saturated porous media belongs to the context of double (or multiple) net porosity [6, 19, 15]. The basic assumption to concile the porous continuum as a multiphasic porous media is to consider the total porosity ϕ split into partial porosities ϕ_α (with $\alpha = 1, \ldots, n$). Thus, the volume occupied by the fluid α is $\phi_\alpha \mathrm{d}\Omega$, and

$$\phi = \sum_{\alpha} \phi_\alpha \tag{2.90}$$

In this framework the saturation degree S_α relative to α is define as

$$S_\alpha = \frac{\phi_\alpha}{\phi} \quad \text{and} \quad \sum_{\alpha} S_\alpha = 1 \tag{2.91}$$

Therefore, the total stress tensor can be expressed as

$$\sigma_{ij} = (1-\phi)\,\sigma^{s}_{ij} - \phi^{\alpha}p^{\alpha}\delta_{ij} \tag{2.92}$$
$$\sigma_{ij} = \sigma^{sk}_{ij} + \sigma^{f\alpha}_{ij} \tag{2.93}$$

where $\sigma_{ij}^{sk} = (1-\phi)\,\sigma_{ij}^{s}$ is the stress tensor related to the solid skeleton, $\sigma_{ij}^{f\alpha} = -\phi^{\alpha} p^{\alpha} \delta_{ij}$ is the stress tensor of fluid phase, p^{α} is the pore pressure of the α phase, being $\alpha = w$ and $\alpha = g$ for water pore and gaseous pressure, respectively.

Nevertheless, a simplified approach can be assumed for partially saturated porous media considering the pore pressure of gaseous phase as a constant and equal to the atmospheric pressure [105, 121]. Then, defining the suction tensor by p_{ij}^{s}

$$p_{ij}^{s} = (\phi^{g} p^{g} - \phi^{w} p^{w})\,\delta_{ij} \tag{2.94}$$

and the total stress can be expressed by

$$\sigma_{ij} = \sigma_{ij}^{sk} + p_{ij}^{s} \tag{2.95}$$

In several geotechnical problems the gas pore pressure can be considered as a constant term that equals the atmospheric pressure. In these cases the suction tensor is counterpart to the water pore pressure, p^{w}.

2.3 Flow theory of poroplasticity

2.3.1 Internal variables of poroplastic materials

Plasticity is a property exhibited by several materials to undergo permanent strains after a complete process of loading and unloading. Hence, poroplasticity is that property of porous media which defines their ability to undergo not only permanent skeleton strains, but also permanent variations in fluid mass content due to irreversible changes in the porosity.

Therefore, owing to the permanent strains and to the permanent changes in porosity, poroplastic evolutions are irreversible and, in contrast to the Thermoporoelastic theory presented in the section before, the total strains ε_{ij} and the porosity ϕ are not enough to fully characterize the current skeleton energy Ψ_s. Thereby, to describe the irreversible evolutions of poroelastoplastic media internal variables such as the plastic porosity ϕ^{p} or the plastic fluid mass content m^{p} must be considered in addition to the plastic strain rates ε_{ij}^{p}, and to the irreversible plastic entropy density s^{p}, in case of non-isothermal process.

Small strain flow rule of poroplastic materials is based on additive decompositions of internal variables into elastic and plastic components

$$\begin{aligned} \dot{\varepsilon}_{ij} &= \dot{\varepsilon}_{ij}^{e} + \dot{\varepsilon}_{ij}^{p} \\ \dot{m} &= \dot{m}^{e} + \dot{m}^{p} \\ \dot{s} &= \dot{s}^{e} + \dot{s}^{p} \end{aligned} \tag{2.96}$$

note that from the relationship between the fluid mass content and the porosity of Eq. (2.40), the second expression of Eq. (2.96) may be substituted by

$$\dot{m} = \rho^f \dot{\phi} = \rho^f \left(\dot{\phi}^e + \dot{\phi}^p \right) \tag{2.97}$$

For finite deformation problems the proposed theory presents some modifications, for details see Appendix A.

Initial, non-deformed stage with $\varepsilon_{ij} = 0$ and $m = 0$, corresponds to initial values of the stress tensor σ^0_{ij}, the pore pressure p^0 and absolute temperature θ^0. Figure 2.3 shows the hypothetical irreversible transformation that occurs in a representative volume element of porous media.

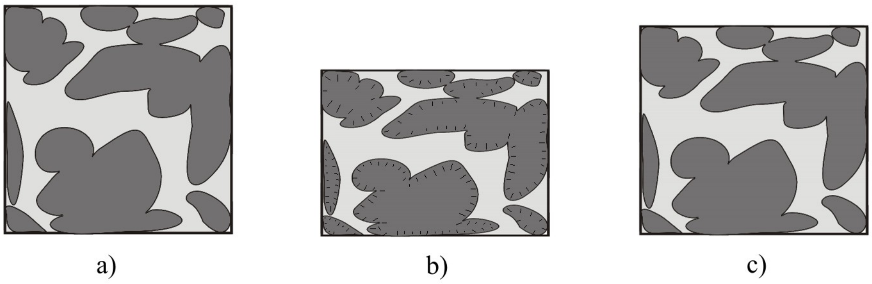

Figure 2.3: Poroplastic deformation process: a) Initial state; b) Current state; c) Final state

The rate of skeleton plastic strains $\dot{\varepsilon}^p_{ij}$ is only related to irreversible evolutions of the skeleton. However, the rate of plastic fluid mass content $\dot{m}^p$ may also be related to the irreversible evolution of the skeleton through its dependence on the porosity by Eq. (2.40). Indeed, the rate of plastic porosity $\dot{\phi}^p$ can be obtained as

$$\dot{\phi}^p = \frac{\dot{m}^p}{\rho_0^{fl}} \tag{2.98}$$

with ρ^f the initial fluid mass density.

Assuming Lagrangian configuration and keeping in mind the mass conservation law, the variation in mass content can then be expressed as

$$m = J \rho^f \phi - \rho_0^{fl} \phi_0 \tag{2.99}$$

being

$$J \equiv 1 + \varepsilon \tag{2.100}$$

which holds in infinitesimal transformations. Thereby is $\varepsilon = \varepsilon_{ii}$. By noting $J^p = (1 + \varepsilon^p)$, with $\varepsilon^p = \varepsilon^p_{ii}$ and being ϕ^d the porosity relative to the state after a complete poroelastic unloading process, results

$$m^p = J^p \rho_0^{fl} \phi^d - \rho_0^{fl} \phi_0 \tag{2.101}$$

Combining Eqs. (2.101) and (2.98) yields to

$$\phi^p = J^p \phi^d - \phi_0 \tag{2.102}$$

From the Jacobian definition and under consideration of Eq. (2.100), the residual differential volume after a complete unloading process can be expressed as

$$\mathrm{d}\Omega^d = J^p \mathrm{d}\Omega \tag{2.103}$$

Combining Eqs. (2.102) and (2.103) leads to

$$\phi^p \mathrm{d}\Omega = \phi^d \mathrm{d}\Omega^d - \phi_0 \mathrm{d}\Omega \tag{2.104}$$

Therefore, the terminology of plastic porosity appears fully justified, since, according to Eq. (2.104), ϕ^p represents the irreversible variation of porous volume, per unit of initial volume $\mathrm{d}\Omega$. The fluid and plastic fluid mass contents m and m^p, respectively, as well as the plastic porosity ϕ^p are Lagrangian variable, since they refer to the initial volume $\mathrm{d}\Omega$.

As previously indicated, under consideration of infinitesimal transformations, the strain tensor trace, ε, represents the volume change in a differential element of the porous media, which is also known as volume dilatation. In turn, the skeleton volume dilatation is related to the volume change of both the porous phase and the solid matrix, ε_s.

Being $d\Omega^s$ and $d\Omega^s_t$ the differential volume occupied by the solid matrix in the reference and current configuration, respectively, the matrix volume dilatation can be expressed as

$$\varepsilon_s = \frac{d\Omega^s_t - d\Omega^s}{d\Omega^s} \tag{2.105}$$

Taking into account that $d\Omega^s_t = (1 - \phi)\, d\Omega_t$ and $d\Omega^s = (1 - \phi_0)\, d\Omega_t / J$, the following expression can be obtained under the assumption expressed in Eq. (2.100)

$$(1 - \phi_0)\, \varepsilon_s = (1 - \phi)\, \varepsilon - (\phi - \phi_0) \tag{2.106}$$

Considering a poroplastic behavior Eq.(2.106) can be reformulated as

$$(1 - \phi_0)\, \varepsilon^p_s = \left(1 - \phi^d\right) \varepsilon^p - \left(\phi^d - \phi_0\right) \tag{2.107}$$

where ε^p_s is the permanent volume dilatation of the matrix, after a complete poroelastic unloading process for the elementary system.

Combining Eqs. (2.102) and (2.107) yields

$$\varepsilon^p = \phi^p + (1 - \phi_0)\, \varepsilon^p_s \tag{2.108}$$

2.3.2 Poroelastic domain and the yield function

The stress tensor σ_{ij} as well as the pore pressure p are sufficient to characterize any elastic loading path. In the loading space there exists an initial domain of poroelasticity including the zero loading point ($\sigma_{ij} = 0; p = 0$). The poroelastic domain $\mathcal{C}_E$ is such that the strain and the change in porosity (or fluid mass content) remain reversible along any loading path starting from the origin and lying entirely within that domain. For an ideal poroplastic material the initial domain of poroelasticity remains unchanged against the plastic evolution along any loading path. In contrast, the initial domain of poroelasticity of a hardening (or softening) poroplastic material exhibits changes in size and shape due to plastic evolutions.

This poroelastic domain $\mathcal{C}_E$ can be defined by means of the scalar loading function $f = f(\sigma_{ij}, p)$ for an ideal poroelastic material.

In the case of a hardening poroplastic material, the previous definitions apply to the current domain of elasticity, provided that the current loading function $f(\sigma_{ij}, p, Q_\alpha)$ involves in addition dissipative stress Q_α accounting for the current hardening state, such as

$$\begin{aligned} &f(\sigma_{ij}, p, Q_\alpha) < 0 \text{ for } (\sigma_{ij}, p) \text{ belonging to the in side of } \mathcal{C}_E \\ &f(\sigma_{ij}, p, Q_\alpha) = 0 \text{ for } (\sigma_{ij}, p) \text{ belonging to the boundary of } \mathcal{C}_E \\ &f(\sigma_{ij}, p, Q_\alpha) > 0 \text{ for } (\sigma_{ij}, p) \text{ belonging to the out side of } \mathcal{C}_E \end{aligned} \tag{2.109}$$

The elastic criterion is now the condition $f(\sigma_{ij}, p, Q_\alpha) < 0$. On the other hand, the plastic criterion is the condition $f(\sigma_{ij}, p, Q_\alpha) = 0$ while the yield surface is the border of $\mathcal{C}_E$, that is the surface defined by $f(\sigma_{ij}, p, Q_\alpha) = 0$. A loading state (σ_{ij}, p) is plastically admissible in the current state if it satisfies the condition $f(\sigma_{ij}, p, Q_\alpha) \leq 0$.

The elastic domain of most plastic materials is convex and this property can be extended to porous materials. The fundamental property of a convex domain is that all points of a segment located in between any couple of points of the same segment who also belong to the border of the domain lie inside the domain. If loading function $f(\sigma_{ij}, p, Q_\alpha)$ is continuously differentiable with respect to both σ_{ij} and p the fundamental property is equivalent to the condition:

$$\begin{aligned} \forall (\tilde{\sigma}_{ij}, \tilde{p}) \neq (\sigma_{ij}, p) \ \text{ with } f(\tilde{\sigma}_{ij}, \tilde{p}, Q_\alpha) = f(\sigma_{ij}, p, Q_\alpha) = 0 \\ (\sigma_{ij} - \tilde{\sigma}_{ij}) \frac{\partial f}{\partial \sigma_{ij}} + (p - \tilde{p}) \frac{\partial f}{\partial p} \geq 0 \end{aligned} \tag{2.110}$$

2.3.3 The flow rule and the plastic work

The plastic criterion $f(\sigma_{ij}, p) = 0$ or $f(\sigma_{ij}, p, Q_\alpha) = 0$, defines if plastic evolutions occurs. The (plastic) flow rule specifies the amount and direction of plastic evolution. If the loading point $(\sigma_{ij}, p, Q_\alpha)$ is on the yield surface but subsequently leaves it the evolutions are also poroelastic (elastic unloading). Since the value of loading function f becomes negative for a loading point (σ_{ij}, p) re-entering the poroelastic domain $\mathcal{C}_E$ (see Fig. 2.4), the elastic unloading condition is $f = 0$ and $\mathrm{d}f < 0$, with

$$\mathrm{d}f = \frac{\partial f}{\partial \sigma_{ij}}\mathrm{d}\sigma_{ij} + \frac{\partial f}{\partial p}\mathrm{d}p + \frac{\partial f}{\partial Q_\alpha}\mathrm{d}Q_\alpha \tag{2.111}$$

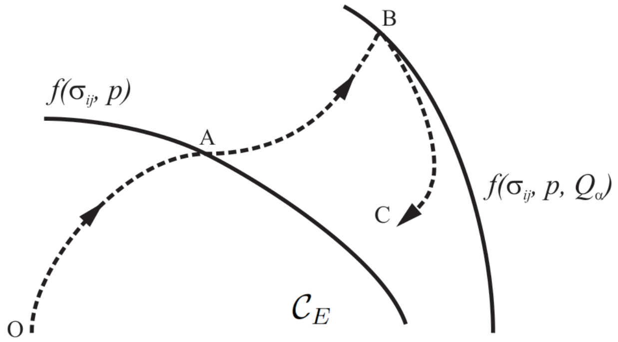

Figure 2.4: The condition $f(\sigma_{ij}, p) < 0$ define the initial domain of poroelasticity $\mathcal{C}_E$ therefore the strain and the change in porosity along a the loading paths such as OA remain reversible. For a hardening poroplastic material the initial domain of poroelasticity is altered by the plastic evolutions occurring along the loading paths such as AB. In order to account for this change an additional hardening force is required Q_α, then the current domain of elasticity is defined by $f(\sigma_{ij}, p, Q_\alpha) < 0$

However, if the loading point remains on the border of $\mathcal{C}_E$ plastic evolutions may occur. The corresponding loading surface differential now satisfies $\dot{f} = \mathrm{d}f = 0$, which is know as *consistency condition*. Taking into account all the above remarks, the flow rule can now be more precisely expressed in the form

$$\dot{\varepsilon}^p_{ij} = \dot{\lambda} h^\varepsilon_{ij}(\sigma_{ij}, p, Q_\alpha) \quad ; \quad \dot{\phi}^p = \dot{\lambda} h^\phi(\sigma_{ij}, p, Q_\alpha) \quad ; \quad \dot{q}_\alpha = \dot{\lambda} h^\alpha(\sigma_{ij}, p, Q_\alpha) \tag{2.112}$$

being q_α the internal thermodynamic variables (with $\alpha = s, p$ for solid or porous phase) and $\dot{\lambda}$ the so-called plastic multiplier that scales the intensity of plastic strain increments $(\dot{\varepsilon}^p_{ij}, \dot{\phi}^p)$ and satisfies the Kuhn-Tucker complementary conditions as follow

$$\dot{\lambda} \geq 0 \quad ; \quad f(\sigma_{ij}, p, Q_\alpha) \leq 0 \quad ; \quad \dot{\lambda} f(\sigma_{ij}, p, Q_\alpha) = 0 \quad ; \quad \dot{\lambda}\mathrm{d}f = 0 \tag{2.113}$$

The functions h^ε_{ij}, h^ϕ and h^α defines the directions of the plastic strain increments $\dot{\varepsilon}^p_{ij}$ and $\dot{\phi}^p$ as well as the corresponding internal variables $\dot{q}_\alpha$, in space $\{\sigma_{ij} \times p \times Q_\alpha\}$.

Assuming the following argument for the free energy of local poroplastic materials

$$\Psi_s = \Psi_s\left(\varepsilon^e_{ij}, \phi^e, q_\alpha\right) \tag{2.114}$$

the irreversible evolution Φ_s of Eq. (2.62) together with the state equation of Eq. (2.69) lead to the total dissipated energy

$$\sigma_{ij}\dot{\varepsilon}^p_{ij} + p\dot{\phi}^p + Q_\alpha \dot{q}_\alpha \geq 0 \tag{2.115}$$

being the dissipative stress for local poroplastic material

$$Q_\alpha = -\frac{\partial \Psi_s}{\partial q_\alpha} \tag{2.116}$$

Owing to the positiveness of plastic multiplier $\dot{\lambda}$ in Eq. (2.113) and considering the flow rule Eq. (2.112), then the positiveness of the total dissipated energy Eq. (2.115) requires

$$\sigma_{ij}h^\varepsilon_{ij} + p\, h^\phi + Q_\alpha h^\alpha \geq 0 \tag{2.117}$$

2.3.4 Principle of Maximal Plastic Work

The principle of maximal plastic work requires the actual plastic strain increment $(\dot{\varepsilon}^p_{ij}, \dot{\phi}^p)$ associated with the current loading $(\sigma_{ij}, p, Q_\alpha)$ to maximize the plastic work over all plastically admissible loadings $(\tilde{\sigma}_{ij}, \tilde{p}, Q_\alpha)$. It is written

$$\begin{aligned} \forall\, (\tilde{\sigma}_{ij}, \tilde{p}, Q_\alpha) \neq (\sigma_{ij}, p, Q_\alpha) \text{ with } f\,(\tilde{\sigma}_{ij}, \tilde{p}, Q_\alpha) \leq 0 \\ (\sigma_{ij} - \tilde{\sigma}_{ij})\, \dot{\varepsilon}^p_{ij} + (p - \tilde{p})\, \dot{\phi}^p \geq 0 \end{aligned} \tag{2.118}$$

In fact, according to [19] the principle of maximal plastic work relies on the more general principle of maximal production of entropy. Since the zero values of ($\tilde{\sigma}_{ij}$, $\tilde{p}$, Q_α) is plastically admissible, the principle of maximal plastic work ensures the fulfillment of Eq. (2.117).

If (σ_{ij}, p, Q_α) lies inside the poroelastic domain $\mathcal{C}_E$, the function h^ε_{ij}, h^ϕ and h^α may take any orientation so that, in order to satisfy Eq. (2.118), ($\dot{\varepsilon}^p_{ij}$, $\dot{\phi}^p$, $\dot{q}_\alpha$) must be zero in conformity with the actual definition of poroelasticity (see Fig. 2.5). Then, considering the vector (σ_{ij}, p, Q_α) on the boundary of poroelastic domain $\mathcal{C}_E$. Since ($\tilde{\sigma}_{ij}$, $\tilde{p}$, Q_α) cannot lie outside the elastic domain, the difference between both vectors (σ_{ij}, p, Q_α) and ($\tilde{\sigma}_{ij}$, $\tilde{p}$, Q_α) can only be oriented towards the border of $\mathcal{C}_E$. In order to fulfill Eq. (2.118), vector ($\dot{\varepsilon}^p_{ij}$, $\dot{\phi}^p$, $\dot{q}_\alpha$) shall be oriented in the normal direction to the border of the elastic domain. Therefore, the normality of the flow rule is expressed in the form

$$\dot{\varepsilon}^p_{ij} = \dot{\lambda}\frac{\partial f}{\partial \sigma_{ij}} \tag{2.119}$$

$$\dot{\phi}^p = \dot{\lambda}\frac{\partial f}{\partial p} \tag{2.120}$$

$$\dot{q}_\alpha = \dot{\lambda} \frac{\partial f}{\partial Q_\alpha} \tag{2.121}$$

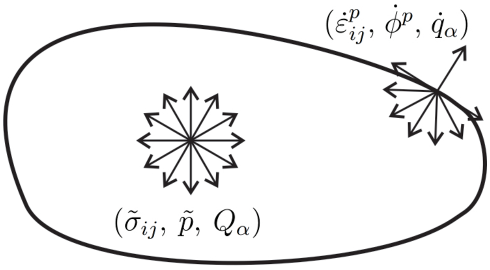

Figure 2.5: The normality of the flow rule and the Principle of maximal plastic work.

Substituting Eqs. (2.119)-(2.121) into Eq. (2.118) yields to

$$(\sigma_{ij} - \tilde{\sigma}_{ij}) \frac{\partial f}{\partial \sigma_{ij}} + (p - \tilde{p}) \frac{\partial f}{\partial p} \geq 0 \tag{2.122}$$

Comparing Eq. (2.122) and Eq. (2.110), the principle of maximal plastic work also implies the convexity of the poroelastic domain $\mathcal{C}_E$ as well as the normality of the flow rule.

This kind of material are so-called standards materials due to the employment of yield function to define the direction of plastic evolution through the definition of the flow rule Eqs. (2.119)-(2.121). This plasticity formulation is said to be associated. In case of non-standards materials a non-associated flow rule based on the plastic potential $g \neq f$ should be defined

$$\dot{\varepsilon}^p_{ij} = \dot{\lambda} \frac{\partial g}{\partial \sigma_{ij}} \tag{2.123}$$

$$\dot{\phi}^p = \dot{\lambda} \frac{\partial g}{\partial p} \tag{2.124}$$

$$\dot{q}_\alpha = \dot{\lambda} \frac{\partial g}{\partial Q_\alpha} \tag{2.125}$$

Finally, owing to the positiveness condition Eq. (2.117) the non-associated plastic potential g should satisfy

$$\sigma_{ij} \frac{\partial g}{\partial \sigma_{ij}} + p \frac{\partial g}{\partial p} + Q_\alpha \frac{\partial g}{\partial Q_\alpha} \geq 0 \tag{2.126}$$

CHAPTER 3

A gradient-based poroplastic theory

The mechanic of porous media constitutes a discipline of great relevance in several knowledge areas like Geophysics, Biomechanics and Materials Science. Its main aim is the description of the kinematic and pore pressure of porous continua when subjected to arbitrary mechanical and/or physical actions.

The definitive advantages of porous mechanics to macroscopically describe or predict complex response behavior of cohesive-frictional materials based on fundamental aspects of their microstructure while accounting for the hydraulic properties and their influence in the resulting failure mechanism were recognized by several authors in the scientific community [10, 14, 55]. Consequently, a tendency to replace the theoretical framework of classical continuum mechanics with that of non-linear porous mechanics was observed. Firstly this process took place in case of soil mechanics, see a.o. [31, 21], but subsequently in the field of concrete, see a.o. [122, 92] and, furthermore, of biomaterials , see a.o. [79, 94].

Further development in classical continuum mechanics was the extension to non-local concepts. The main aim was the regularization of post peak response behavior regarding mesh size and element orientation in case of finite element analyses, based on fundamental aspects of the material microstructure, see a.o. [117, 40, 36, 2, 130].

In recent years significant progresses and relevant contributions were made in non-local gradient formulations for non-porous materials. Thermodynamic frameworks were considered in the proposals of [2, 3, 95, 96, 125, 46, 53, 130]. Phenomenological aspects of the considered materials at the microscopic level of observation were taken into account in non-local gradient formulations by [97, 9, 63]. Objective descriptions of the gradient internal length based on crystal-plasticity concepts were due to [8, 61, 62, 33], while based on actual confining pressure in case of quasi-brittle materials like concrete as proposed by [130]. Considerations of material anisotropy in the formulation of internal variables evolution laws in case of gradient plasticity are due to [4, 126]. Geometrical analysis of bifurcation condition in case of non-local gradient formulations as proposed by [127, 37]. Formulation of gradient enhanced coupled damage-plasticity material models and related finite element implementations, see [117, 67, 27].

Recently, non-local concepts were extended for the formulation of porous material models, see a.o. [64, 57, 77]. Likewise, the consideration of microscopic aspects in the formulation of non-local constitutive theories for porous materials are due to [140, 81, 134].

In spite of the strong development of constitutive modelling for porous media, explained before, there is still a need of thermodynamically consistent theoretical frameworks. This is particularly the case of non-local models for porous materials. Thermodynamic concepts should lead to dissipative stress formulations in hardening and softening regimes that allow non-constant descriptions of the internal variables of non-local character to accurately predict the sensitivity of porous material failure behavior to both confinement and saturation levels.

In this work the thermodynamically consistent formulation for non-porous gradient-based elastoplasticity by Vrech and Etse, 2009 [129, 130] that follows general thermodynamic approach proposed by Svedberg and Runesson, 1997 [116, 118, 117], for non-local damage formulation is extended for porous media. Main feature of present proposal is the definition of a gradient-based characteristic length in terms of both the governing stress and hydraulic conditions to capture the variation of the transition from brittle to ductile failure mode of cohesive-frictional porous materials with the confinement level and saturation [76].

3.1 A thermodynamically consistent gradient-based poroplastic theory

The thermodynamic framework of classical or local plasticity is extended to non-local gradient-based elastoplastic porous material.

Following [111, 18] we assume that arbitrary thermodynamic states of the dissipative material during isothermal processes are completely determined by the elastic strain $\varepsilon_{ij}^e = \varepsilon_{ij} - \varepsilon_{ij}^p$, the elastic entropy $s^e = s - s^p$ and the internal variables q_α with $\alpha = s, p$ for solid or porous phase, which are considered here as scalar variables. Furthermore, isothermal situation is considered, i.e. θ is treated as a known parameter. This means that θ, s^e and s^p become irrelevant quantities and the elastic entropy s^e does not need to be included as an additional argument of the thermodynamic state.

When considering poroplastic materials the elastic porosity $\phi^e = \phi - \phi^p$ needs also to be included as a thermodynamic argument, see [18]. Based on [117, 130, 76] we further assume that the internal variables q_α, are the only ones of non-local character. The extension to more than two scalar internal variables is straightforward. Hence, both q_α and $q_{\alpha,i}$ will appear as arguments in the free energy Ψ_s, such that

$$\Psi_s = \Psi_s \left(\varepsilon_{ij}^e, \phi^e, q_\alpha, q_{\alpha,i} \right) \tag{3.1}$$

Note that by restricting non-local effects to the internal variables the energy balance in Eq. (2.49) remains unchanged. This is because the strain rate tensor remains local and the energy density is not expressed in terms of its arguments that involve non-local effects through internal variables, like in Eq. (3.1).

Upon differentiation of Eq. (3.1) and combining with the intrinsic dissipation of Eq. (2.55) on the whole domain Ω, under consideration of Eqs. (2.96) and Eq. (2.97),

$$\int_{\Omega}\left[\left(\sigma_{ij}-\frac{\partial\Psi_s}{\partial\varepsilon^e_{ij}}\right)\dot{\varepsilon}_{ij}+\left(p-\frac{\partial\Psi_s}{\partial\phi^e}\right)\dot{\phi}+\frac{\partial\Psi_s}{\partial\varepsilon^e_{ij}}\dot{\varepsilon}^p_{ij}+\frac{\partial\Psi_s}{\partial\phi^e}\dot{\phi}^p \right.$$
$$\left. -\sum_{\alpha}\frac{\partial\Psi_s}{\partial q_\alpha}\dot{q}_\alpha-\sum_{\alpha}\frac{\partial\Psi_s}{\partial q_{\alpha,i}}\dot{q}_{\alpha,i}\right]\mathrm{d}\Omega\geq 0 \quad (3.2)$$

and integrating the gradient term by parts, it follows

$$\int_{\Omega}\left[\left(\sigma_{ij}-\frac{\partial\Psi_s}{\partial\varepsilon^e_{ij}}\right)\dot{\varepsilon}_{ij}+\left(p-\frac{\partial\Psi_s}{\partial\phi^e}\right)\dot{\phi}+\frac{\partial\Psi_s}{\partial\varepsilon^e_{ij}}\dot{\varepsilon}^p_{ij}+\frac{\partial\Psi_s}{\partial\phi^e}\dot{\phi}^p \right.$$
$$\left. -\sum_{\alpha}\frac{\partial\Psi_s}{\partial q_\alpha}\dot{q}_\alpha-\sum_{\alpha}\left(\frac{\partial\Psi_s}{\partial q_{\alpha,i}}\dot{q}_\alpha\right)_{,i}\dot{q}_\alpha\right]\mathrm{d}\Omega-\int_{\partial\Omega}\sum_{\alpha}n_i\frac{\partial\Psi_s}{\partial q_{\alpha,i}}\dot{q}_\alpha\;\mathrm{d}\partial\Omega\geq 0 \quad (3.3)$$

On the above equation, the Divergence Theorem was applied being n_i the (outward) unit normal to the surface $\partial\Omega$.

Then, the dissipative stress in the domain Ω and on the boundary $\partial\Omega$ are defined as Q_α and $Q^{(b)}_\alpha$, respectively

$$Q_\alpha=-\frac{\partial\Psi_s}{\partial q_\alpha}-\left(\frac{\partial\Psi_s}{\partial q_{\alpha,i}}\right)_{,i} \qquad \text{in } \Omega \quad (3.4)$$

$$Q^{(b)}_\alpha=-\frac{\partial\Psi_s}{\partial q_{\alpha,i}}n_i \qquad \text{on } \partial\Omega \quad (3.5)$$

and the Eq. (3.3) can be expressed as

$$\int_{\Omega}\left[\left(\sigma_{ij}-\frac{\partial\Psi_s}{\partial\varepsilon^e_{ij}}\right)\dot{\varepsilon}_{ij}+\left(p-\frac{\partial\Psi_s}{\partial\phi^e}\right)\dot{\phi}+\frac{\partial\Psi_s}{\partial\varepsilon^e_{ij}}\dot{\varepsilon}^p_{ij}+\frac{\partial\Psi_s}{\partial\phi^e}\dot{\phi}^p \right.$$
$$\left. +\sum_{\alpha}Q_\alpha\dot{q}_\alpha\right]\mathrm{d}\Omega+\int_{\partial\Omega}\sum_{\alpha}Q^{(b)}_\alpha\dot{q}_\alpha\;\mathrm{d}\partial\Omega\geq 0 \quad (3.6)$$

In standard form (as for local theory), it is postulated that the last inequality must hold for any choice of domain Ω and for any independent thermodynamic process. As a result, Coleman's equation are formally obtained like for the local continuum theory Eq. (2.69)

$$\sigma_{ij}=\frac{\partial\Psi_s}{\partial\varepsilon^e_{ij}} \quad ; \quad p=\frac{\partial\Psi_s}{\partial\phi^e} \quad (3.7)$$

being the dissipative energy

$$\mathfrak{D} = \sigma_{ij}\dot{\varepsilon}^{p}_{ij} + p\dot{\phi}^{p} + \sum_{\alpha} Q_{\alpha}\dot{q}_{\alpha} \geq 0 \qquad \text{in } \Omega \tag{3.8}$$

$$\mathfrak{D}^{(b)} = \sum_{\alpha} Q^{(b)}_{\alpha}\dot{q}_{\alpha} \geq 0 \qquad \text{on } \partial\Omega \tag{3.9}$$

In the particular case of non-porous material ($p = 0$) above equations takes similar form to those obtained by [117, 130] for isothermal situations.

From the above Eq. (3.8) and Eq. (3.9), it can be concluded that the difference between this simplified non-local theory and the local one presented in Section 2.3.3 (see Eq. (2.115)) is the additional gradient term in the expression of the dissipative stresses Q_{α}, and the boundary dissipation term $Q^{(b)}_{\alpha}$.

Consequently, the dissipative stress Q_{α} can be decomposed into the local and non-local components

$$Q_{\alpha} = Q^{loc}_{\alpha} + Q^{nloc}_{\alpha} \tag{3.10}$$

with

$$Q^{loc}_{\alpha} = -\frac{\partial \Psi_s}{\partial q_{\alpha}} \tag{3.11}$$

$$Q^{nloc}_{\alpha} = -\left(\frac{\partial \Psi_s}{\partial q_{\alpha,i}}\right)_{,i} \tag{3.12}$$

Remark: while the global inequality in Eq. (3.6) is necessary in order to satisfy the Clausius-Duhem inequality, the inequalities Eqs. (3.8) and (3.9) are only sufficient conditions.

It is interesting to compare the rate of dissipation expression in Eq. (3.3), when non-porous media are considered, with that corresponding to the unified treatment of thermodynamically consistent gradient plasticity by Gudmundson, 2004, [44]. When applying integration by parts, followed by the Divergence Theorem, to the gradient terms of the rate of dissipation, see Eq. (7) of [44], this formulation leads to dissipative non-local stresses on the boundary, similarly to the present proposal when particularized to non-porous media.

However, a relevant difference between Gudmundson formulation and the present one is that the free energy density in the first one is expressed as function of the elastic strain, plastic strain, and plastic strain gradient tensors. Consequently, the dissipation includes the differences between the rate of change of the free energy with respect to the plastic strains and plastic strain gradients, on the one hand, and the internal stresses conjugated to both kinematic fields, on the other hand. These internal stresses are denoted by Gudmundson as microstresses and moment stresses, respectively. In the present formulation, and based on [117, 130], the free energy density is expressed in terms of the elastic strains, the internal variables and their gradients (being the only ones of non-local character). So, the rate of dissipation in Eq. (3.3) does not include the so-called microstresses and moment stresses.

3.1.1 Thermodynamically consistent constitutive relations

Based on previous works [117, 130, 35], the following additive expression of the free energy corresponding to non-local gradient poroplastic materials is adopted

$$\Psi_s\left(\varepsilon_{ij}^e, m^e, q_\alpha, q_{\alpha,i}\right) = \Psi^e\left(\varepsilon_{ij}^e, m^e\right) + \Psi^{p,loc}\left(q_\alpha\right) + \Psi^{p,nloc}\left(q_{\alpha,i}\right) \tag{3.13}$$

whereby Ψ^e is the elastic energy of the porous media deduced in Section 2.2.5. Considering the relation Eq. (2.40), the expression Eq. (2.85) for the elastic counterpart of the free energy for isothermal process, neglecting initial stress and pressures, can be expressed as

$$\Psi^e = \frac{1}{2}\varepsilon_{ij}C_{ijkl}\varepsilon_{kl} + \frac{1}{2}\mathrm{M}\left(\phi^e\right)^2 - \mathrm{M}B_{ij}\varepsilon_{ij}\phi^e \tag{3.14}$$

Whereas $\Psi^{p,loc}$ and $\Psi^{p,nloc}$ are the local and non-local gradient contributions due to dissipative hardening/softening behaviors, which are expressed in terms of the internal variables q_α and their gradient $q_{\alpha,i}$, respectively.

Once the Coleman's relations are deduced from Eq. (3.7) the following expressions can be obtained

$$\sigma_{ij} = C_{ijkl}\varepsilon_{kl}^e - \mathrm{M}B_{ij}\phi^e \tag{3.15}$$

$$p = -\mathrm{M}B_{ij}\varepsilon_{ij}^e + \mathrm{M}\phi^e \tag{3.16}$$

being M the Biot's module, $B_{ij} = b\delta_{ij}$ with b the Biot coefficient, and $C_{ijkl} = C_{ijkl}^s + \mathrm{M}B_{ij}B_{kl}$ is the undrained elastic constitutive tensor, whereby C_{ijkl}^s is the fourth-order elastic tensor which linearly relates stress and strain, both presented in Section 2.2.5.

3.1.2 Rate form of constitutive equations

In the undrained condition and considering the additive decomposition of the free energy potential in Eq. (3.13) and the flow rule of Eq. (2.123) and Eq. (2.124), the following rate expressions of the stress tensor $\dot{\sigma}_{ij}$ and pore pressure $\dot{p}$ are obtained from Eq. (3.15) and Eq. (3.16)

$$\dot{\sigma}_{ij} = C_{ijkl}\dot{\varepsilon}_{kl} - C_{ijkl}\dot{\lambda}\frac{\partial g}{\partial \sigma_{kl}} - \mathrm{M}B_{ij}\dot{\phi} + \mathrm{M}B_{ij}\dot{\lambda}\frac{\partial g}{\partial p} \tag{3.17}$$

$$\dot{p} = -\mathrm{M}B_{ij}\dot{\varepsilon}_{ij} + \mathrm{M}B_{ij}\dot{\lambda}\frac{\partial g}{\partial \sigma_{ij}} + \mathrm{M}\dot{\phi} - \mathrm{M}\dot{\lambda}\frac{\partial g}{\partial p} \tag{3.18}$$

After multiplying Eq. (3.18) by B_{ij} and combining with Eq. (3.17), a more suitable expression of the rate of the stress tensor for drained condition is achieved

$$\dot{\sigma}_{ij} = C^s_{ijkl}\dot{\varepsilon}_{kl} - B_{ij}\dot{p} - C^s_{ijkl}\dot{\lambda}\frac{\partial g}{\partial \sigma_{kl}} \tag{3.19}$$

while the evolution law of the local and non-local dissipative stress in Eq. (3.10) results

$$\dot{Q}_\alpha = \dot{Q}^{loc}_\alpha + \dot{Q}^{nloc}_\alpha \tag{3.20}$$

with

$$\dot{Q}^{loc}_\alpha = -\dot{\lambda}H^{loc}_\alpha \frac{\partial g}{\partial Q_\alpha} \tag{3.21}$$

$$\dot{Q}^{nloc}_\alpha = l^2_\alpha \left(H^{nloc}_{\alpha\, ij}\dot{\lambda}_{,j}\frac{\partial g}{\partial Q_\alpha} + \dot{\lambda}H^{nloc}_{\alpha\, ij}Q_{\alpha,j}\frac{\partial^2 g}{\partial {Q_\alpha}^2}\right)_{,i} \tag{3.22}$$

Thereby, local hardening/softening module H^{loc}_α have been introduced as well as the new non-local hardening/softening tensor $H^{nloc}_{\alpha\, ij}$ as defined in [117]

$$H^{loc}_\alpha = \frac{\partial^2 \Psi^{p,loc}}{\partial {q_\alpha}^2} \quad , \quad H^{nloc}_{\alpha\, ij} = \frac{1}{l^2_\alpha}\frac{\partial^2 \Psi^{p,nloc}}{\partial q_{\alpha,i}\partial q_{\alpha,j}} \tag{3.23}$$

$H^{nloc}_{\alpha\, ij}$ is a second order positive defined tensor. For the characteristic length l_α three alternative definitions can be given, see [84, 116, 127]. On the one hand, it can be defined as a convenient dimensional parameter so as H^{loc}_α and $H^{nloc}_{\alpha\, ij}$ will get the same dimension. On the other hand, as a physical entity that characterizes the material microstructure. Alternatively, l_α can be interpreted as an artificial numerical stabilization mechanism for the non-local theory.

3.1.3 Differential equation for the plastic multiplier

The complementary Kuhn-Tucker condition in Eq. (2.113) together with the plastic consistency condition, leads to

$$\dot{f} = \frac{\partial f}{\partial \sigma_{ij}}\dot{\sigma}_{ij} + \frac{\partial f}{\partial p}\dot{p} + \frac{\partial f}{\partial Q_\alpha}\dot{Q}_\alpha = 0 \tag{3.24}$$

From Eq. (3.17), Eq. (3.18) and Eq. (3.20), the following differential equation for undrained condition can be obtained

$$\dot{f} = \dot{\lambda}\left(-\frac{\partial f}{\partial \sigma_{ij}} C_{ijkl} \frac{\partial g}{\partial \sigma_{kl}} + \mathrm{M}\frac{\partial f}{\partial \sigma_{ij}} B_{ij} \frac{\partial g}{\partial p} + \mathrm{M}\frac{\partial f}{\partial p} B_{ij} \frac{\partial g}{\partial \sigma_{ij}} - \mathrm{M}\frac{\partial f}{\partial p}\frac{\partial g}{\partial p} - H_{\alpha}^{loc}\frac{\partial f}{\partial Q_{\alpha}}\frac{\partial g}{\partial Q_{\alpha}}\right)$$
$$+ \left(\frac{\partial f}{\partial \sigma_{ij}} C_{ijkl} - \mathrm{M}\frac{\partial f}{\partial p} B_{kl}\right)\dot{\varepsilon}_{kl} + \left(\mathrm{M}\frac{\partial f}{\partial p} - \frac{\partial f}{\partial \sigma_{ij}} B_{ij}\right)\dot{\phi}$$
$$+ \frac{\partial f}{\partial Q_{\alpha}}\left[l_{\alpha}^{2}\left(H_{\alpha\, ij}^{nloc}\dot{\lambda}_{,j}\frac{\partial g}{\partial Q_{\alpha}} + \dot{\lambda} H_{\alpha\, ij}^{nloc} Q_{\alpha,j}\frac{\partial^2 g}{\partial {Q_{\alpha}}^2}\right)_{,i}\right] = 0 \quad (3.25)$$

also, a more suitable differential equation for the drained condition can be obtained when Eq. (3.19) instead of Eq. (3.17) is combined with Eqs. (3.18) and (3.20).

$$\dot{f} = \dot{\lambda}\left(-\frac{\partial f}{\partial \sigma_{ij}} C_{ijkl}^{s} \frac{\partial g}{\partial \sigma_{kl}} - H_{\alpha}^{loc}\frac{\partial f}{\partial Q_{\alpha}}\frac{\partial g}{\partial Q_{\alpha}}\right)$$
$$+ \frac{\partial f}{\partial \sigma_{ij}} C_{ijkl}^{s}\dot{\varepsilon}_{kl} + \left(\frac{\partial f}{\partial p} - \frac{\partial f}{\partial \sigma_{ij}} B_{ij}\right)\dot{p}$$
$$+ \frac{\partial f}{\partial Q_{\alpha}}\left[l_{\alpha}^{2}\left(H_{\alpha\, ij}^{nloc}\dot{\lambda}_{,j}\frac{\partial g}{\partial Q_{\alpha}} + \dot{\lambda} H_{\alpha\, ij}^{nloc} Q_{\alpha,j}\frac{\partial^2 g}{\partial {Q_{\alpha}}^2}\right)_{,i}\right] = 0 \quad (3.26)$$

For the sake of clarity last equation is rewritten in compacted form

$$-\dot{f}^{nloc} + \left(h + h^{nloc}\right)\dot{\lambda} = \dot{f}^{e} - \dot{f} \quad (3.27)$$

where $\dot{f}^{e}$ is the local loading function, h the generalized plastic modulus, h^{nloc} the gradient plastic modulus, and $\dot{f}^{nloc}$ the gradient loading function defined as

$$\dot{f}^{nloc} = l_{\alpha}^{2}\frac{\partial f}{\partial Q_{\alpha}}\left\{\frac{\partial g}{\partial Q_{\alpha}}\left[H_{\alpha\, ij}^{nloc}\dot{\lambda}_{,ij} + H_{\alpha\, ij,j}^{nloc}\dot{\lambda}_{,i}\right] + 2\frac{\partial^2 g}{\partial {Q_{\alpha}}^2} Q_{\alpha,i} H_{\alpha\, ij}^{nloc}\dot{\lambda}_{,j}\right\} \quad (3.28)$$

$$h^{nloc} = -l_{\alpha}^{2}\frac{\partial f}{\partial Q_{\alpha}}\left\{\frac{\partial^2 g}{\partial {Q_{\alpha}}^2}\left[H_{\alpha\, ij}^{nloc} Q_{\alpha,ij} + H_{\alpha\, ij,j}^{nloc} Q_{\alpha,i}\right] + \frac{\partial^3 g}{\partial {Q_{\alpha}}^3} Q_{\alpha,i} H_{\alpha\, ij}^{nloc} Q_{\alpha,j}\right\} \quad (3.29)$$

Both, the local yield function and the generalized plastic modulus can be decomposed into the components ($\dot{f}_{s}^{e}$, h_s) and ($\dot{f}_{p}^{e}$ and h_p) related to the solid skeleton and to the porous phase, respectively. This decomposition is valid for undrained and drained conditions.

$$\dot{f}^{e} = \dot{f}_{s}^{e} + \dot{f}_{p}^{e} \quad (3.30)$$
$$h = h_s + h_p + \bar{H} \quad (3.31)$$

with

$$\bar{H} = H_{\alpha}^{loc} \frac{\partial f}{\partial Q_{\alpha}} \frac{\partial g}{\partial Q_{\alpha}} \tag{3.32}$$

where, for drained condition, it can be obtained

$$\dot{f}_s^{e,d} = \frac{\partial f}{\partial \sigma_{ij}} C_{ijkl}^s \dot{\varepsilon}_{kl} \tag{3.33}$$

$$\dot{f}_p^{e,d} = \left(\frac{\partial f}{\partial p} - \frac{\partial f}{\partial \sigma_{ij}} B_{ij} \right) \dot{p} \tag{3.34}$$

$$h_s^d = \frac{\partial f}{\partial \sigma_{ij}} C_{ijkl}^s \frac{\partial g}{\partial \sigma_{kl}} \tag{3.35}$$

$$h_p^d = 0 \tag{3.36}$$

while for undrained condition

$$\dot{f}_s^{e,u} = \frac{\partial f}{\partial \sigma_{ij}} C_{ijkl} \dot{\varepsilon}_{kl} - \mathrm{M} \frac{\partial f}{\partial p} B_{ij} \dot{\varepsilon}_{ij} \tag{3.37}$$

$$\dot{f}_p^{e,u} = \dot{\phi} \left(\mathrm{M} \frac{\partial f}{\partial p} - \frac{\partial f}{\partial \sigma_{ij}} B_{ij} \right) \tag{3.38}$$

$$h_s^u = \frac{\partial f}{\partial \sigma_{ij}} C_{ijkl} \frac{\partial g}{\partial \sigma_{kl}} \tag{3.39}$$

$$h_p^u = -\mathrm{M} \left(\frac{\partial f}{\partial \sigma_{ij}} B_{ij} \frac{\partial g}{\partial p} + \frac{\partial f}{\partial p} B_{ij} \frac{\partial g}{\partial \sigma_{ij}} - \frac{\partial f}{\partial p} \frac{\partial g}{\partial p} \right) \tag{3.40}$$

When all state variables are spatially homogeneous it can be assumed that the dissipative stress gradient is negligible, then $Q_{\alpha,i} = 0$ and consequently $\partial^2 g / \partial {Q_{\alpha}}^2 = 0$, see [131, 32, 80, 117]. Thereby

$$h^{nloc} = 0 \quad \text{and} \quad \dot{f}^{nloc} = l_{\alpha}^2 \frac{\partial f}{\partial Q_{\alpha}} \frac{\partial g}{\partial Q_{\alpha}} H_{\alpha\, ij}^{nloc} \dot{\lambda}_{,ij} \tag{3.41}$$

and the pertinent differential equation to evaluate $\dot{\lambda}$ in this particular case results

$$-\dot{f}^{nloc} + h\dot{\lambda} = \dot{f}^{e} - \dot{f} \tag{3.42}$$

3.1.4 Gradient form of elastoplastic constitutive equations

Under consideration of plastic loading, the plastic multiplier can be easily determined from Eq. (3.42). Replacing it in the constitutive equations Eq. (3.17) or Eq. (3.19) for undrained and drained hydraulic condition, respectively, leads to

$$\dot{\sigma}_{ij} = C^s_{ijkl}\dot{\varepsilon}_{kl} - B_{ij}\dot{p} - C^s_{ijkl}\frac{\partial g}{\partial \sigma_{kl}}\left(\dot{f}^e + \dot{f}^{nloc}\right)/h \tag{3.43}$$

$$\dot{\sigma}_{ij} = C_{ijkl}\dot{\varepsilon}_{kl} - \mathrm{M}B_{ij}\dot{\phi} + \left(\mathrm{M}B_{ij}\frac{\partial g}{\partial p} - C_{ijkl}\frac{\partial g}{\partial \sigma_{kl}}\right)\left(\dot{f}^e + \dot{f}^{nloc}\right)/h \tag{3.44}$$

Taking into account the definitions of $\dot{f}^e$ and $\dot{f}^{nloc}$ in the above equations results

$$\dot{\sigma}_{ij} = E^{ep,sd}_{ijkl}\dot{\varepsilon}_{kl} + E^{ep,pd}_{ij}\dot{p} - E^{g,spd}_{ij}\dot{f}^g \tag{3.45}$$

$$\dot{\sigma}_{ij} = E^{ep,su}_{ijkl}\dot{\varepsilon}_{kl} + E^{ep,pu}_{ij}\dot{\phi} - E^{g,spu}_{ij}\dot{f}^g \tag{3.46}$$

being $\boldsymbol{E}^{ep,s}$ the elastoplastic fourth-order operator of solid skeleton, $\boldsymbol{E}^{ep,p}$ the elastoplastic second-order operators of porous phase and $\boldsymbol{E}^{g,sp}$ the continuum gradient-elastoplastic second-order tensor of both constituents. The superscript ^{d} or ^{u} indicates the considered hydraulic condition, drained or undrained, respectively. For more details about the matrix of Eq. (3.45) and Eq. (3.46) see Appendix B.

3.2 Particular cases of analysis

In this Section some particular cases are adressed in order to show different material behaviour

Non-local behavior restricted to the solid phase In some engineering materials non-local dissipative behavior may be fully restricted to the granular or solid phase. The thermodynamically consistent constitutive formulation presented in previous sections can be easily adjusted to reproduce this particular form of non-local behavior. In this case the porous phase does not follow an irreversible thermodynamical process, then $\dot{\phi}^p = 0$ and $\dot{q}_p = 0$. Consequently Eq. (3.8) takes the form

$$\mathfrak{D} = \sigma_{ij}\dot{\varepsilon}^p_{ij} + Q_s\dot{q}_s \geq 0 \tag{3.47}$$

This non-local formulation which requires only one characteristic length, is also covered by the unified description of strain gradient plasticity by Gudmundson, 2004 [44].

It is relevant to note that the condition $\dot{\phi}^p = 0$ usually arises in constitutive models that do not rigorously fulfill the Second Law of Thermodynamic. Models based on Mixtures Theory (presented in Section 2.1) by [20, 54, 107, 73] are typical examples of this type of constitutive formulations. The same can be said of models based on fictitious simplifications of the material behaviour such as the proposal by [58, 25] that make use of artificial state combinations.

Non-local behavior restricted to the porous phase Experimental evidence demonstrates that under certain stress states and hydraulic conditions, localization phenomena may develop only in the porous phase [71, 65, 105]. This particular behavior can also be modeled with the thermodynamic non-local formulation proposed in this work. To this end, the gradients of internal variables that control the non-local behavior of the solid phase are neglected while the gradient terms of internal variables corresponding to the porous phase are the only ones with non-local characteristics.

CHAPTER 4

Thermodynamically consistent poroplastic models

Following the presentation of the thermodynamically consistent gradient-based theory in Chapter 3 the particularization for an specific material model is proposed. In this regard two well known material models for porous media are considered, the modified Cam Clay plasticity model employed in mechanical prediction of saturated and partially saturated porous media [13, 14, 85] as well as the Parabolic Drucker-Prager material model commonly used in constitutive formulations for concrete.

The usual material models employed in non-porous media cover a wide range of cohesive-frictional materials but have some difficulties in capturing the plastic evolution of clays. Indeed, soils cannot sustain tensile stresses, nor large confining pressure, whereas the observed dilatancy can be either positive (dilation) or negative (contraction), depending on the ratio between the shear stress and the effective confinement.

This Chapter is focused on the presentation of main features of theses material models and the particularization of the thermodynamically consistent gradient-based theory of porous media proposed in [35] for clays and concrete materials. On the other hand, the mathematical definition of both internal characteristic lengths for solid skeleton and porous media, is presented, as well as the thermodynamically consistent plastic potential function.

4.1 Modified Cam Clay plasticity model

From research of Roscoe et al. (1958) [100] at Cambridge University a plasticity model family for saturated soil was developed by introducing an isotropic hardening function for the evolution of the yield function. Based on this, the Cam Clay material model was proposed by Schofield and Wroth (1968) [106]. Then, the Modified Cam Clay plasticity model was proposed by Roscoe and Burland (1968) [99] for normally consolidated clays. Due to its accurate predictions of consolidated clay mechanical behavior and to the reduced number of involved parameters, the Cam Clay material theory has been extended to a wide range of soils including unsaturated ones [5, 13], and cyclic external actions [88].

Main assumptions of the originally proposed Modified Cam Clay plasticity model are:

a- The yield function is an ellipse defined in the (σ', τ) plane

b- The volumetric component of the plastic strain on the Critical State Line (CSL) is null while the plastic flow develops under constant volume

c- Associated plastic flow is considered

d- The hardening law is increasing, convex and asymptotic to a certain value, thus the Drucker condition is fulfilled and the Second Principle of the Thermodynamic is not violated

The yield function is defined by

$$f\left(\sigma, \tau, p, Q_\alpha\right) = \left(\sigma - \beta p + \frac{\tau^2}{M^2\left(\sigma - \beta p\right)}\right) - Q_\alpha \tag{4.1}$$

where $\sigma = I_1/3$ is the total hydrostatic stress and $\sigma' = \sigma - \beta p$ is the effective hydrostatic stress, $\tau = \sqrt{3J_2}$ is the shear stress, M the Critical State Line (CSL) slope and Q_α the thermodynamically consistent dissipative stress equivalent to the preconsolidation pressure p_{co}, see Fig. 4.1. Also I_1 and J_2 are the first and second invariants of the stress tensor and the deviator tensor, respectively.

The preconsolidation pressure p_{co} is the upper bound of the admissible current effective pressure σ' and turns out to be the maximum effective pressure to which the material has been subjected during the past plastic loadings.

4.1.1 Plastic potential

On the other hand, experimental results showed that the conventional critical state model, often overestimates the value of the volumetric compressibility coefficient K_0 therefore a non-associated potential function should be defined. To avoid overestimation of the volumetric compressibility coefficient K_0 by the conventional critical state model a non-associated flow rule was introduced by [7, 114, 75].

Thereby, the following plastic potential is proposed

$$g\left(\sigma, \tau, p, Q_\alpha\right) = \eta\left[\left(\sigma - \beta p\right)^2 - \left(\sigma - \beta p\right)Q_\alpha\right] + \left(\frac{\tau}{M}\right)^2 \tag{4.2}$$

η is a coefficient that limits the influence of the volumetric pressure during softening regime (see Fig. 4.2).

The gradients of the plastic potential in Eq. (4.2) are summarized in Appendix C.

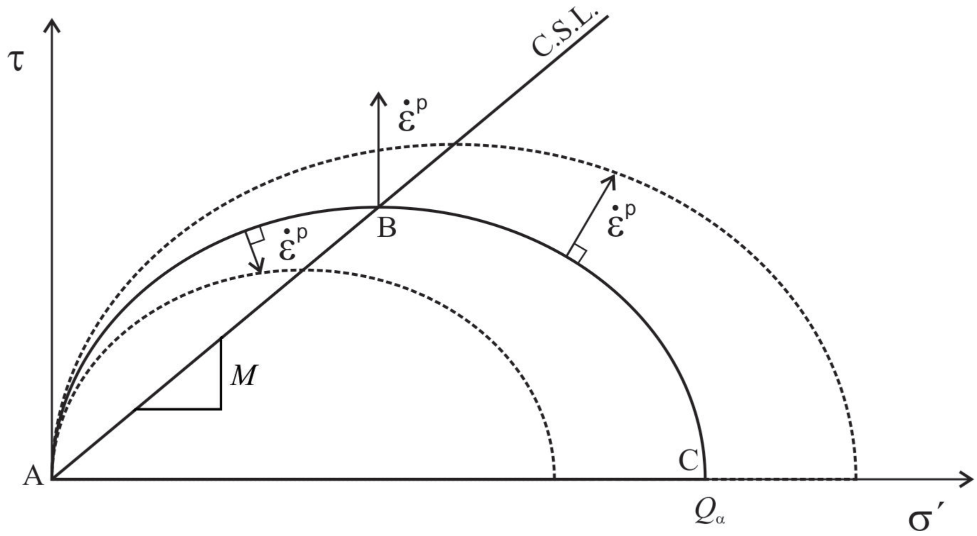

Figure 4.1: Modified CamClay plasticity model. The material exhibits plastic contraction for $\sigma' > Q_\alpha/2$ (surface BC) and plastic dilatancy for $\sigma' < Q_\alpha/2$ (surface AB), whereas for $\sigma' = Q_\alpha/2$ the plastic evolution occurs at constant volume and therefore the plastic flow occurs indefinitely at constant loading (ideal plastic material) so that the line is known as critical states (C.S.L.).

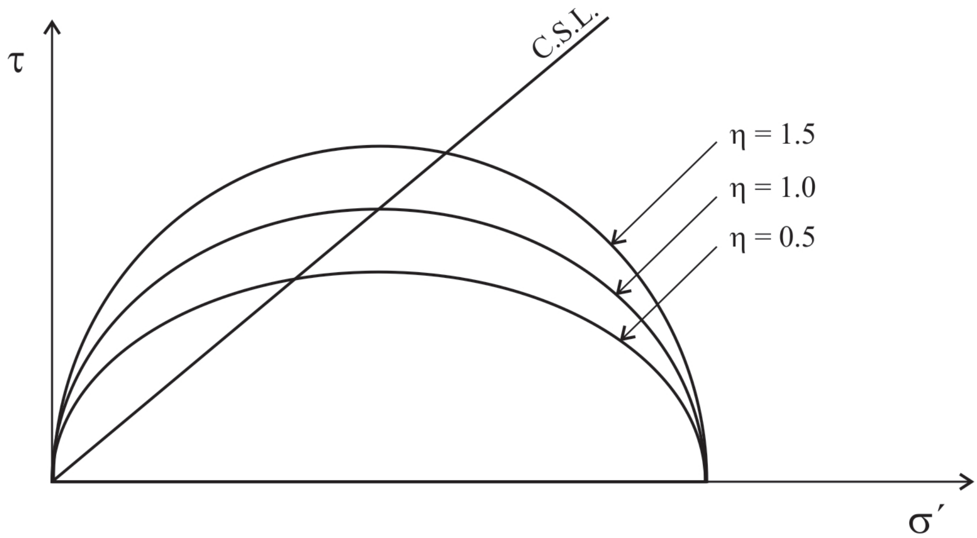

Figure 4.2: Modified Cam Clay plasticity model and plastic potential

4.1.2 Hardening law

The thermodynamic consistency is achieved by assuming the following expression for the dissipative part of the free energy in Eq. (3.13)

$$\Psi^p\left(\varepsilon^p, \varepsilon^p_{,i}\right) = \Psi^{p,loc}\left(\varepsilon^p\right) + \Psi^{p,nloc}\left(\varepsilon^p_{,i}\right) = -\frac{1}{\chi}p^0_{co}\exp\left(\chi\varepsilon^p\right) - \left(\frac{1}{2}l^2_\alpha H^{nloc}_{\alpha\,ij}\varepsilon^p_{,j}\right)_{,i} \tag{4.3}$$

where the coefficient χ is defined by

$$\chi = -\frac{\beta\left(1+e_0\right)}{\gamma-\kappa} \tag{4.4}$$

being β an adjustment coefficient (assumed $\beta = 1$ in this work), e_0 the initial void ratio, γ a hardening parameter and κ the swelling index (obtained from the odometry test).

The volumetric plastic strain of the continuous porous media, ε^p (see Eq. (2.108)), is expressed as a function of the state variables in order to describe the plastic evolutions of the porous and solid phases, in terms of the plastic porosity ϕ^p and the volumetric plastic strain of soil grain ε^p_s, respectively [18].

$$\varepsilon^p = \phi^p + \left(1-\phi_0\right)\varepsilon^p_s \tag{4.5}$$

From Eq. (3.11) and Eq. (3.12) the following expressions for local and non-local dissipative stresses are obtained

$$Q^{loc}_\alpha\left(\varepsilon^p\right) = -\frac{\partial\Psi_s}{\partial\varepsilon^p} = p^0_{co}\exp\left(\chi\left(\phi^p + \left(1-\phi_0\right)\varepsilon^p_s\right)\right) \tag{4.6}$$

$$Q^{nloc}_\alpha\left(\varepsilon^p_{,i}\right) = -\left(\frac{\partial\Psi_s}{\partial\varepsilon^p_{,i}}\right)_{,i} = l^2_s H^{nloc}_{s\,ij}\varepsilon^p_{s\,,ij} + l^2_p H^{nloc}_{p\,ij}\phi^p_{,ij} \tag{4.7}$$

where l_s and l_p are the internal characteristic lengths for solid skeleton and porous phase, respectively.

4.2 Parabolic Drucker-Prager plasticity model

The Drucker-Prager plasticity model has been used in several constitutive formulations of cohesive–frictional materials. The classic formulation of the Drucker-Prager criterion (1952) [29] is a simple modification of the von Mises criteria including an additional parameter as a function of the first invariant of the stress tensor. This simple material model allows to reproduce with sufficient precision the mechanical behavior of such materials which exhibit very different strength in tensile and compression.

The original version of the Drucker-Prager material model is expressed by the following yield function

$$f\left(I_1, J_2\right) = \sqrt{J_2} + \alpha I_1 - k \tag{4.8}$$

both parameter α and k are calibrated with the uniaxial stress strength in compression and tension, f_t and f_c, respectively. The coefficient α is called internal frictional coefficient, while k represents the strength under pure shear. Additionally, whether all principal stress are equal, i. e. $\sigma_1 = \sigma_2 = \sigma_3 = \sigma$ the mean strength is $\sigma = k/\alpha$. Thus, the coefficient k/α is known as cohesive pressure.

$$\alpha = \frac{f_c - f_t}{\sqrt{3}\,\left(f_c + f_t\right)} \quad ; \quad k = \frac{2 f_c f_t}{\sqrt{3}\,\left(f_c + f_t\right)} \tag{4.9}$$

When $f_t = f_c$, $\alpha = 0$, and Eq. (4.8) approaches the classical von Mises criterion. The yield function Eq. (4.8) represents a conical surface in the principal stress space while a lineal function in the invariant space

The main shortcoming of the linear Drucker-Prager formulation is the excessive plastic dilatancy. The parabolic version of the Drucker-Prager criterion leads to a more accurate predictions of the plastic dilatancy. For non-porous materials this criterion is expressed by (see Fig. 4.3)

$$f\left(I_1, J_2\right) = J_2 + \alpha I_1 - k \tag{4.10}$$

being the friction and cohesion parameters,

$$\alpha = \frac{f_c - f_t}{3} \quad ; \quad k = \frac{f_c f_t}{3} \tag{4.11}$$

Regarding to porous media, the parabolic Drucker-Prager material model is rewritten considering the pore pressure effect

$$f\left(\sigma, J_2, p, Q_\alpha\right) = J_2 + \alpha\left(\sigma - \beta p\right) - Q_\alpha \tag{4.12}$$

4.2.1 Plastic Potential

To improve the volumetric dilatancy predictions [127, 87] of concrete under low confinement levels, the further following non associated plastic potential is considered

$$g\left(\sigma, J_2, p, Q_\alpha\right) = J_2 + \eta\alpha\left(\sigma - \beta p\right) - Q_\alpha \tag{4.13}$$

The influence of the non-associative parameter η can be showed in Fig. 4.4.

The gradients of the plastic potential presented in Eq. (4.13) are summarized in Appendix C.

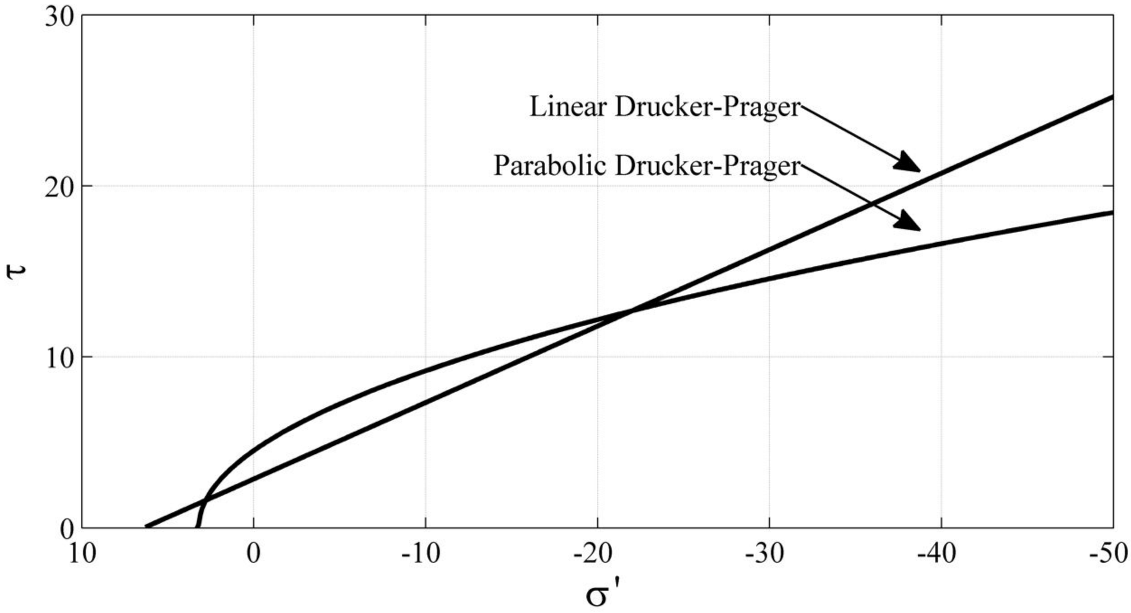

Figure 4.3: Linear and Parabolic Drucker-Prager strength criterion

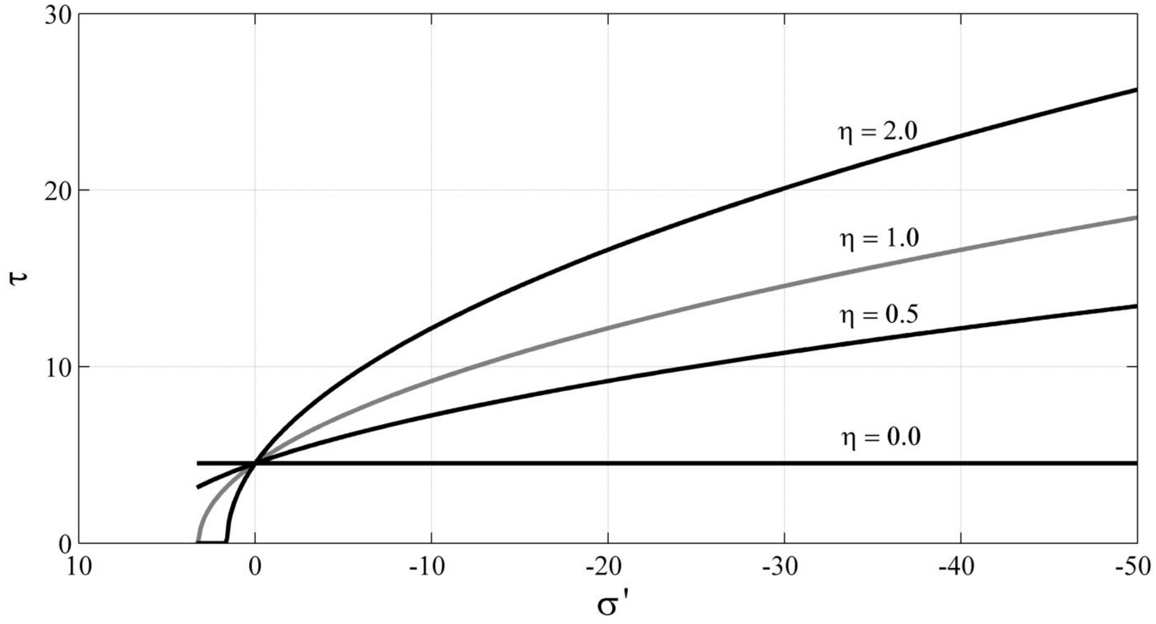

Figure 4.4: Parabolic Drucker-Prager strength criterion and Plastic Potential

4.3 Mathematical expressions of the internal lengths

In the present constitutive formulation the shear band width is controlled by both internal characteristic lengths, the one for the solid skeleton l_s and the other for the porous phase l_p.

In quasi-brittle porous materials like soils and concrete the strength degradation process in the post-peak regime may be controlled by two independent variables, the acting confining pressure during softening process and the pore water content. This dependence can be mathematically described through the expression defining the internal characteristic length.

From Vrech and Etse (2009) [130] the internal characteristic length for solid phase takes the following form (see Fig. 4.5)

$$l_s(\sigma') = \begin{cases} 0 & \text{for } \sigma' \leq 0 \\ \frac{l_{s,m}}{2}\left[1+\sin\left(\frac{\pi}{Q_\alpha/2}\sigma' - \frac{\pi}{2}\right)\right] & \text{for } 0 < \sigma' \leq Q_\alpha/2 \\ l_{s,m} & \text{for } \sigma' > Q_\alpha/2 \end{cases} \tag{4.14}$$

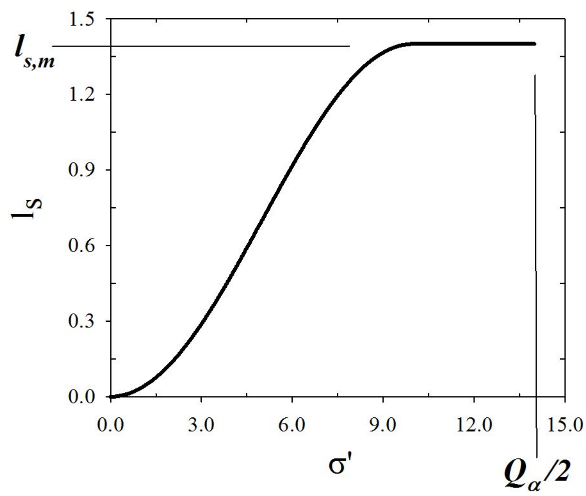

Figure 4.5: Internal characteristic length of solid phase vs. σ'

The internal characteristic length of the porous phase is governed by the saturation degree S_w or, indirectly by the acting pore pressure. As the soil specimen dries, l_p tends to zero, and brittle failure behavior is expected. On the other hand, when the water content increases, l_p tends to its maximum value $l_{p,m}$, and ductile failure response is expected.

The saturation degree of the porous medium can be associated with the pore pressure (or suction) by a logarithmic expression [41, 66] which depends on different experimental coefficients, i.e. the soil-water characteristic curve. Another option to describe the relationship between the saturation degree and the pore pressure is an hyperbolic function as proposed by Mroginski et al. (2010) [73]. This function can be easily inverted, also no further algorithm for the solution of the root is required. Then,

$$p = \frac{1}{2\,b}\ln\left(\frac{a+S_w}{a-S_w}\right) \tag{4.15}$$

being a and b two setting parameters. In Fig. 4.6a the Eq. (4.15) is plotted, being p_{100} the pore water pressure corresponding to a fully saturated specimen.

Thus, the following expression for the internal characteristic length of the porous phase is proposed

$$l_p\left(p\right) = \begin{cases} 0 & \text{for } p \leq 0 \\ a\,l_{p,m}\tanh\left(b\,l_p\right) & \text{for } 0 < p \leq p_{100} \end{cases} \tag{4.16}$$

In Fig. 4.6b the Eq. (4.16) is plotted

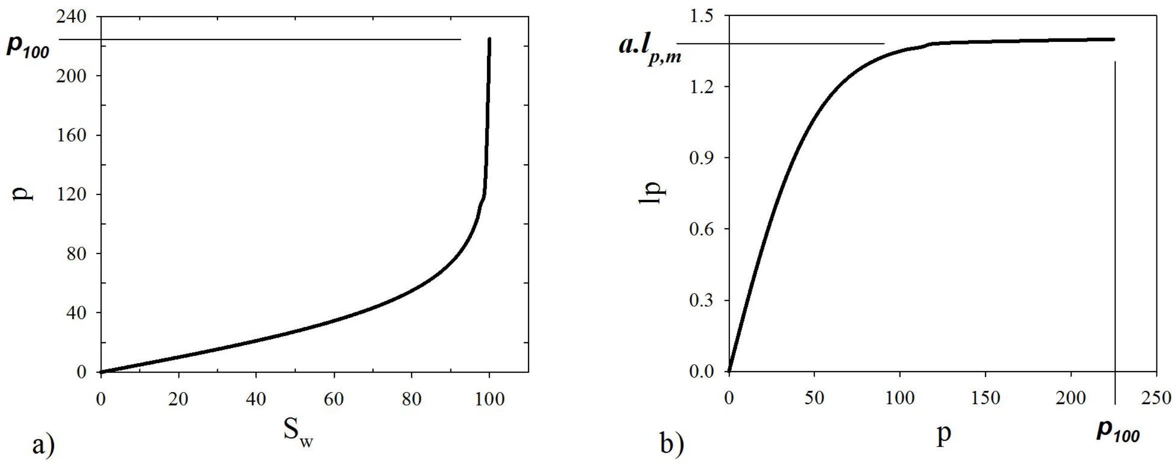

Figure 4.6: a) Saturation degree vs. Pore pressure; b) Internal characteristic length of porous phase vs. Pore pressure

CHAPTER 5

Instability analysis in the form of discontinuous bifurcation

In this Chapter the discontinuous bifurcation analysis for local and non-local porous media will be treated as well as the deduction of the critical hardening module considering both drained and undrained hydraulic boundary conditions.

5.1 Basics concepts about failure definition

The generalized failure in continuous media is usually preceded by local discontinuities or jumps signalized by the kinematic fields.

A large number of material failure studies have been developed in the framework of continuous mechanics [84, 40, 124, 56]. Thereby, the succession of events that begins at microscopic scale and cause the progressive deterioration of materials, which are usually modelled as continuous ones were clearly defined.

Considering an arbitrary domain Ω, the discontinuity S which divides the body domain in two sub domains Ω^+ and Ω^-, can be characterized by its normal unit vector $\boldsymbol{n}$ on point P (see Fig. 5.1).

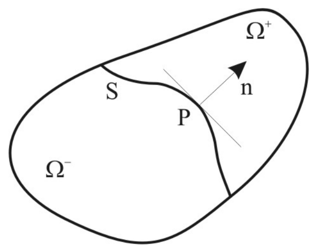

Figure 5.1: Discontinuity surface S

The aforementioned discontinuity should be analyzed from three different points of view. Therefore, the following failure shapes are defined

1. *Discrete failure*: this type of analysis lies beyond to the continuum mechanic and belongs to the fracture mechanic. The discontinuity is presented in the velocity field, i.e. $[[\dot{\boldsymbol{u}}]] \neq 0$

2. *Localized failure*: this failure mode is characterized by the continuity in the velocities, whereas its gradient exhibits the discontinuity, i.e. $[[\dot{\boldsymbol{u}}]] = 0$ and $[[\dot{\boldsymbol{\varepsilon}}]] \neq 0$

3. *Diffuse failure*: this behavior is generally presented in ductile materials. In this case both the velocity field and its gradient remains continuous, i.e. $[[\dot{\boldsymbol{u}}]] = 0$ and $[[\dot{\boldsymbol{\varepsilon}}]] = 0$.

In the previous definitions the operador $[[\bullet]]$ is the jump operator, defined by

$$[[\bullet]] = \bullet^{+} - \bullet^{-} \tag{5.1}$$

These concepts of the mechanics of continuum solids can be appropriately extrapolated to the mechanics of porous media considering that the medium is composed by a solid skeleton surrounded, in the general case, by several fluids phases. The influence of these fluid phases is taken into account by means of the pore pressure.

Thus, concerning to porous media the localization analysis may present two different approaches based on the assumed discontinuity hypothesis in the porous phase. The first one consists on attributing the whole localization phenomenon exclusively to the solid phase. In this approach the discontinuities are verified in the rate of deformation, remaining the fluids phases continuous. On the other hand, the second alternative assumes that the discontinuities occur in both the solid and fluid phases. Even though this phenomenon is unusual, some researchers state that both hypotheses have been observed in the nature of the cohesive-frictional soils and their validity depends on the hydraulic conditions and confinement level of the medium. Further, when drained boundary condition (the net pressure is dissipated) is observed the first hypothesis seems to be worth [14, 31]. On the other hand, according to the confinement level and the external actions, at the onset of localized failure in the solid skeleton an expansion of the porous medium may induce a jump or discontinuity in the fluid phase, and it would be valid the second hypothesis [105].

5.2 Discontinuous bifurcation analysis in local porous media

It has been widely accepted that when dissipative constitutive models of quasi-brittle and ductile materials are subjected to monotonic loading in the inelastic regime, they may exhibit spatial discontinuities of the kinematic fields [52, 101] depending on the particular boundary condition but also on the degree of non-associative, water content, inhomogeneities, etc. The occurence of cracks and shear bands experimentally observed in cementitious and granular materials as well as in metals are related to the so-called localized failure mode.

In case of non-porous constitutive theories, different authors performed numerical and theoretical analyses to obtain model predictions of localized failure modes in the form of discontinuous bifurcation, see a.o. [39, 84, 16, 40, 124, 56].

In case of porous media, localization analysis should not be restricted to the consideration of discontinuities taking place only in the solid phase, see [12, 14, 105]. Contrarily, discontinuities may develop in all different phases during monotonic loading and/or changes in the humidity conditions of porous media. From the mathematic stand point this assumption means that both the field of velocity gradients and the rate of fluid mass content are discontinuous and their jumps are defined as

$$[[\dot{\varepsilon}_{ij}]] = 1/2\,(g_i n_j + n_i g_j) \tag{5.2}$$

$$[[\dot{m}]] = -\,[[M_{i,i}]] = -n_i g_i^{\mathrm{M}} \tag{5.3}$$

Applying Hadamard relation [47, 18] to the tensors of zero and second order, p and σ_{ij}, respectively, the following balance equations are obtained (see Appendix D for details)

$$\mathrm{c}\,[[p_{,i}]] + [[\dot{p}]]\,n_i = 0 \tag{5.4}$$

$$\mathrm{c}\,[[\sigma_{ij,j}]] + [[\dot{\sigma}_{ij}]]\,n_j = 0 \tag{5.5}$$

Drained state

In drained state the instability analysis is restricted to the solid skeleton. The fluid flow in deformable porous media is governed by the Darcy's law. Thus, neglecting inertial forces, the relative flow vector of fluid mass M_i is then expressed as

$$M_i = -\rho^f k_{ij} p_{,j} \tag{5.6}$$

where k_{ij} is the permeability tensor of porous media. During quasi-static loading the fluid subjected to strong pressure gradients may exhibit a spontaneous diffusion process, with very fast pressure degradation. Thereby, the relative flow vector of fluid mass should remain continuous. Then, from Eq. (5.6) follows

$$[[M_i]] = -\rho^f k_{ij}\,[[p_{,j}]] = 0 \tag{5.7}$$

The last expression leads to the conclusion that pore pressure gradient does not present discontinuities $[[p_{,i}]] = 0$. Thus, Eq. (5.4) can only be fulfilled if the rate of pore pressure remains continuous, i.e. $[[\dot{p}]] = 0$.

Considering the momentum balance equation for quasi-static problems, applying the jump operator to the incremental constitutive equation, Eq. (3.45), and substituting the resulting expression into Eq. (5.5), we obtain

$$[[\dot{\sigma}_{ij}]]\,n_j = E^{ep,sd}_{ijkl}\,[[\dot{\varepsilon}_{kl}]]\,n_j = 0 \tag{5.8}$$

being $E_{ijkl}^{ep,sd}$ the solid skeleton elastoplastic tensor, as described in Section 3.1.4. Introducing Eq. (5.2) in Eq. (5.8) results

$$[[\dot{\sigma}_{ij}]]\, n_j = A_{ij}^{d,loc} g_j = 0 \tag{5.9}$$

where the elastoplastic acoustic tensor for local plasticity in porous media under drained condition is decomposed in its elastic, $A_{ij}^{d,e,s}$, and elastoplastic parts, $A_{ij}^{d,ep,s}$, as

$$A_{ij}^{d,loc} = E_{ijkl}^{ep,sd} n_l n_k = A_{ij}^{d,e,s} - A_{ij}^{d,ep,s} \tag{5.10}$$

being

$$\begin{aligned} A_{ij}^{d,e,s} &= C_{ijkl}^{s} n_l n_k \\ A_{ij}^{d,ep,s} &= \frac{C_{ijmn}^{s} g_{mn}^{s} f_{pq}^{s} C_{pqkl}^{s}}{h} n_l n_k \end{aligned} \tag{5.11}$$

From now on the following brief notation is considered for partial derivatives:

$$\begin{aligned} f_{ij}^{s} &= \partial f/\partial \sigma_{ij} \quad ; f^{p} = \partial f/\partial p \quad ; f_{\alpha}^{Q} = \partial f/\partial Q_{\alpha} \\ g_{ij}^{s} &= \partial g/\partial \sigma_{ij} \quad ; g^{p} = \partial g/\partial p \quad ; g_{\alpha}^{Q} = \partial g/\partial Q_{\alpha} \end{aligned} \tag{5.12}$$

The non-trivial solutions of Eq. (5.9) could be obtained by the spectral analysis of the local acoustic tensor $A_{ij}^{d,loc}$. Then, the localization condition of drained porous media is achieved as

$$\det\left(A_{ij}^{d,loc}\right) = 0 \tag{5.13}$$

From this assumptions, porous effects can be neglected when drained conditions are presented in the porous media. Then, the discontinuity regarding to the above bifurcation condition is related only to the strain velocity field. Consequently, the localization tensor in fully drained condition has the same form as in classical elastoplastic continua. However, since the localization condition in Eq. (5.13) involves only the drained poroelastic properties, the fluid pressure is concerned in the localization phenomenon through its influence on the current values of both the loading function f and the generalized plastic modulus h.

Undrained state

In undrained state the variation of fluid mass content in the solid skeleton vanishes, $\dot{m} = 0$. The pore pressure can be obtained from the solid phase kinematics, $g_i \equiv g_i^{\mathrm{M}}$.

Applying the jump operator to Eq. (3.46) and Eq. (5.2),

$$[[\dot{\sigma}_{ij}]]\, n_j = A_{ij}^{u,loc} g_j = 0 \tag{5.14}$$

where, in the same way as in the previous Section, the elastoplastic acoustic tensor for local plasticity under undrained condition can be decomposed in its elastic and plastic parts referred to both the solid phase, $A_{ij}^{u,e,s}$ and $A_{ij}^{u,ep,s}$, and the porous phase, $A_{ij}^{u,e,p}$ and $A_{ij}^{u,ep,p}$, as well as a coupled elastoplastic acoustic tensor for solid and porous phases ,$A_{ij}^{u,ep,sp}$, as

$$A_{ij}^{u,loc} = E_{ijkl}^{ep,su} n_l n_k = A_{ij}^{u,e,s} + A_{ij}^{u,e,p} - A_{ij}^{u,ep,s} - A_{ij}^{u,ep,p} + A_{ij}^{u,ep,sp} \tag{5.15}$$

being

$$\begin{aligned}
A_{ij}^{u,e,s} &= A_{ij}^{d,e,s} = C_{ijkl}^{s} n_l n_k \\
A_{ij}^{u,e,p} &= \mathrm{M} B_{ij} B_{kl} n_l n_k \\
A_{ij}^{u,ep,s} &= \frac{C_{ijmn} g_{mn}^{s} f_{pq}^{s} C_{pqkl}}{h} n_l n_k \\
A_{ij}^{u,ep,p} &= \mathrm{M}^2 \frac{g^p B_{ij} B_{kl} f^p}{h} n_l n_k \\
A_{ij}^{u,ep,sp} &= \mathrm{M} \left(\frac{C_{ijmn} g_{mn}^{s} B_{kl} f^p}{h} + \frac{g^p B_{ij} C_{klmn} f_{mn}^{s}}{h} \right) n_l n_k
\end{aligned} \tag{5.16}$$

The localization condition follows from the spectral properties analysis of the acoustic tensor

$$\det \left(A_{ij}^{u,loc} \right) = 0 \tag{5.17}$$

From the comparison between Eq. (5.13) and Eq. (5.17) it can be concluded that the hydraulic border conditions appreciably affect the localization condition by the solid-fluid coupling matrix.

5.3 Bifurcation analysis in non-local gradient-based porous media

In the previous Section the discontinuous bifurcation problem of local porous medium has been studied. The aforementioned analysis is hold in case of brittle failure modes. This is the case of some cementitious sandy soils cemented with iron oxide (so-called Sandstone) as well as concrete in tensile or uniaxial compression states. In these situations strain localization is generated in a region of null thickness $l_\alpha = 0$.

In case of quasi-brittle and, moreover, ductile failure modes, shear bands or microcracking zones of non-zero thicknesses develop during failure processes. This is typically the case of cementitious and granular materials under triaxial compression with medium or high confinements, and of metals. The size of finite localization zones that develop during failure processes of quasi-brittle and ductile materials can be defined by the so-called characteristic length $l_\alpha \neq 0$ [84, 124, 127].

In the following the conditions for the occurrence of localized failure modes in the form of discontinuous bifurcation in non-local gradient elastoplastic porous media are analyzed. It is assumed homogeneous fields of stress and strain rates just before the onset of localization. Contrarily to the case of local poroplastic media discussed in Chapter 2, the plastic consistency, see Eq. (3.42), is now a function of both the plastic multiplier $\dot{\lambda}$, and its second gradient $\dot{\lambda}_{,ij}$.

The jump operator of the current stress on the discontinuity surface should satisfy the equilibrium equation

$$\dot{\sigma}_{ij,j} = 0 \tag{5.18}$$

where the incremental stress tensor is defined by Eq. (3.17) or Eq. (3.19), depending on the assumed hydraulic border conditions.

Eventual instabilities of equilibrium states are evaluated through the condition for the loss of ellipticity of the differential equations of equilibrium. This condition is commonly investigated by a wave propagation analysis [1, 120, 12, 67, 117]. Thus, considering a homogeneous state before the onset of localization the following harmonic perturbation with respect to the incremental field variables, i.e. displacements, mass content and plastic multiplier, for an infinite porous medium is assumed, which corresponds to the assumption of stationary planar waves

Following [117, 1] the solutions of the field variables, i.e. displacements, mass content and plastic multiplier, are expressed in terms of plane wave

$$\begin{bmatrix} \dot{u}\left(\boldsymbol{x},t\right) \\ \dot{\gamma}\left(\boldsymbol{x},t\right) \\ \dot{\lambda}\left(\boldsymbol{x},t\right) \end{bmatrix} = \begin{bmatrix} \dot{\mathcal{U}}\left(t\right) \\ \dot{\mathcal{M}}\left(t\right) \\ \dot{\mathcal{L}}\left(t\right) \end{bmatrix} \exp\left(\frac{i2\pi}{\delta}\boldsymbol{n}\cdot\boldsymbol{x}\right) \tag{5.19}$$

being $\dot{\gamma}$ the mass content, $\boldsymbol{x}$ the position vector (in Cartesian coordinates), $\boldsymbol{n}$ the wave normal direction and δ the wave length. Moreover $\dot{\mathcal{U}}$, $\dot{\mathcal{M}}$ and $\dot{\mathcal{L}}$ are spatially homogeneous amplitudes of the wave solutions.

Replacing Eqs. (5.19) in Eqs. (3.42), (5.18) and, (3.17) or (3.19) (depending on the assumed hydraulic conditions), representing the differential expression of plastic consistency, the equilibrium condition, and the incremental constitutive relations, respectively, follows that the equilibrium condition on the discontinuity surface is fulfilled if

$$\left(\frac{2\pi}{\delta}\right)^2 \left\{C^s_{ijkl} - \frac{C^s_{ijmn} g^s_{mn} f^s_{pq} C^s_{pqkl}}{h + \bar{h}^{nloc}}\right\} n_l n_k \, \dot{\mathcal{U}} = 0 \tag{5.20}$$

in case of drained conditions, and if

$$\left(\frac{2\pi}{\delta}\right)^2 \left\{C_{ijkl} - \frac{C_{ijmn} g^s_{mn} f^s_{pq} C_{pqkl}}{h + \bar{h}^{nloc}} - \mathrm{M}^2 \frac{g^p B_{ij} B_{kl} f^p}{h + \bar{h}^{nloc}} + \right.$$

$$\mathrm{M}\left(\frac{C_{ijmn}g^s_{mn}B_{kl}f^p}{h+\bar{h}^{nloc}}+\frac{g^pB_{ij}C_{mnkl}f^s_{mn}}{h+\bar{h}^{nloc}}\right)\Bigg\}\, n_l n_k\,\dot{\mathcal{U}}=0 \quad (5.21)$$

in the undrained case. Being $\bar{h}^{nloc}$ the generalized gradient modulus as

$$\bar{h}^{nloc}=l^2_\alpha\left(f^Q_\alpha g^Q_\alpha H^{nloc}_{\alpha\, ij}\right)n_j n_i\left(\frac{2\pi}{\delta}\right)^2 \tag{5.22}$$

The expressions between brackets on Eq. (5.20) and Eq. (5.21) correspond to the non local acoustic tensor for porous media under drained and undrained conditions $A^{d,nloc}_{ij}$ and $A^{u,nloc}_{ij}$, respectively,

$$A^{d,nloc}_{ij}=A^{d,e,s}_{ij}-A^{d,nl,s}_{ij} \tag{5.23}$$
$$A^{u,nloc}_{ij}=A^{u,e,s}_{ij}+A^{u,e,p}_{ij}-A^{u,nl,s}_{ij}-A^{u,nl,p}_{ij}+A^{u,nl,sp}_{ij} \tag{5.24}$$

where the submatrix of $A^{d,nloc}_{ij}$ and $A^{u,nloc}_{ij}$ are obtained by inspection

$$\begin{aligned}
A^{d,nl,s}_{ij}&=\frac{C^s_{ijmn}g^s_{mn}f^s_{pq}C^s_{pqkl}}{h+\bar{h}^{nloc}}\\
A^{u,nl,s}_{ij}&=\frac{C_{ijmn}g^s_{mn}f^s_{pq}C_{pqkl}}{h+\bar{h}^{nloc}}\\
A^{u,nl,p}_{ij}&=\mathrm{M}^2\frac{g^pB_{ij}B_{kl}f^p}{h+\bar{h}^{nloc}}\\
A^{u,nl,sp}_{ij}&=\mathrm{M}\left(\frac{C_{ijmn}g^s_{mn}B_{kl}f^p}{h+\bar{h}^{nloc}}+\frac{g^pB_{ij}C_{mnkl}f^s_{mn}}{h+\bar{h}^{nloc}}\right)
\end{aligned} \tag{5.25}$$

From the comparison between the bifurcation analysis carried out for local, and non local porous media, Eqs. (5.13), (5.15) and Eqs. (5.23) ,(5.24), respectively, follows that the difference between both lies only in the generalized (non-local) gradient modulus $\bar{h}^{nloc}$. Precisely the effect of $\bar{h}^{nloc}$ at the finite-element level is the regularization of the post-peak regime.

5.4 Spectral analysis for discontinuous bifurcation condition

Since the existence of discontinuous bifurcation requires the singularity of the acoustic tensor deduced above, the eigenvalue problem should be studied [83, 102]. In this work the eigenvalue analysis is restricted to the undrained acoustic tensor for gradient poroplasticity given that when the Biot modulus M tends to zero it can be easily shown that the tensor $A^{u,nloc}_{ij}$ tends to $A^{d,nloc}_{ij}$. Therefore, the critical hardening/softening module, H^{crit}, for undrained condition tends to the drained one, as well.

The classical eigenvalue problem may be written as

$$\left(Q_{ij} - \delta_{ij}\lambda^{(i)}\right) y^{(i)} = 0 \tag{5.26}$$

being $\lambda^{(i)}$ and $y^{(i)}$ the eigenvalues and eigenvectors, respectively, and Q_{ij}:

$$Q_{ij} = \delta_{ij} - \frac{1}{h + \bar{h}^{nloc}} \left(P^e_{ik} b^s_k a^s_j + \mathrm{M}^2 P^e_{ik} b^p_k a^p_j - \mathrm{M} P^e_{ik} \left(b^s_k a^p_j + b^p_k a^s_j\right)\right) \tag{5.27}$$

with

$$\begin{aligned}
b^s_j &= n_i C_{ijkl} g^s_{kl} \\
a^s_k &= f^s_{ij} C_{ijkl} n_l \\
b^p_j &= n_i B_{ij} g^p \\
a^p_j &= f^p B_{kl} n_l \\
P^e_{ik} &= \left(A^{u,e,s}_{ij} + A^{u,e,p}_{ij}\right)^{-1}
\end{aligned} \tag{5.28}$$

The matrix $P^e_{ik} b_k a_j$ can always be written as $p_i a_j$, where $p_i = P^e_{ik} b_k$. Therefore two rows of the matrix $P^e_{ik} b_k a_j$ will be proportional to the remaining one and the actual rank of Q_{ij} is one. Then, $\lambda^{(1)} = \lambda^{(2)} = 1$, and the remaining eigenvalue could be obtained considering the following property

$$Q_{jj} = \lambda^{(1)} + \lambda^{(2)} + \lambda^{(3)} = 2 + \lambda^{(3)} \tag{5.29}$$

and,

$$\lambda^{(3)} = 1 - \frac{1}{h + \bar{h}^{nloc}} \left(P^e_{ik} b^s_k a^s_j + \mathrm{M}^2 P^e_{ik} b^p_k a^p_j - \mathrm{M} P^e_{ik} \left(b^s_k a^p_j + b^p_k a^s_j\right)\right) \tag{5.30}$$

From this spectral analysis it can be seen that there exists only one possibility for a nontrivial solution of Eq. (5.26), i. e. $\lambda^{(3)} = 0$. From Eq. (5.28) and Eq. (5.30) the corresponding expression for the hardening modulus is obtained

$$\begin{aligned}
\bar{H} = P^e_{ik} b^s_k a^s_j + \mathrm{M}^2 P^e_{ik} b^p_k a^p_j - \mathrm{M} P^e_{ik} \left(b^s_k a^p_j + b^p_k a^s_j\right) \\
- f^s_{ij} C_{ijkl} g^s_{kl} + \mathrm{M}\left(f^s_{ij} B_{ij} g^p + f^p B_{ij} g^s_{ij} - f^p g^p\right) - \bar{h}^{nloc}
\end{aligned} \tag{5.31}$$

Assuming the isotropy of the elastic stiffness tensor of the solid phase C^s_{ijkl}, and considering $C_{ijkl} = C^s_{ijkl} + \mathrm{M} B_{ij} B_{kl}$, the following elastic stiffness tensor for poroelastic continuous media is obtained

$$C_{ijkl} = G\left(\delta_{ik}\delta_{jl} + \delta_{il}\delta_{jk}\right) + \omega \delta_{ij}\delta_{kl} \tag{5.32}$$

where G is the shear modulus, ν the Poisson ratio and $\omega = 2G\nu/(1-2\nu) + \mathrm{M}b^2$. The elastic acoustic tensor for gradient poroplasticity $A_{ij}^{u,e} = A_{ij}^{u,e,s} + A_{ij}^{u,e,p}$ defined in Eq. (5.23) and its inverse P_{ij}^{e} become

$$A_{ij}^{u,e} = G\left(\gamma n_i n_j + \delta_{ij}\right) \qquad ; \qquad P_{ij}^{e} = \frac{1}{G}\left(-\phi n_i n_j + \delta_{ij}\right) \tag{5.33}$$

being $\phi = \left[G + \mathrm{M}b^2\left(1-2\nu\right)\right]\left[2G\left(1-\nu\right) + \mathrm{M}b^2\left(1-2\nu\right)\right]^{-1}$ and $\gamma = 1/(1-2\nu) + \mathrm{M}b^2/G$. With these expressions the hardening modulus given by Eq. (5.31) take the following form

$$\begin{aligned}\bar{H} = {} & 4G\phi n_i f_{ij}^{s} n_j n_k g_{kl}^{s} n_l + f_{ii}^{s} g_{ii}^{s}\left[\frac{\omega^2}{G}\left(1-\phi\right) - \omega\right] + 4G n_i f_{ij}^{s} g_{jk}^{s} n_k \\ & - 2G f_{ij}^{s} g_{ij}^{s} + 2\omega\left(1-\phi\right) n_i \left(g_{kk}^{s} f_{ij}^{s} + f_{kk}^{s} g_{ij}^{s}\right) n_j - 2\mathrm{M}b\left(1-\phi\right) n_i\left(g^p f_{ij}^{s} + f^p g_{ij}^{s}\right) n_j \\ & + \left(g^p f_{ii}^{s} + f^p g_{ii}^{s}\right)\left[\mathrm{M}b - \frac{\mathrm{M}b\omega}{G}\left(1-\phi\right)\right] + f^p g^p \left[\frac{\mathrm{M}^2 b^2}{G}\left(1-\phi\right) - \mathrm{M}\right] - \bar{h}^{nloc}\end{aligned} \tag{5.34}$$

A more convenient expression could be obtained considering the decomposition of f_{ij}^{s} and g_{ij}^{s} into their deviatoric and volumetric parts.

$$\bar{f}_{ij}^{s} = f_{ij}^{s} - \frac{1}{3}\delta_{ij} f^{s} \qquad ; \qquad \bar{g}_{ij}^{s} = g_{ij}^{s} - \frac{1}{3}\delta_{ij} g^{s} \tag{5.35}$$

where $\bar{f}_{ij}^{s}$ and f^s denote the deviatoric and volumetric parts of f_{ij}^{s}, as well as $\bar{g}_{ij}^{s}$ and g^s denote the deviatoric and volumetric parts of g_{ij}^{s}, respectively.

With this notation the hardening module of Eq. (5.34) can be rewritten as

$$\begin{aligned}\frac{\bar{H}}{4G} = {} & -\frac{1}{2}\bar{f}_{ij}^{s}\bar{g}_{ij}^{s} - \alpha_0 n_i \bar{f}_{ij}^{s} n_j n_k \bar{g}_{kl}^{s} n_l + \alpha_1 f^s g^s + n_i\left(\alpha_2 g^s \bar{f}_{ij}^{s} + \alpha_2 f^s \bar{g}_{ij}^{s} + \bar{g}_{ij}^{s}\bar{f}_{ij}^{s}\right) n_j \\ & + \alpha_3 n_i\left(g^p \bar{f}_{ij}^{s} + f^p \bar{g}_{ij}^{s}\right) n_j + \alpha_4\left(f^p g^s + g^p f^s\right) + \alpha_5 f^p g^p - \frac{\bar{h}^{nloc}}{4G}\end{aligned} \tag{5.36}$$

being

$$\begin{aligned}\alpha_0 &= \phi \\ \alpha_1 &= \frac{\omega\left(1-\phi\right)}{G}\left(\frac{1}{3} + \frac{\omega}{4G}\right) - \left(\frac{\omega}{4G} + \frac{\phi}{9} + \frac{1}{18}\right) \\ \alpha_2 &= \frac{1-\phi}{3} + \frac{\omega\left(1-\phi\right)}{2G} \\ \alpha_3 &= \frac{\mathrm{M}b\left(1-\phi\right)}{2G} \\ \alpha_4 &= \frac{\mathrm{M}b}{4G}\left[1 - \left(1-\phi\right)\frac{\omega}{G}\right] - \frac{\mathrm{M}b\left(1-\phi\right)}{6G} \\ \alpha_5 &= \left(1-\phi\right)\left(\frac{\mathrm{M}b}{2G}\right)^2 - \frac{\mathrm{M}}{4G}\end{aligned} \tag{5.37}$$

In order to obtain the analytical solution, we should only consider the particular case of identical principal directions for f^s_{ij} and g^s_{ij}

$$\bar{f}^s_{ij} = \begin{bmatrix} \bar{f}^s_1 & 0 & 0 \\ 0 & \bar{f}^s_2 & 0 \\ 0 & 0 & \bar{f}^s_3 \end{bmatrix} \qquad ; \qquad \bar{g}^s_{ij} = \begin{bmatrix} \bar{g}^s_1 & 0 & 0 \\ 0 & \bar{g}^s_2 & 0 \\ 0 & 0 & \bar{g}^s_3 \end{bmatrix} \tag{5.38}$$

where $\bar{f}^s_1, \bar{f}^s_2, \bar{f}^s_3$ and $\bar{g}^s_1, \bar{g}^s_2, \bar{g}^s_3$ denote the corresponding principal values according to $\bar{f}^s_1 \geq \bar{f}^s_2 \geq \bar{f}^s_3$.

On the other hand, for cohesive-frictional material like soils, a non-associative flow rule for volumetric strain may be consider, whereas the deviatoric parts remains associative, i. e. $\bar{f}^s_i = \bar{g}^s_i$ and $f^s \neq g^s$.

With these assumptions Eq. (5.36) becomes

$$\frac{\bar{H}}{4G} = -\alpha_0 \left(\bar{f}^s_i n^2_i\right)^2 + \left(r\bar{f}^s_i + \left(\bar{f}^s_i\right)^2\right) n^2_i + \alpha_4 \left(f^p g^s + g^p f^s\right) + k - \frac{\bar{h}^{nloc}}{4G} \tag{5.39}$$

being $r = \alpha_2 \left(f^s + g^s\right) - \alpha_3 \left(f^p + g^p\right)$ and $k = -\frac{1}{2}\left(\bar{f}^s_i\right)^2 + \alpha_1 f^s g^s + \alpha_5 f^p g^p$.

Using the Lagrange multiplier method the extreme properties of $\bar{H}$ can be studied

$$\ell = \frac{\bar{H}}{4G} - \lambda \left(n^2_1 + n^2_2 + n^2_3 - 1\right) \tag{5.40}$$

where λ is the Lagrangian multiplier. It appears that the hardening modulus and its critical directions is highly dependent of two coefficients, r and c_{13} or c_{31}.

$$c_{13} = \bar{f}^s_1 + (1 - 2\alpha_0)\, \bar{f}^s_3 + r \qquad ; \qquad c_{31} = \bar{f}^s_3 + (1 - 2\alpha_0)\, \bar{f}^s_1 + r \tag{5.41}$$

Then, the critical hardening modulus can be obtained by

$$r \leq 0 \begin{cases} \bar{H} = \frac{G}{\alpha_0}\left(\bar{f}^s_1 + \bar{f}^s_3 + r\right)^2 - \bar{f}^s_1 \bar{f}^s_3 + c & ;\text{for } c_{13} \geq 0 \\ \bar{H} = 4G\,(1 - \alpha_0)\, \bar{f}^{s2}_3 + r\bar{f}^s_3 + c & ;\text{for } c_{13} \leq 0 \end{cases} \tag{5.42}$$

$$r \geq 0 \begin{cases} \bar{H} = \frac{G}{\alpha_0}\left(\bar{f}^s_1 + \bar{f}^s_3 + r\right)^2 - \bar{f}^s_1 \bar{f}^s_3 + c & ;\text{for } c_{31} \leq 0 \\ \bar{H} = 4G\,(1 - \alpha_0)\, \bar{f}^{s2}_1 + r\bar{f}^s_1 + c & ;\text{for } c_{31} \geq 0 \end{cases} \tag{5.43}$$

with $c = \alpha_4 \left(f^p g^s + f^s g^p\right) + k - \bar{h}^{nloc}/4G$

On the other hand, the critical directions obtained by this analysis are summarized in Table 5.1, considering two different cases: $r \geq 0$ and $r \leq 0$, being $\rho = 2\alpha_0\left(\bar{f}^s_1 - \bar{f}^s_3\right)$

Finally, a special case is presented when $\bar{f}^s_1 = \bar{f}^s_2 = \bar{f}^s_3 = 0$. In this trivial situation the hardening modulus remains constant.

$$\bar{H} = 4Gc \tag{5.44}$$

	$r \leq 0$		$r \geq 0$	
	$c_{13} \geq 0$	$c_{13} < 0$	$c_{31} \leq 0$	$c_{31} > 0$
$\bar{f}_1^s > \bar{f}_2^s > \bar{f}_3^s$	$n_1^2 = c_{13}/\rho$ $n_2^2 = 0$ $n_3^2 = -c_{31}/\rho$	$n_1^2 = 0$ $n_2^2 = 0$ $n_3^2 = 1$	$n_1^2 = c_{31}/\rho$ $n_2^2 = 0$ $n_3^2 = -c_{31}/\rho$	$n_1^2 = 1$ $n_2^2 = 0$ $n_3^2 = 0$
$\bar{f}_1^s = \bar{f}_2^s > \bar{f}_3^s$	$n_1^2 + n_2^2 = c_{13}/\rho$ $n_3^2 = -c_{31}/\rho$	$n_1^2 = n_2^2 = 0$ $n_3^2 = 1$	$n_1^2 + n_2^2 = c_{13}/\rho$ $n_3^2 = -c_{31}/\rho$	$n_1^2 + n_2^2 = 1$ $n_3^2 = 0$
$\bar{f}_1^s > \bar{f}_2^s = \bar{f}_3^s$	$n_1^2 = c_{13}/\rho$ $n_2^2 + n_3^2 = -c_{31}/\rho$	$n_1^2 = 0$ $n_2^2 + n_3^2 = 1$	$n_1^2 = c_{13}/\rho$ $n_2^2 + n_3^2 = -c_{31}/\rho$	$n_1^2 = 1$ $n_2^2 = n_3^2 = 0$

Table 5.1: Critical directions for $\bar{H}$

5.5 Analytical localization analysis

In this Section the spectral properties of the acoustic localization tensors for gradient plasticity discussed above are evaluated for several numerical examples considering drained and undrained hydraulic boundary conditions.

Plane strain condition is assumed. The stress state domain is included in Appendix E Two types of material models are considered. On the one hand, the modified Cam Clay criterion for saturated porous media [14] based on non-associated flow rule. On the other hand, the Parabolic Drucker-Prager for young concretes considered as partially saturated porous media (see Chapter 4).

5.5.1 Analytical prediction of critical hardening module for Cam Clay plasticity model

In this Section the spectral analysis of the localization tensor in Section 5.4 will be applied for the modified Cam Clay plasticity model described in Chapter 4 under consideration of both drained and undrained hydraulic conditions.

The material properties considered in the following examples are summarized in Table 5.2. Three different equilibrium stress states on the yield surface are considered, see Fig. 5.2.

The evolution of the hardening module for each bifurcation angle as well as the critical hardening module predicted in Section 5.4, are plotted in Fig. 5.3 and Fig. 5.4 for drained and undrained hydraulic conditions, respectively.

5.5.2 Discontinuous bifurcation analysis and transition point for Cam Clay model

In this Section several numerical results with two main purposes the spectral properties study of the localization tensors are presented, and the identification of the transition point between ductile and brittle failure shapes.

Material parameters	Value
CSL slope, M	0.856
Preconsolidation pressure, p_{co}	100.00 Mpa
Initial pore pressure, p	10.00 Mpa
Initial porosity, ϕ_0	0.4
Bulk compressibility coefficient, K_0	1000.00
Solid compressibility coefficient, K_s	1500.00
Fluid compressibility coefficient, K_{fl}	500.00
Biot coefficient, $b = 1 - K_0/K_s$	0.33
Biot module inverse, $M1 = M^{-1} = (b - \phi_0)/K_s + \phi_0/K_f$	$3.56 * 10^{-4}$
Young module, E	20000.0 MPa
Poisson ratio, ν	0.2
Local hardening/softening module, $H_s^{loc} = H_p^{loc}$	$-0.1 * E$
Non-associativity coefficient, η	0.25

Table 5.2: Material parameters for Cam Clay material model

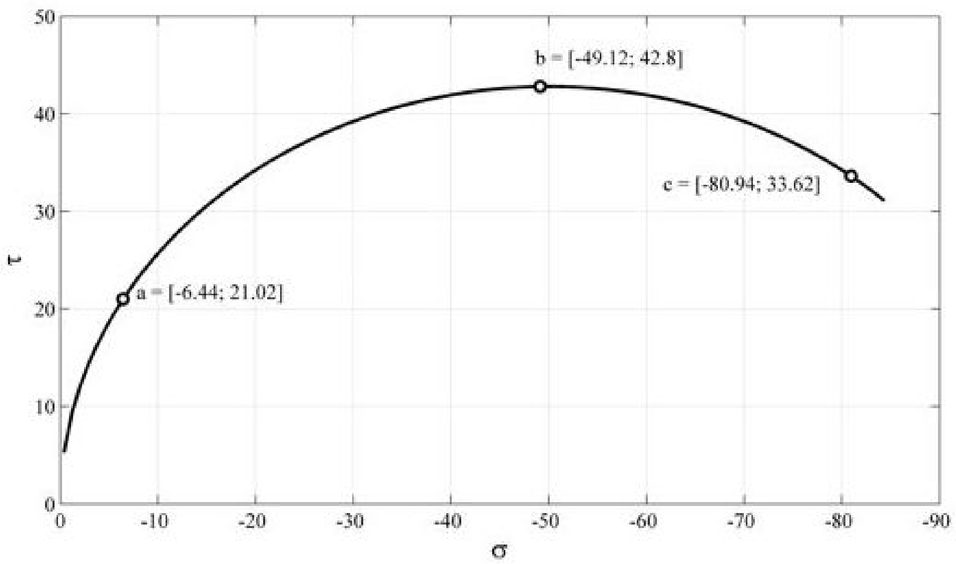

Figure 5.2: Stress states on Cam Clay yield surface

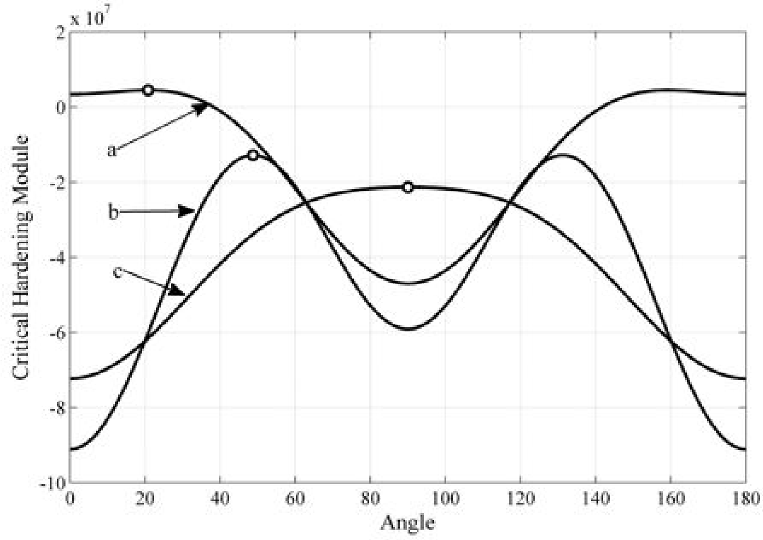

Figure 5.3: Critical hardening module of the Cam Clay model considering drained condition for stress states a, b and c

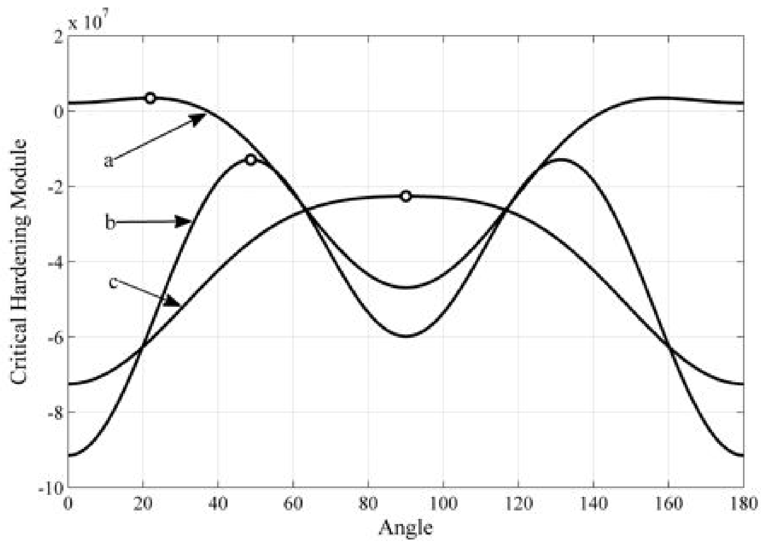

Figure 5.4: Critical hardening module of the Cam Clay model considering undrained condition for stress states a, b and c

On the other hand, the study of the critical hardening module in the principal stresses space allows to establish whether the discontinuous bifurcation condition can be fulfilled in hardening regime.

Furthermore, the influence of the pore water pressure and of the volumetric non-associativity of the proposed material model on the discontinuous bifurcation condition are analyzed in the spaces (σ',det(A),p) and (σ',det(A),η), respectively.

In first place, the critical hardening module in the principal stress space is showed in Fig. 5.5. This kind of analysis is of great importance since it allows to establish whether the discontinuous bifurcation condition is fulfilled not only in the softening regime but, moreover, in hardening.

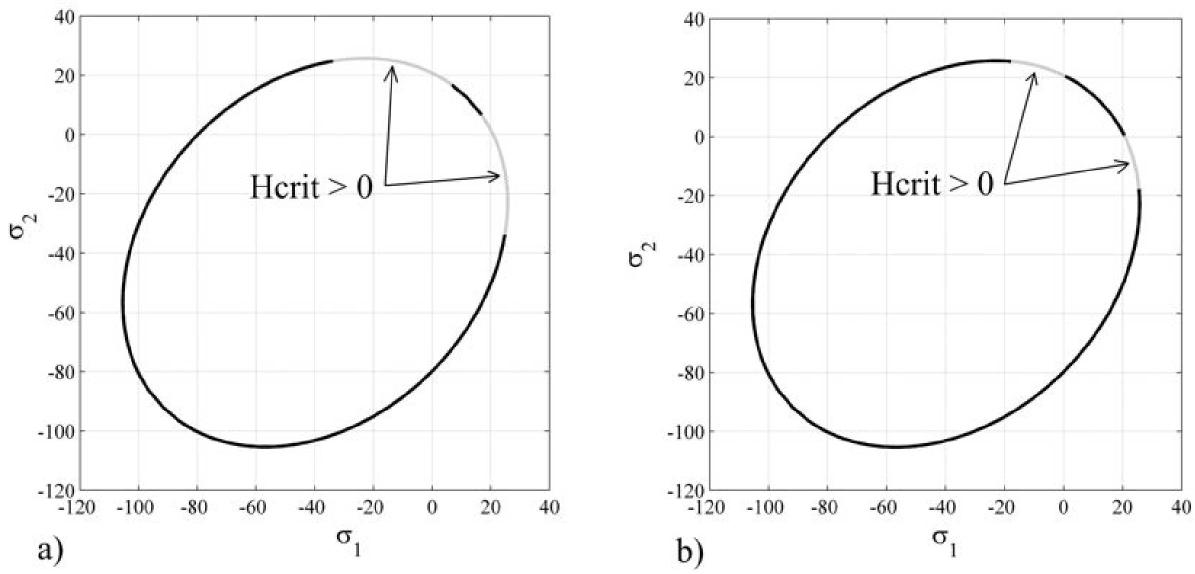

Figure 5.5: Critical hardening module in principal stress space for Cam Clay model, considering: a) drained condition; b) undrained condition

Following, the discontinuous bifurcation condition is analyzed on the initial yield surface considering the materials properties presented in Table 5.2. Also the regularization capabilities of this non-local gradient-based model for porous media is showed.

In Fig. 5.6 the acoustic tensor determinant for drained boundary conditions in both classical and gradients plasticity is presented. It can be clearly seen that the discontinuous bifurcation condition is not fulfilled in case of the gradient-based plasticity model. Positive value of the determinant of the acoustic tensor are indicated in the normal outward direction to the yield surface. This means that the proposed model is able to provide objective solutions regarding finite element sizes and orientations.

when this proposed gradient-based plasticity is considered, thus the objectivity of the numerical solution is achieved.

Likewise, the discontinuous bifurcation condition for undrained porous media is presented in Fig. 5.7. Here also the numerically regularization property of this gradient-based formulation for undrained porous media can be obsedved.

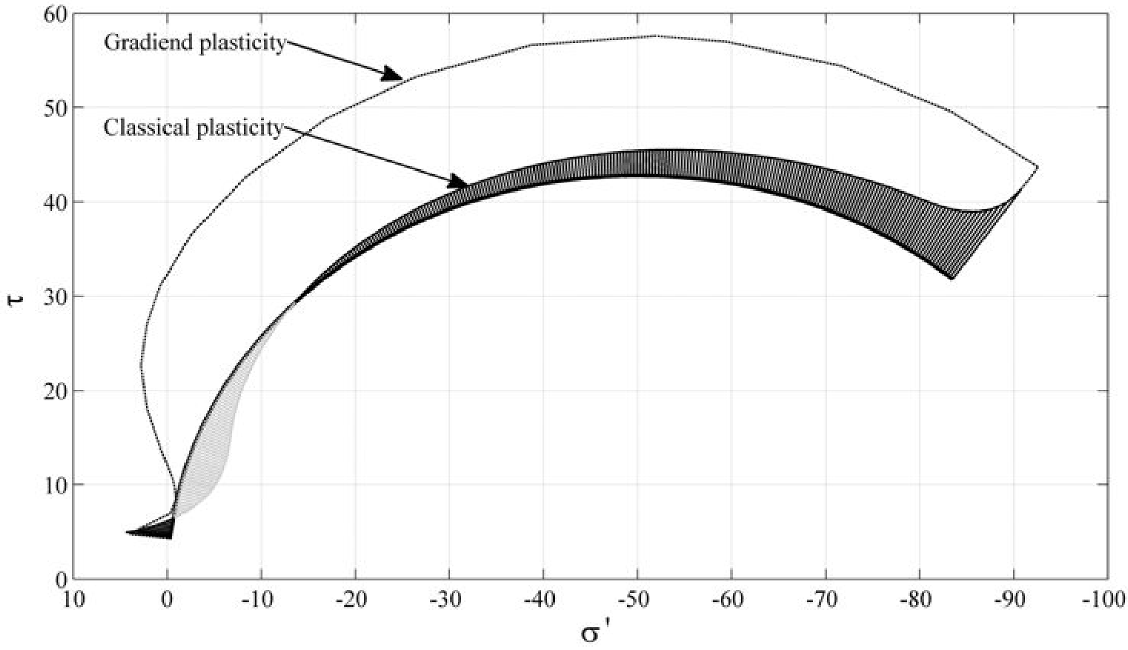

Figure 5.6: Evolution of the localization indicator for Cam Clay plasticity considering drained condition on yield surface

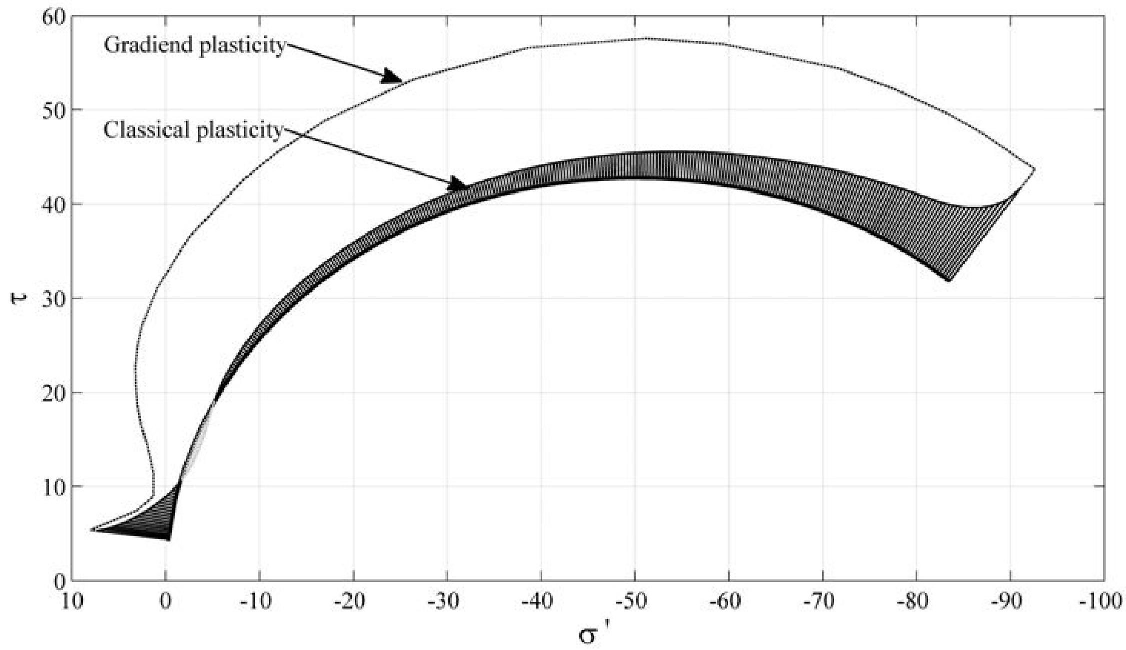

Figure 5.7: Evolution of the localization indicator for Cam Clay plasticity considering undrained condition on yield surface

An interesting alternative of the above results consists in representing the determinant of the localization acoustic tensor over the maximum strength curve of the material model, which is Critical States Line (CSL) of the modified Cam Clay.

On the CSL, the gradients of both the yield surface and plastic potential are paralell to τ axis. Therefore the influence of the hydrostatic component is despicable. Thus, the plastic potential tends to yield surface and the plastic flow becomes associated. In the same way, the derivatives of the yield surface and of the plastic potential with respect to the pore pressure tend to zero on the CSL. Therefore, the performance of the localization indicators on the CSL in case of undrained conditions agree with those corresponding to drained conditions. Figure 5.8 shows the discontinuous bifurcation condition on the CSL for drained hydraulic condition, considering classical and gradient poroplasticity.

For a more clear evaluation of the influence of the water pore pressure on the performance of the indicator for localized failure, the zones of the stress space associated with negative values of *det Q* are highlighted in Fig. 5.9 and Fig. 5.10, for drained and undrained conditions, respectively.

Finally, the influence of the volumetric non-associativity of the modified Cam Clay material model on the indicator for localized failure is presented in Fig. 5.11a and Fig. 5.11b, considering both drained and undrained conditions, respectively.

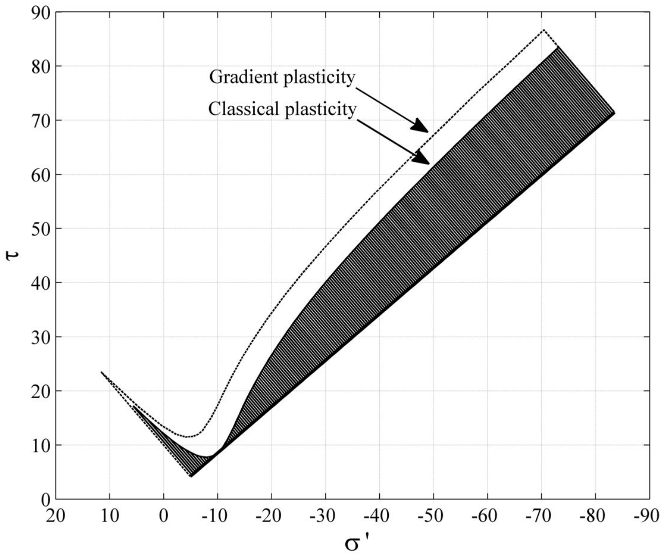

Figure 5.8: Bifurcation condition for Cam Clay plasticity considering drained condition on the CSL

5.5.3 Discontinuous bifurcation analysis and transition point for brittle-ductile behaviour. Parabolic Drucker-Prager poroplastic material.

Similarly to Section 5.5.2, in this Section the analysis of the spectral properties of the localization tensor for the case of the parabolic Drucker-Prager gradient-based poroplastic

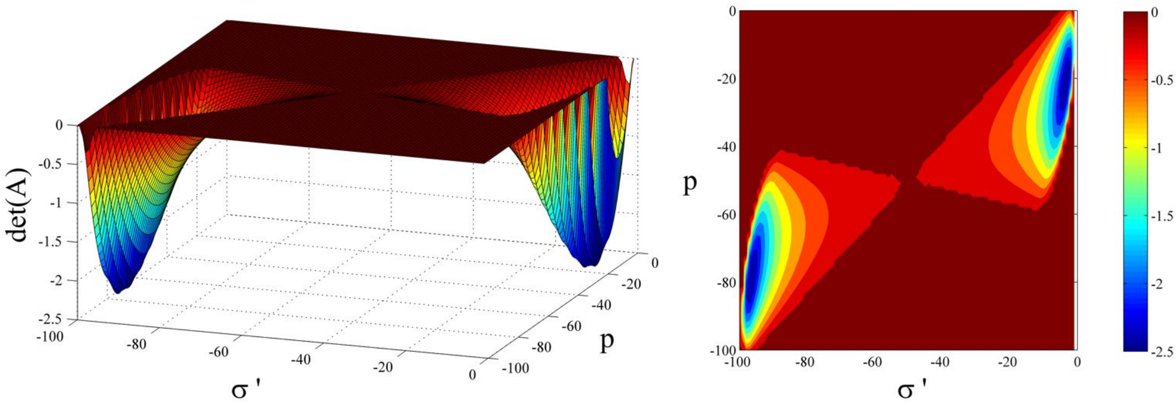

Figure 5.9: Discontinuous bifurcation condition in (σ',det(A),p) space for Cam Clay plasticity considering drained condition. Only negative values of *det* Q are scaled.

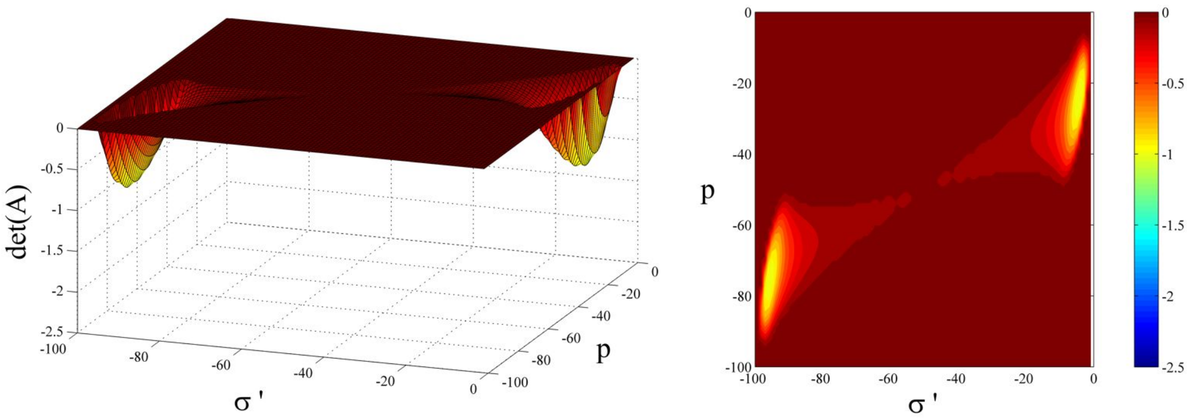

Figure 5.10: Discontinuous bifurcation condition in (σ',det(A),p) space for Cam Clay plasticity considering undrained condition. Only negative values of *det* Q are scaled.

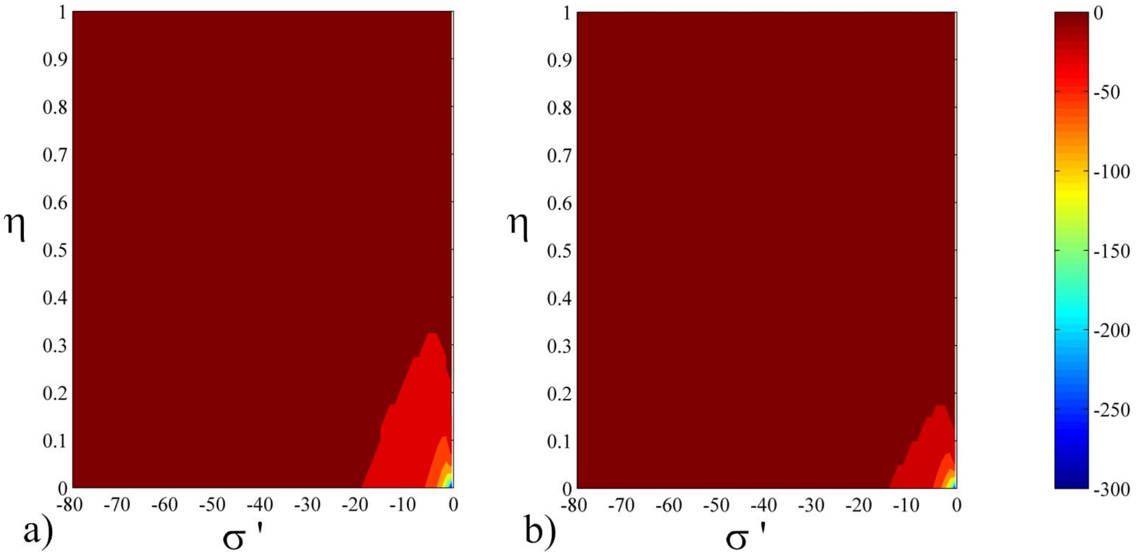

Figure 5.11: Discontinuous bifurcation condition in (σ',det(A),η) space for Cam Clay plasticity, considering a) drained condition; b) undrained condition

material model (see Chapter 4) is performed. The aim of this section is to evaluate with the thermodynamically consistent poroplastic constitutive theory proposed in this thesis, the localization properties of cohesive-frictional porous materials like concrete under drained and undrained conditions.

Also the critical hardening module for localization is evaluated to establish whether the discontinuous bifurcation condition can be fulfilled in hardening regime, prior to peak.

Furthermore, the influence of the water pore pressure and of the non-associativity degree of the proposed material model on the performance of the localization indicator is analyzed in the spaces (σ',det(A),p) and (σ',det(A),η), respectively.

The material properties employed in the following examples are summarized in Table 5.3. The solution of the critical hardening module in the principal stress space is presented in Fig. 5.12.

It can be seen from Fig. 5.12 that the critical domain where the localization tensor is singular in the principal stress space is slightly higher when drained hydraulic boundary condition is assumed. Similar conclusions were obtained from the results in Fig. 5.5 regarding to Cam Clay material model.

Now, the discontinuous bifurcation condition is analyzed on the initial yield surface considering the materials properties of Table 5.3.

In Fig. 5.13 the determinant of the localization tensor for drained boundary conditions in both classical and gradients plasticity is presented. It can be clearly seen that the discontinuous bifurcation condition is not fulfilled, thus the objectivity of the numerical solution regarding mesh size and orientation is achieved.

Similarly, the discontinuous bifurcation condition for undrained porous media is presented in Fig. 5.14. Here also the numerically regularization property of this gradient-based

Material parameters	Value
Compressive strength, f_c	22.0 MPa
Tensile strength, f_t	2.8 MPa
Initial pore pressure, p	10.0 MPa
Initial porosity, ϕ_0	0.1
Bulk compressibility coefficient, K_0	1000.0
Solid compressibility coefficient, K_s	25000.0
Fluid compressibility coefficient, K_{fl}	100.0
Young module, E	19300.0 MPa
Poisson ratio, ν	0.2
Local hardening/softening module, $H_s^{loc} = H_p^{loc}$	$-0.1 * E$
Non-associativity coefficient η (from Eq. (4.13))	0.1

Table 5.3: Material parameters for parabolic Drucker-Prager criterion

formulation for undrained porous media can be observed.

In undrained condition, the localization condition is not achieved. Contrarily to the previous case, the undrained boundary condition leads to diffuse failure form and, consequently, to regularization of the post peak behaviour.

For a more clear evaluation of the influence of the water pore pressure on the performance of the indicator for localized failure, the zones of the stress space associated with negative values of $det\, Q$ are highlighted in Fig. 5.9 for drained boundary condition.

In Fig. 5.16 the performance of the discontinuous bifurcation condition is presented for

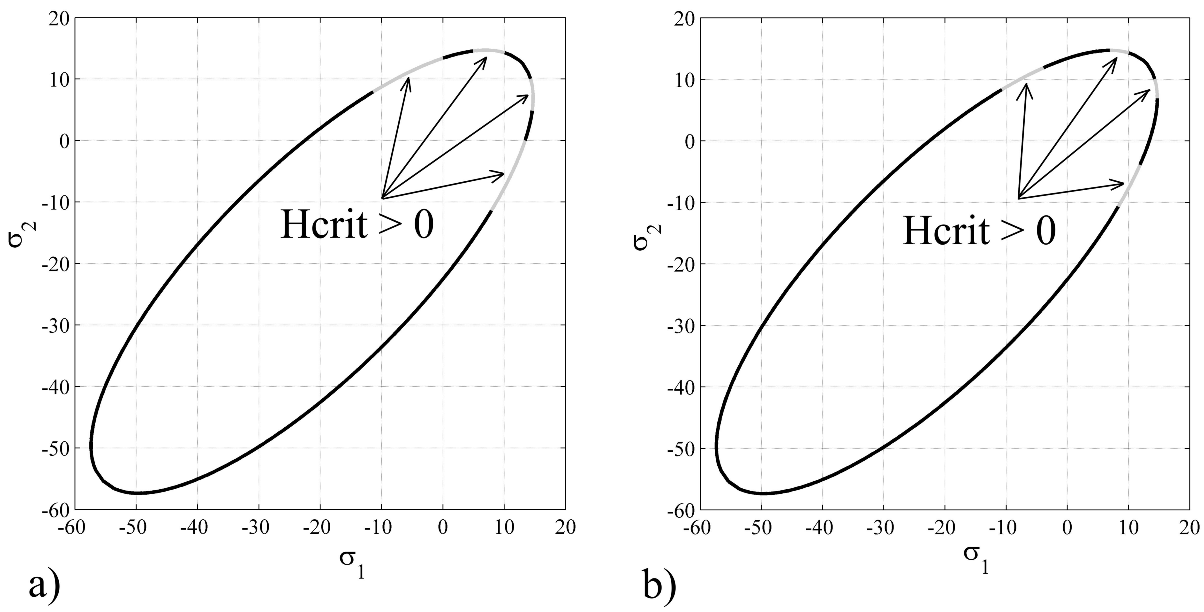

Figure 5.12: Performance of the critical hardening along the maximal strength criterion of the parabolic Drucker-Prager gradient poroplastic material, considering: a) drained condition ; b) undrained condition

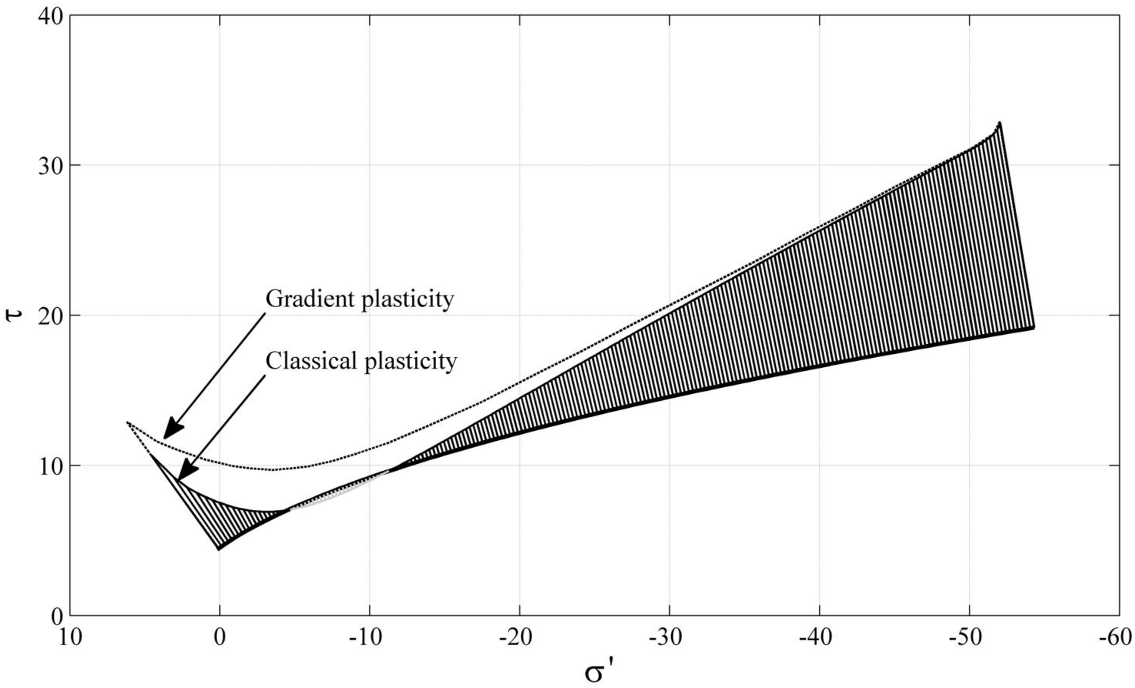

Figure 5.13: Performance of the localization indicator for parabolic Drucker-Prager gradient poroplastic material considering drained condition along the maximal strength surface

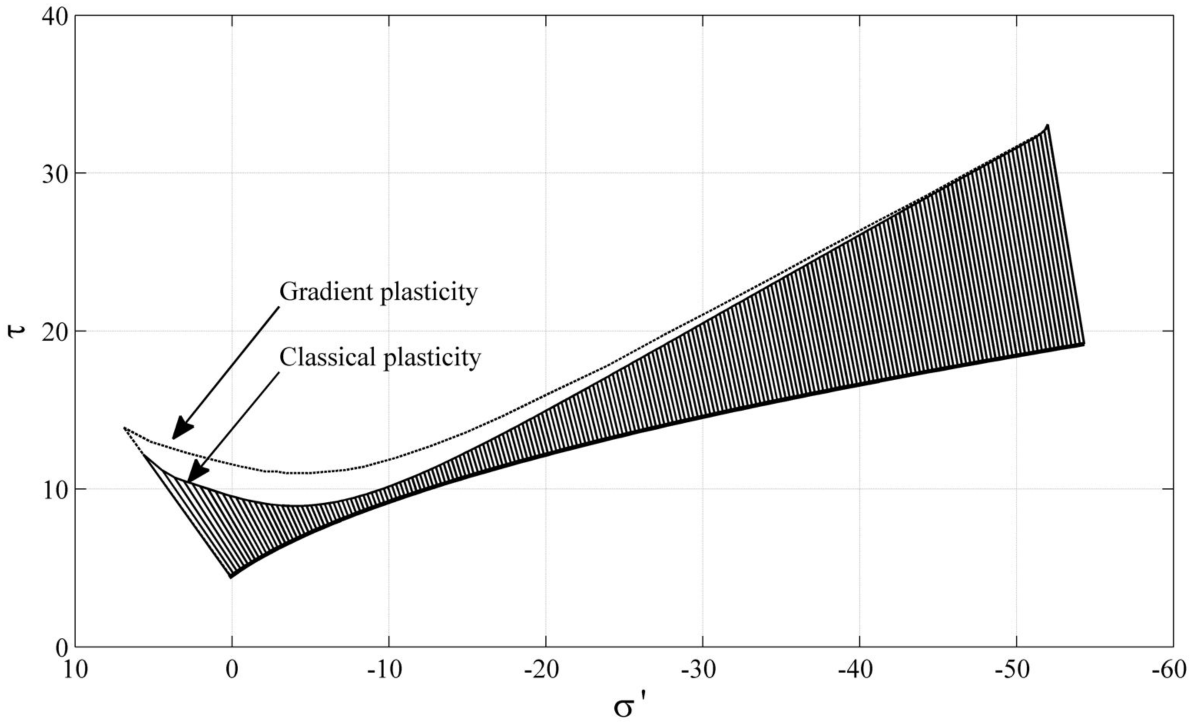

Figure 5.14: Performance of the localization indicator for parabolic Drucker-Prager gradient poroplastic material considering undrained condition along the maximal strength surface

undrained hydraulic conditions. In this case the localization condition is never achieved, since the determinant of the acoustic tensor remains positive for all possible pore pressures.

Finally, the influence of the volumetric non-associativity degree of the parabolic Drucker-Prager material model is studied. The discontinuous bifurcation condition for both drained and undrained hydraulic boundary conditions are presented in Fig. 5.17 and Fig. 5.18, respectively. From Fig. 5.18 it can be seen that under undrained condition the localization indicator of the parabolic Drucker-Prager material model is indifferent to the volumetric non-associativity degree as indicated in Eq. (4.13).

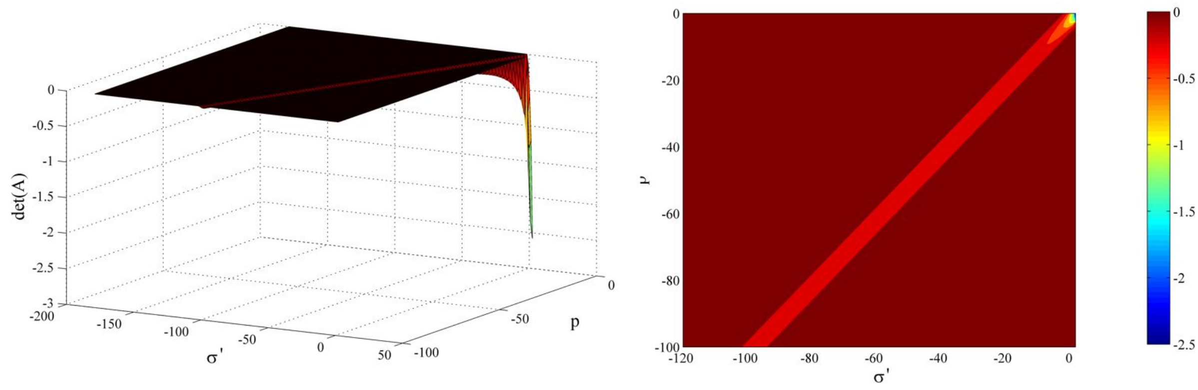

Figure 5.15: Discontinuous bifurcation condition in (σ',det(A),p) space for parabolic Drucker-Prager poroplasticity considering drained condition

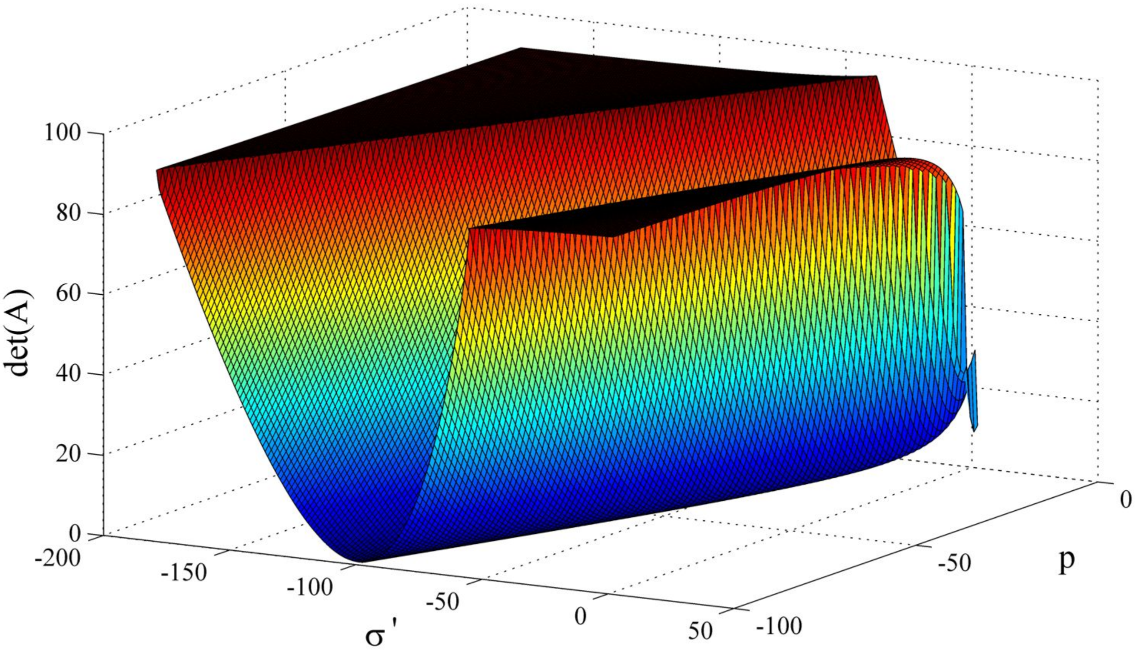

Figure 5.16: Discontinuous bifurcation condition in (σ',det(A),p) space for Parabolic Drucker-Prager poroplasticity considering undrained condition

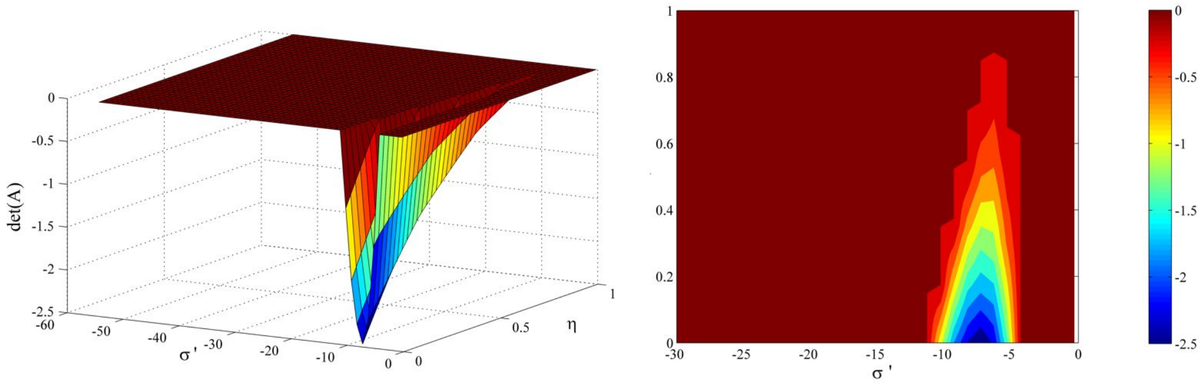

Figure 5.17: Discontinuous bifurcation condition in (σ',det(A),η) space for Parabolic Drucker-Prager poroplasticity considering drained condition

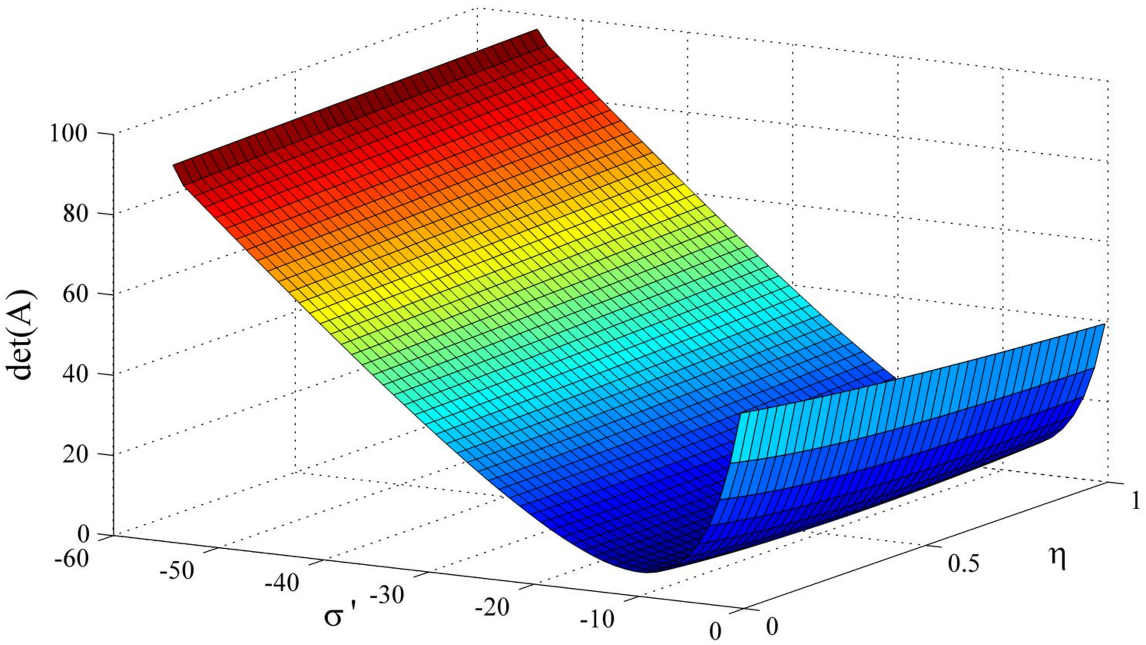

Figure 5.18: Discontinuous bifurcation condition in (σ',det(A),η) space for Parabolic Drucker-Prager poroplasticity considering undrained condition

CHAPTER 6

A finite element formulation for gradient-based poroplasticity

Having established the basic principles of the thermodynamically consistent gradient-based theory for porous media in Chapter 3 as well as its particularization for the Modified Cam Clay and Parabolic Drucker-Prager poroplastic models in Chapter 4, the present Chapter focuses in the formulation of a new C_1-continuous FE formulation for gradient-based constitutive formulation of porous media with the capacity to reproduce both localized and diffuse failure modes that characterized quasi-brittle materials like concretes and soils, see Mroginski and Etse (2013) [75]. A distinguish aspect of this FE formulation is the inclusion of interpolation functions of first order continuity (C_1) only for the internal variables while the kinematic fields remain with the classical C_0-continuous interpolation functions. Similarly to [118, 128] present FE formulation considers gradient material models with internal variables being the only ones of non-local character. This reduces the involved complexity of the FE formulation.

After presenting the finite element formulation, its iterative algorithm to solve the field variable increments of boundary value problems related to gradient-based poroplastic media is discussed and clarified.

The governing equations will be discretized in the framework of the Galerkin method. The solution of the boundary value problem should enforce the equilibrium condition, fluid mass balance and yield condition at the end of each increment by considering the hydro-mechanical coupling.

6.1 Incremental formulation

An incremental formulation of the above boundary value problem introduces residual terms, which make the stress update necessary. The transition from elastic to plastic regimes within a loading step must also be considered. At the end of the $j+1$ iteration of current load step, the incremental equilibrium condition, the fluid mass balance, and the yield condition are studied in a weak form. Thereby, bold symbol for tensors are used instead of the indicial notation employed in previous Chapters, i.e.

$$\int_{\Omega} \delta \boldsymbol{\varepsilon}^T : \boldsymbol{\sigma}_{j+1} \, \mathrm{d}\Omega - \int_{\partial\Omega} \delta \mathbf{u}^T \mathbf{t}_{j+1} \, \mathrm{d}\partial\Omega = 0 \tag{6.1}$$

$$\int_{\Omega} \delta p \, \dot{m}_{j+1} \, \mathrm{d}\Omega - \int_{\Omega} \nabla \delta p \cdot \mathbf{w}_{j+1} \, \mathrm{d}\Omega + \int_{\partial\Omega} \delta p \, \mathbf{w}_{j+1} \cdot \mathbf{n} \, \mathrm{d}\partial\Omega = 0 \tag{6.2}$$

$$\int_{\Omega} \delta \lambda \; f \left. (\boldsymbol{\sigma}, p, Q_\alpha) \right|_{j+1} \, \mathrm{d}\Omega = 0 \tag{6.3}$$

Differently to the local plasticity algorithm, Eq. (6.3) is not strictly satisfied but in a weak form. Furthermore, it is only fulfilled when the convergence is reached and not necessarily during the iterative process.

Considering the decomposition of stress tensor in the $j+1$ iteration as $\boldsymbol{\sigma}_{j+1} = \boldsymbol{\sigma}_j + \Delta\boldsymbol{\sigma}$, and replacing in Eq. (6.1) results

$$\int_{\Omega} \delta \boldsymbol{\varepsilon}^T : \Delta\boldsymbol{\sigma} \, \mathrm{d}\Omega = \int_{\partial\Omega} \delta \mathbf{u}^T \mathbf{t}_{j+1} \, \mathrm{d}\partial\Omega - \int_{\Omega} \delta \boldsymbol{\varepsilon}^T : \boldsymbol{\sigma}_j \, \mathrm{d}\Omega \tag{6.4}$$

replacing $\Delta\boldsymbol{\sigma}$ in the last equation by the linearized form of Eq. (3.19),

$$\int_{\Omega} \delta \boldsymbol{\varepsilon}^T : (\mathbf{C}^s : \Delta\boldsymbol{\varepsilon} - \mathbf{B}\Delta p - \mathbf{C}^s : \mathbf{g}^s \Delta\lambda) \, \mathrm{d}\Omega = \int_{\partial\Omega} \delta \mathbf{u}^T \mathbf{t}_{j+1} \mathrm{d}\partial\Omega - \int_{\Omega} \delta \boldsymbol{\varepsilon}^T : \boldsymbol{\sigma}_j \mathrm{d}\Omega \tag{6.5}$$

It can be observed that Eq. (6.5) is very similar to the incremental equilibrium condition of classical plasticity as it does not include an explicit dependence on the Laplacian of the plastic multiplier.

Considering the incremental decomposition of the infiltration vector $\mathbf{w}_{j+1} = \mathbf{w}_j + \Delta\mathbf{w}_{j+1}$ and the rate of the fluid mass content $\dot{m}$ obtained from the combination between Eq. (2.97) and Eq. (3.18), the Eq. (6.2) can be reformulated as

$$\begin{aligned} \int_{\Omega} \delta p \left(\frac{\Delta p}{M} + \mathbf{B} : \Delta\boldsymbol{\varepsilon} - (\mathbf{B} : \mathbf{g}^s - \mathrm{g}^p) \, \Delta\lambda \right) \, \mathrm{d}\Omega = \\ \Delta t \int_{\Omega} \nabla \delta p \cdot (\mathbf{w}_j + \Delta\mathbf{w}) \, \mathrm{d}\Omega - \Delta t \int_{\partial\Omega} \delta p \, \mathbf{w}_{j+1} \cdot \mathbf{n} \, \mathrm{d}\partial\Omega \end{aligned} \tag{6.6}$$

considering the generalized Darcy's law for porous media [18, 66, 109].

$$\mathbf{w} = -\mathbf{k} \cdot \nabla p \tag{6.7}$$

the following expression is obtained

$$\int_{\Omega} \delta p \left(\frac{\Delta p}{M} + \mathbf{B} : \Delta \boldsymbol{\varepsilon} - \left(\mathbf{B} : \mathbf{g}^s - \mathrm{g}^p \right) \Delta \lambda \right) \, \mathrm{d}\Omega =$$
$$- \Delta t \int_{\Omega} \nabla \delta p \cdot \mathbf{k} \cdot \nabla p_j \, \mathrm{d}\Omega - \Delta t \int_{\Omega} \nabla \delta p \cdot \mathbf{k} \cdot \nabla \Delta p \, \mathrm{d}\Omega - \Delta t \int_{\partial\Omega} \delta p \; \mathbf{w}_{j+1} \cdot \mathbf{n} \, \mathrm{d}\partial\Omega \quad (6.8)$$

Following [84] the yield function f can be approximated with sufficient accuracy by means of a linear Taylor series around $\left(\boldsymbol{\sigma}_j, p_j, Q_{\alpha_j}\right)$ as

$$f\left(\boldsymbol{\sigma}, p, Q_\alpha\right)\big|_{j+1} = f\left(\boldsymbol{\sigma}, p, Q_\alpha\right)\big|_{j} + \mathbf{f}^s : \Delta\boldsymbol{\sigma} + \mathrm{f}^p \Delta p + \mathrm{f}^Q_\alpha \Delta Q_\alpha \quad (6.9)$$

When all state variables are spatially homogeneous it can be assumed that the dissipative stress gradient is negligible, then $\nabla Q_\alpha = 0$, see [131, 32, 80, 117]. Also, from the additive decomposition of the dissipative stress in Eq. (3.20) follows

$$\dot{Q}_\alpha = \dot{Q}^{loc}_\alpha + \dot{Q}^{nloc}_\alpha = -H^{loc}_\alpha \mathrm{g}^Q_\alpha \dot{\lambda} + l^2_\alpha \mathbf{H}^{nloc}_\alpha \mathrm{g}^Q_\alpha \nabla^2 \dot{\lambda} \quad (6.10)$$

by replacing Eq. (3.19) and Eq. (6.10) in Eq. (6.9) the weak form of the yield condition is obtained

$$\int_{\Omega} \delta\lambda \; f\left(\boldsymbol{\sigma}, p, Q_\alpha\right)\big|_{j+1} \, \mathrm{d}\Omega = \int_{\Omega} \delta\lambda \; f\left(\boldsymbol{\sigma}, p, Q_\alpha\right)\big|_{j} \, \mathrm{d}\Omega + \int_{\Omega} \delta\lambda \; \mathbf{f}^s : \mathbf{C}^s : \Delta\boldsymbol{\varepsilon} \, \mathrm{d}\Omega +$$
$$\int_{\Omega} \delta\lambda \left[\left(\mathrm{f}^p - \mathbf{f}^s : \mathbf{B} \right) \Delta p - \mathbf{f}^s : \mathbf{C}^s : \mathbf{g}^s \Delta\lambda \right.$$
$$\left. + \mathrm{f}^Q_\alpha \left(-H^{loc}_\alpha \mathrm{g}^Q_\alpha \Delta\lambda + l^2_\alpha \mathbf{H}^{nloc}_\alpha \mathrm{g}^Q_\alpha \nabla^2 \Delta\lambda \right) \right] \mathrm{d}\Omega = 0 \quad (6.11)$$

6.2 Galerkin discretization

In this section the original formulation proposed by De Borst and Mühlhaus (1992) [22] for solid materials is extended to porous media. As it can be observed in Eqs. (6.5), (6.8) and (6.11) at most first order derivatives of the displacement and pore pressure fields appear as well as second order derivative of the plastic multiplier. Therefore, displacement and pressure field discretizations require C_0-continuous shape functions that are indicated as $\mathbf{N}_u$ and $\mathbf{N}_p$, respectively. However, C_1-continuous shape functions, called $\mathbf{H}$, are required for the plastic multiplier discretization. Then, the FE approximations can be expressed as

$$\mathbf{u} = \mathbf{N}_u \; \bar{\mathbf{u}} \quad (6.12)$$
$$p = \mathbf{N}_p \; \bar{p} \quad (6.13)$$
$$\lambda = \mathbf{H} \; \bar{\lambda} \quad (6.14)$$

where $\bar{\mathbf{u}}$, $\bar{p}$ and $\bar{\lambda}$ are the nodal displacement vector, the pore pressure and the plastic multiplier, respectively. Hence considering $\boldsymbol{\varepsilon} = \nabla^s \mathbf{u} = \nabla^s \mathbf{N}_u \ \bar{\mathbf{u}} = \bar{\mathbf{B}} \ \bar{\mathbf{u}}$ and replacing the above entities in Eqs. (6.5), (6.8) and (6.11) the following set of integral equations is obtained

$$\begin{aligned}
&\left\{ \int_\Omega \delta \bar{\mathbf{u}}^T \bar{\mathbf{B}}^T : \mathbf{C}^s : \bar{\mathbf{B}} \ \mathrm{d}\Omega \right\} \Delta \bar{\mathbf{u}} - \left\{ \int_\Omega \delta \bar{\mathbf{u}}^T \bar{\mathbf{B}}^T : \mathbf{B} \mathbf{N}_p \ \mathrm{d}\Omega \right\} \Delta \bar{p} \\
&\quad - \left\{ \int_\Omega \delta \bar{\mathbf{u}}^T \bar{\mathbf{B}}^T : \mathbf{C}^s : \mathbf{g}^s \mathbf{H} \ \mathrm{d}\Omega \right\} \Delta \bar{\lambda} = \int_{\partial\Omega} \delta \bar{\mathbf{u}}^T \mathbf{N}_u^T \mathbf{t}_{j+1} \mathrm{d}\partial\Omega - \int_\Omega \delta \bar{\mathbf{u}}^T \bar{\mathbf{B}}^T : \boldsymbol{\sigma}_j \mathrm{d}\Omega
\end{aligned} \tag{6.15}$$

$$\begin{aligned}
&\left\{ \int_\Omega \delta \bar{p} \ \mathbf{N}_p^T \mathbf{B} : \bar{\mathbf{B}} \ \mathrm{d}\Omega \right\} \Delta \bar{\mathbf{u}} + \left\{ \int_\Omega \delta \bar{p} \left[\frac{\mathbf{N}_p^T \mathbf{N}_p}{M} + \Delta t \left(\nabla \mathbf{N}_p \right)^T \cdot \mathbf{k} \cdot \nabla \mathbf{N}_p \right] \mathrm{d}\Omega \right\} \Delta \bar{p} \\
&\qquad + \left\{ \int_\Omega \delta \bar{p} \mathbf{N}_p^T \left[\mathrm{g}^p - \mathbf{B} : \mathbf{g}^s \right] \mathbf{H} \ \mathrm{d}\Omega \right\} \Delta \bar{\lambda} = \\
&\quad - \left\{ \Delta t \int_\Omega \delta \bar{p} \left(\nabla \mathbf{N}_p \right)^T \cdot \mathbf{k} \cdot \nabla \mathbf{N}_p \ \mathrm{d}\Omega \right\} \bar{p}_j - \Delta t \int_{\partial\Omega} \delta \bar{p} \mathbf{N}_p^T \mathbf{w}_{j+1} \cdot \mathbf{n} \ \mathrm{d}\partial\Omega
\end{aligned} \tag{6.16}$$

$$\begin{aligned}
&\left\{ \int_\Omega \delta \bar{\lambda} \mathbf{H}^T \mathbf{f}^s : \mathbf{C}^s : \bar{\mathbf{B}} \ \mathrm{d}\Omega \right\} \Delta \bar{\mathbf{u}} + \left\{ \int_\Omega \delta \bar{\lambda} \mathbf{H}^T \left[\mathrm{f}^p - \mathbf{f}^s : \mathbf{B} \right] \mathbf{N}_p \ \mathrm{d}\Omega \right\} \Delta \bar{p} \\
&\quad + \left\{ - \int_\Omega \delta \bar{\lambda} \mathbf{H}^T \left[\mathbf{f}^s : \mathbf{C}^s : \mathbf{g}^s + \bar{H}_\alpha^{loc} \right] \mathbf{H} + l_\alpha^2 \mathbf{H}^T \bar{\mathbf{H}}_\alpha^{nloc} \mathbf{P} \ \mathrm{d}\Omega \right\} \Delta \bar{\lambda} = \\
&\qquad\qquad - \int_\Omega \delta \bar{\lambda} \mathbf{H}^T \ f \left(\boldsymbol{\sigma}_j, p_j, Q_{\alpha_j} \right) \ \mathrm{d}\Omega
\end{aligned} \tag{6.17}$$

where

$$\nabla^2 \left(\Delta \lambda \right) = \nabla^2 \left(\mathbf{H} \right) \Delta \bar{\lambda} = \mathbf{P} \Delta \bar{\lambda} \tag{6.18}$$

$$\bar{H}_\alpha^{loc} = \mathrm{f}_\alpha^Q H_\alpha^{loc} \mathrm{g}_\alpha^Q \tag{6.19}$$

$$\bar{\mathbf{H}}_\alpha^{nloc} = \mathrm{f}_\alpha^Q \mathbf{H}_\alpha^{nloc} \mathrm{g}_\alpha^Q \tag{6.20}$$

Equations (6.15)-(6.17) must hold for any admissible variation of $\delta\bar{\mathbf{u}}$, $\delta\bar{p}$ and $\delta\bar{\lambda}$. Thus, the algebraic equation system in matrix form of the proposed FE formulation for gradient-dependent poroplastic media can be expressed as

$$\begin{bmatrix} -\mathbf{K}_{\mathrm{ss}} & \mathbf{Q}_{\mathrm{sp}} & \mathbf{Q}_{\mathrm{s}\lambda} \\ \mathbf{Q}_{\mathrm{ps}} & \mathbf{K}_{\mathrm{pp}} + \Delta t \mathbf{H}_{\mathrm{pp}} & \mathbf{Q}_{\mathrm{p}\lambda} \\ \mathbf{Q}_{\lambda\mathrm{s}} & \mathbf{Q}_{\lambda\mathrm{p}} & -\mathbf{K}_{\lambda\lambda} \end{bmatrix} \begin{bmatrix} \Delta\bar{\mathbf{u}} \\ \Delta\bar{p} \\ \Delta\bar{\lambda} \end{bmatrix} = \begin{bmatrix} \mathbf{F}_{\mathrm{s}}^{\mathrm{int}} - \mathbf{F}_{\mathrm{s}}^{\mathrm{ext}} \\ -\mathbf{F}_{\mathrm{p}} \\ -\mathbf{F}_{\lambda} \end{bmatrix} \tag{6.21}$$

1) Compute matrices of Eq. (6.21) according to Appendix F 2) Solve the algebraic system of Eq. (6.21) in terms of the increments $\Delta\bar{\mathbf{u}}$, $\Delta\bar{p}$ and $\Delta\bar{\lambda}$ 3) Update primary variables $\Delta\bar{\mathbf{u}}_{j+1} = \Delta\bar{\mathbf{u}}_j + \Delta\bar{\mathbf{u}}$, $\Delta\bar{p}_{j+1} = \Delta\bar{p}_j + \Delta\bar{p}$ and $\Delta\bar{\lambda}_{j+1} = \Delta\bar{\lambda}_j + \Delta\bar{\lambda}$ 4) On each integration point compute: $\Delta\boldsymbol{\varepsilon}_{j+1} = \bar{\mathbf{B}}\ \Delta\bar{\mathbf{u}}_{j+1}$ $\Delta\lambda_{j+1} = \mathbf{H}\ \Delta\bar{\lambda}_{j+1}$ $\nabla^2(\Delta\lambda_{j+1}) = \mathbf{P}\ \Delta\bar{\lambda}_{j+1}$ $q_{\alpha_{j+1}} = q_{\alpha_0} + \mathrm{g}_\alpha^Q \Delta\lambda_{j+1}$ $\nabla^2 q_{\alpha_{j+1}} = \nabla^2 q_{\alpha_0} + \mathrm{g}_\alpha^Q \nabla^2(\Delta\lambda_{j+1})$ $\boldsymbol{\sigma}^t = \boldsymbol{\sigma}_0 + \mathbf{C}^s : \Delta\boldsymbol{\varepsilon}_{j+1} - \mathbf{B}\mathbf{N}_p \Delta\bar{p}_{j+1}$ IF $f\left(\boldsymbol{\sigma}^t, q_\alpha, \nabla^2 q_\alpha\right)\big\|_{j+1} > 0$ $\boldsymbol{\sigma}_{j+1} = \boldsymbol{\sigma}^t - \Delta\lambda_{j+1}\mathbf{C}^s : \mathbf{g}^s$ ELSE $\boldsymbol{\sigma}_{j+1} = \boldsymbol{\sigma}^t$ END 5) Check convergence criterion, i.e. balance between internal and external energy. If it is not achieved go to 1

Table 6.1: Gradient-poroplasticity algorithm for selective C_1-continuous FE

Submatrices of Eq. (6.21), presented in Appendix F, were obtained from Eqs. (6.15)-(6.17).

In Table 6.1 the solution algorithm of the boundary value problem is summarized.

The main and most important difference between this selective C_1-continuous FE formulation and the one based on C_0 continuity approximations for gradient plasticity proposed by [118, 128] is the solution procedure. While present formulation requires only the solution of Eq. (6.21), the FE approaches proposed by the aforementioned authors require an additional global iteration to obtain the plastic multiplier.

Another meaningfully characteristic of present FE approach for gradient-poroplasticity as compared to standards classical plasticity related formulations is that the return mapping algorithm for the plastic multiplier is not longer required, since this state parameter is obtained from Eq. (6.21).

6.3 FE stability and boundary conditions

In this Section the stability requirements of the proposed FE are analysed.

As previously discussed, the gradient-based plasticity formulation for porous media proposed in Chapter 3 which is particularized here for saturated soils, involves the Laplacian of the plastic multiplier in its variational form. Therefore, C_1-continuous shape function are needed in order to appropriately describe the plastic multiplier field in the element domain as well as on its boundary.

Consolidation problems in saturated soils require the fulfilment of the Babuska-Brezzi condition [107, 73] to avoid instabilities in their numerical solution procedures. This is particularly necessary when approaching the undrained limit state, where the permeability matrices turn zero. In this case, the system to be solved turns similar to those corresponding to incompressible elastic solids and, therefore, no real solution of Eq. (6.21) may arise. Nevertheless, if the undrained limit state can never be achieved the choice of finite element shape functions is wide.

In present formulation the isoparametric 8-node quadrilateral FE for 2D problems is adopted for the kinematic field. This element was sufficiently tested in several problems regarding multiphasic fluid flow in porous media [43, 66, 59, 107, 92, 25, 73]. The Babuska-Brezzi condition is properly satisfied by considering shape functions for the displacement field $\mathbf{N}_u$ that are of higher order than the one considered for the pressure field $\mathbf{N}_p$. This FE was also extensively used in gradient-plasticity problems [84, 28] related to non-porous materials with accurate results. Actually, this type of FE behaves as the combination of three separated elements. On the one hand, two FEs based on C_0 approximations for the displacements (eight-node FE) and the pore pressure (four-node FE), respectively. On the other hand, a four-nodes rectangular FE with hermitian shape functions to approximate the plastic multiplier, as proposed in [27].

Figure 6.1 shows the proposed FE for porous media with the corresponding degrees of freedom of each element node, while Fig. 6.2 illustrates the Hermitian shape functions for the plastic multiplier interpolation of element node 1. In Appendix G the mathematical description of each Hermitian interpolation function is presented.

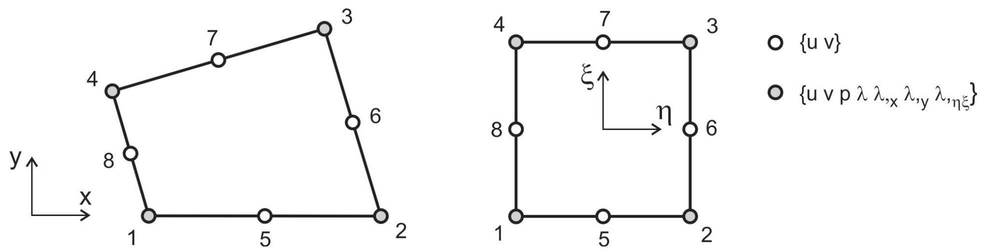

Figure 6.1: 8-node quadrilateral FE for gradient-plasticity in porous media

The additional degrees of freedom in the proposed FE formulation for porous media require their corresponding boundary conditions. To this end, the boundary conditions proposed by [84, 28] to avoid the FE stiffness matrix to turn singular should be

$$\partial_n \lambda = 0 \tag{6.22}$$
$$\partial_{nm} \lambda = 0 \tag{6.23}$$

where n and m denote the normal and tangential directions to the model boundary, respectively.

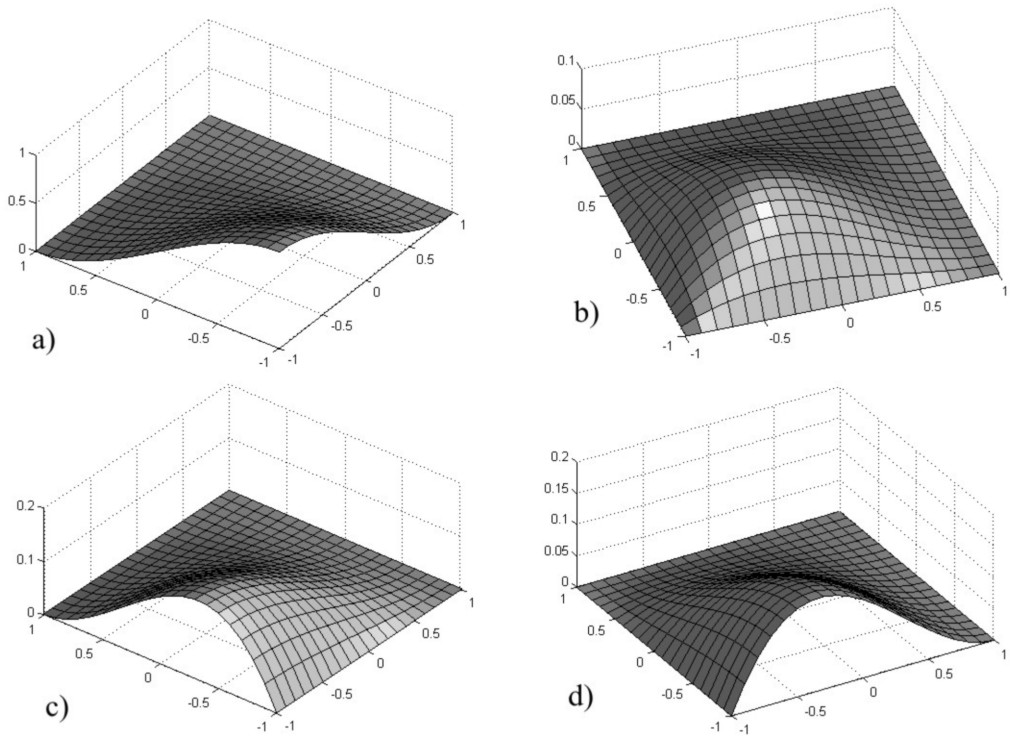

Figure 6.2: Hermitian shape function for node 1: a) for plastic multiplier λ, b) for $\partial\lambda/\partial xy$, c) for $\partial\lambda/\partial x$ and, d) for $\partial\lambda/\partial y$

These boundary conditions can easily be applied in either the global coordinated system or the reference coordinate system when the surface normal is directed along either of the global coordinates.

CHAPTER 7

Boundary value problems

In this Chapter numerical evaluations of boundary value problems related to porous media that are discretized with the FE formulated in Chapter 6 are presented in order to test the numerical tools and failure behavior prediction, considering both the gradient-enhanced constitutive theory presented in Chapter 3 as well as the non-associated Cam Clay model described in Chapter 4. The influence of the gradient characteristic length on the ductility in post-peak regime is also evaluated.

7.1 Plain strain localization analysis. Mesh objectivity.

Firstly, a plane strain specimen under biaxial state of loading is considered. Figure 7.1 shows geometry and boundary conditions of the specimen while material parameters are given in Table 7.1. The dimensions assumed are $B = 60mm$ and $H = 120mm$. Drained conditions for the porous phase are considered in this numerical example.

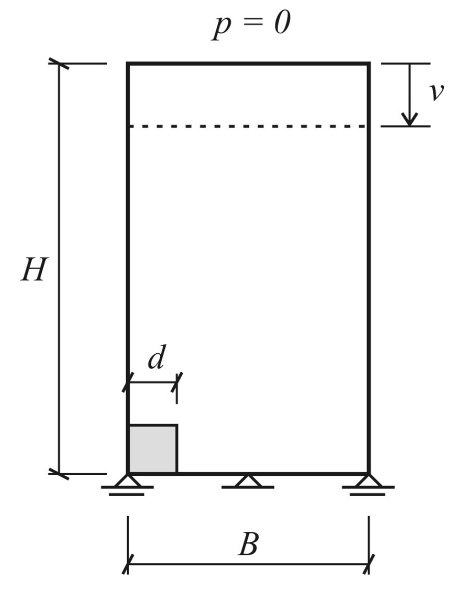

Figure 7.1: Geometry and boundary conditions

Material parameters	Value
CSL slope, M	1.00
Preconsolidation pressure, p_{co}	100.00 MPA
Initial porosity, ϕ_0	0.4
Bulk compressibility coefficient, K_0	1000.00
Solid compressibility coefficient, K_s	1500.00
Fluid compressibility coefficient, K_{fl}	500.00
Biot coefficient, $b = 1 - K_0/K_s$	0.33
Young module, E	20000.0 MPA
Poisson ratio, ν	0.2
Local hardening/softening module, $H_s^{loc} = H_p^{loc}$	$-0.1 * E$

Table 7.1: Soil material parameters

To create an inhomogeneous loading state and to induce localized failure mode a weakened region of $d = 10mm$ in the bottom left-hand corner of the specimen was considered by assigning a yield strength which is 10% reduced as compared to the material outside this weakened zone (see Fig. 7.1).

The supplementary boundary conditions considered in this analysis due to the additional degrees of freedom of the problem are: $\partial_x \lambda = 0$ along the left and right boundaries, $\partial_y \lambda = 0$ along the top and bottom boundaries, and $\partial_{xy} \lambda = 0$ along the whole boundary.

Four different meshes (three structured, Fig. 7.2a, 7.2c and 7.2d, and one non-structured, Fig. 7.2b) were considered in this analysis in order to evaluate the FE mesh size and orientation sensitivities of the numerical predictions. The characteristic length of the saturated soil is assumed constant $l_s = 3.5mm$. As can be observed in Fig. 7.2 the localization band width remains practically constant in all different meshes when the gradient length is set constant, $w = 2\pi l_s \cong 20mm$. This result demonstrates the capability of the proposed FE formulation to capture the considered non-local effects through the gradient theory.

The mesh objectivity or softening regularization capabilities of the numerical predictions can also be demonstrated by observing the good agreement between the load-displacement curves of the four different meshes in Fig. 7.3. Also the stress path of the material point where the plastic process initiates is illustrated in Fig. 7.4.

7.2 Influence of the internal characteristic length in the failure mode and shear band width

A second set of analysis of this test was performed with three different gradient characteristic lengths and totally drained conditions. Only the 12x24 regular mesh of Fig. 7.2 was used in this case. Figure 7.5 shows FE predictions considering $l_s = 3.0mm$, $l_s = 3.5mm$ and $l_s = 4mm$, being its localization band width $w \cong 15mm$, $w \cong 20mm$ and $w \cong 25mm$, respectively. It can be clearly observed in these results that the proposed FE formula-

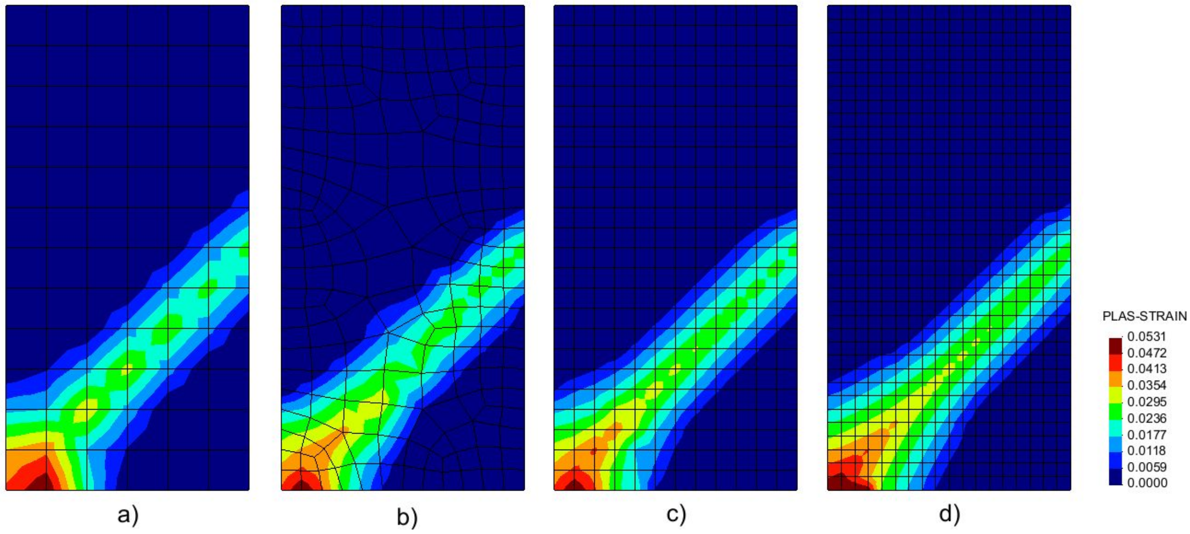

Figure 7.2: FE discretization and shear band width in terms of plastic strains isolines

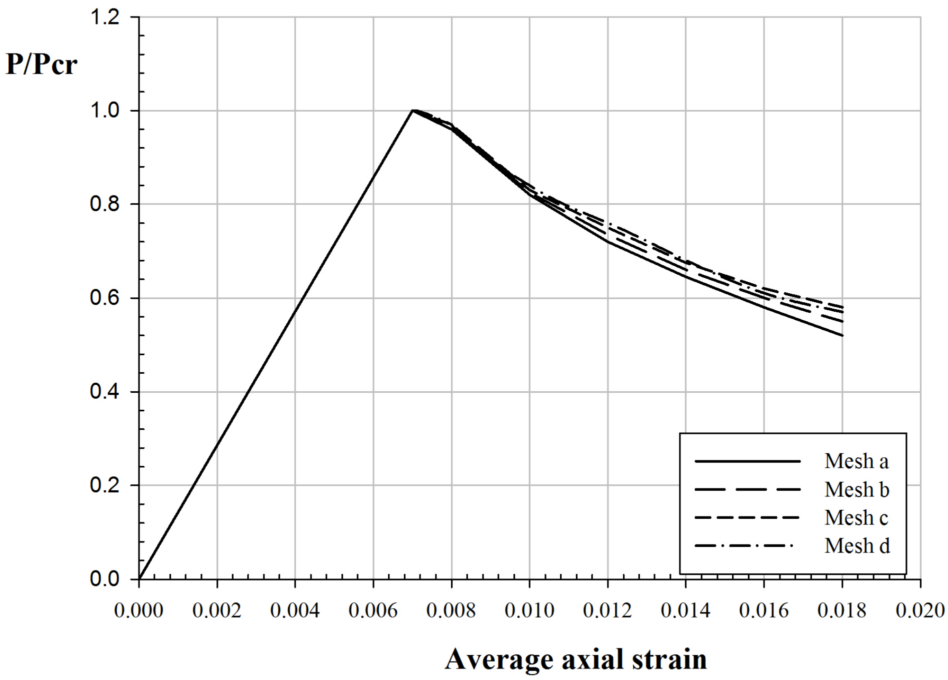

Figure 7.3: Normalized load-displacement curves for different mesh sizes and orientations

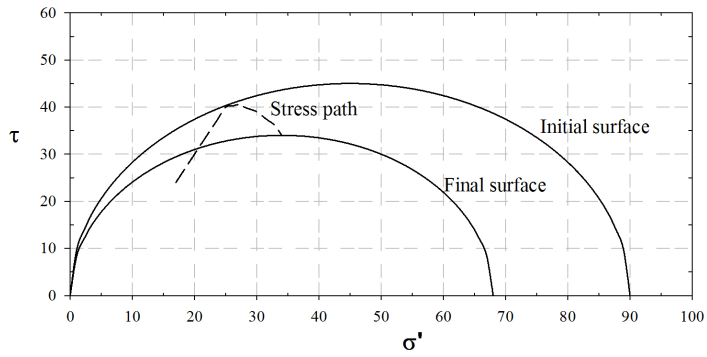

Figure 7.4: Stress path and yield surface evolution

tion is able to reproduce the model sensitivity to the characteristic length. A significant improvement of the ductility takes place under increasing l_s.

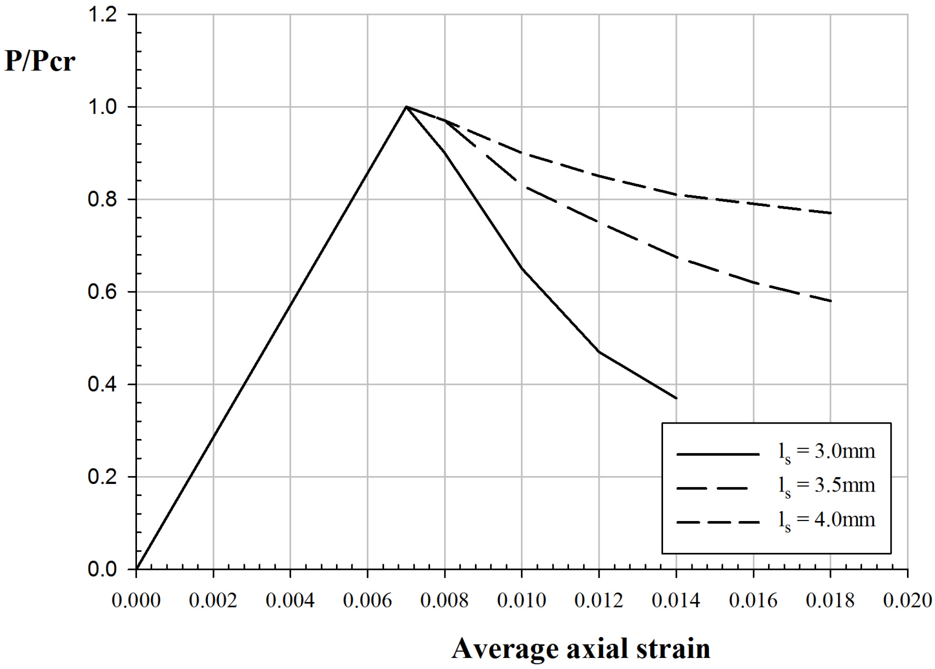

Figure 7.5: Normalized load-displacement curve for variable l_s

The equivalent plastic strain distribution at residual strength of the numerical analysis can be observed in Fig. 7.6. The increment of the shear band width with increasing internal characteristic length can be clearly recognized.

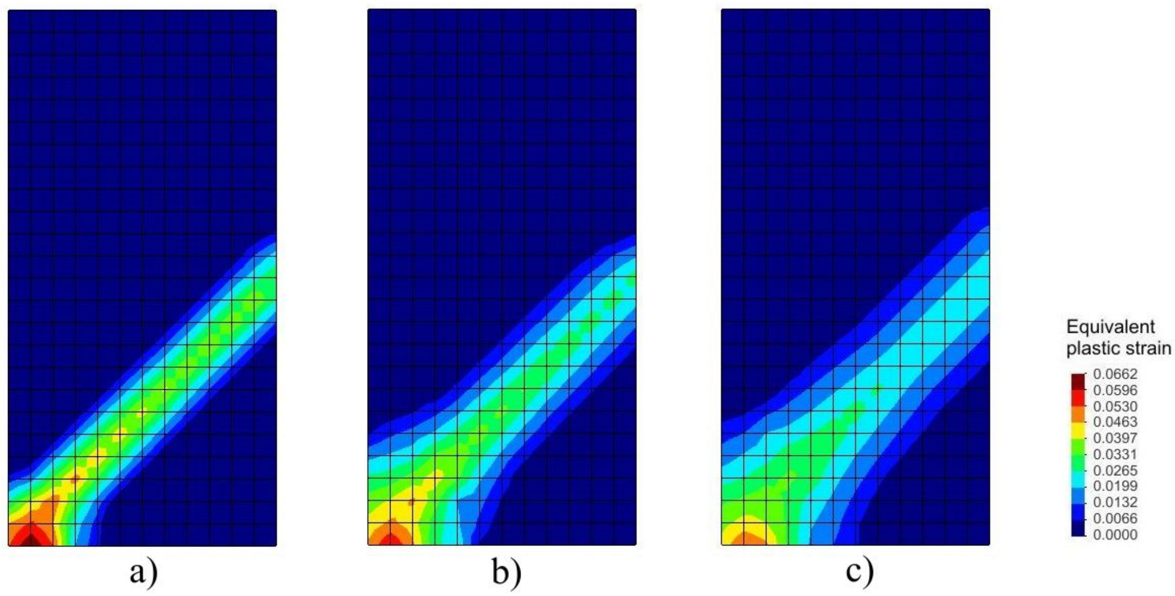

Figure 7.6: Equivalent plastic strain for different constant values of: a) $l_s = 3.0mm$, b) $l_s = 3.5mm$ and c) $l_s = 4mm$

7.3 Influence of the confinement pressure

The third set of analysis was carried out varying the confinement pressure in the soil specimen. As explained before, the internal characteristic length of the solid skeleton l_s is a function of the acting confining pressure according to Eq. (4.14) (see Fig. 4.5).

In this third set of analysis three different confining pressures were applied, $\sigma' = 24\,MPa$, $\sigma' = 29\,MPa$ and $\sigma' = 38\,MPa$, being the corresponding charcteristics lengths of each confining pressure 3.3 mm, 4.4 mm and 6.0 mm, respectively, and the extreme value of the internal characteristic length of the solid phase is $l_{s,m} = 7mm$, according to Eq. (4.14). Figure 7.7 shows the variation of the shear band width with the increasing confinement.

7.4 Influence of the pore pressure

Finally, an additional numerical example of the previous test was performed considering three different levels of initial pore pressure: $p = 20$, $p = 40$ and $p = 60$. Thus, according to Eq. (4.16) the corresponding charcteristics lengths were 3.3 mm, 4.4 mm and 6.0 mm, respectively. Also the coefficients of the Eq. (4.16) are $a = 1.0$, $b = 0.02$ and the extreme value of the internal characteristic length of the porous phase is $l_{p,m} = 7mm$. In Fig. 7.8 the equivalent plastic strain in the soil specimen is depicted. As in previous set of analysis, it can be easily recognize in this case the transition from ductile to brittle failure mode as the pore pressure level reduces.

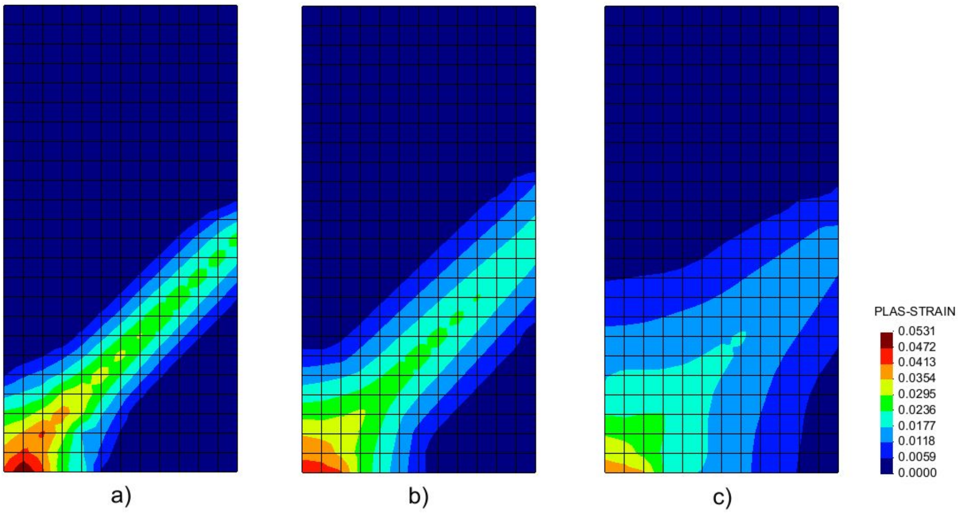

Figure 7.7: Equivalent plastic strain distribution considering l_s as a function of confining pressure for: a) $\sigma' = 24\,MPa$, b) $\sigma' = 29\,MPa$ and c) $\sigma' = 38\,MPa$

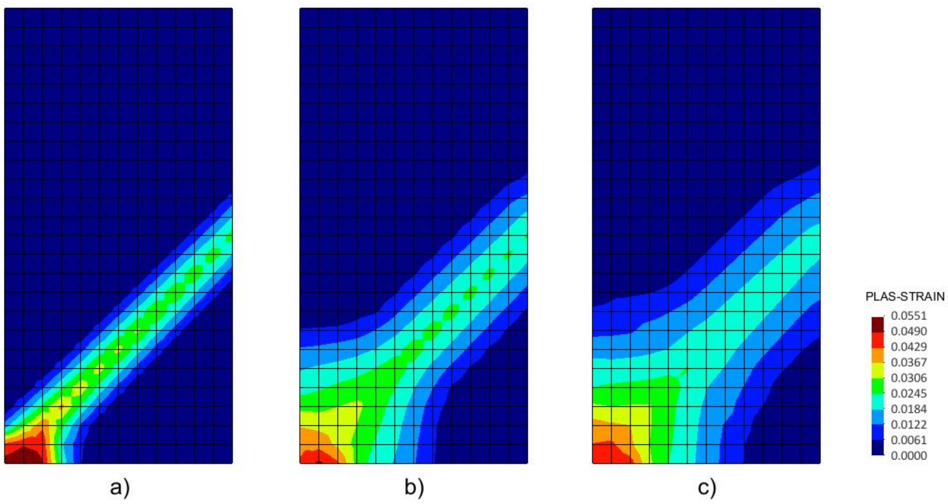

Figure 7.8: Equivalent plastic strain distribution considering l_p as a function of pore pressure, a) $p = 20$, b) $p = 40$ and c) $p = 60$

CHAPTER 8

Conclusions

In this work a general thermodynamically consistent gradient-based constitutive theory to describe non-local behavior of porous media is proposed. The proposal is an extension of the gradient-based thermodynamically consistent theory by [116] and [130] for non-porous continua. In the present proposal the internal variables are the only ones of non-local character while in the classical framework of gradient plasticity the non-local gradient fields involve the entire kinematic variables.

The kinematic of porous material in this work is modelled at the macroscopic level of observation, based on the Generalized Theory of Porous Media [18], that is considered as an open thermodynamic system characterized by the presence of occluded sub-regions.

Discontinuous bifurcation theory to predict localized failure modes was consistently extended in this thesis to account for porous media. Accordingly, the analytical expression of the localization tensor for gradient regularized in porous media as well as the analytical expression of the critical hardening were obtained. These failure indicators were particularized for both drained and undrained hydraulic conditions.

The thermodynamically consistent constitutive theory and its related localization indicators as proposed in this work can be applied to the analysis of failure behavior of different types of porous materials like soils, bones and concrete.

Two well known material models were extended and enriched by means of the proposed thermodynamically consistent gradient poroplastic constitutive theory. On the one hand, the modified Cam Clay plasticity model employed in mechanical prediction of saturated and partially saturated soils and, on the other hand, the Parabolic Drucker-Prager model commonly used for concrete. Moreover, the mathematical definition of both internal characteristic length for solid skeleton and porous phase, was presented and discussed, as well as the thermodynamically consistent plastic potential function.

In order to solve the boundary value problem, a new finite element formulation for porous media based on thermodynamically consistent gradient-based plasticity theory is proposed. The element formulation includes C_0 continuous approximations for both the pore pressure and the displacements fields, while a C_1-continuous interpolation function for the internal variable. Therefore, hermitian functions need to be considered to approximate the gradient fields that are included in the variational problem due to the non-local gradient formulation assumed at the constitutive level. The inclusion of the additional field variable, i.e. the gradients to the plastic multiplier, requires the consideration of additional boundary conditions in the finite element formulation.

A distinguish and novel consideration in the proposed finite element is the associated numerical approach for the solution of the plastic multiplier and the related Laplacian that only involves one iteration procedure. This leads to stable numerical solutions during failure processes of gradient-based poroplastic continua.

The numerical analyses presented in this work demonstrate the predictive capabilities of the proposed enhanced gradient-based constitutive theory as well as the robustness of the finite element formulation also proposed in this thesis, to reproduce failure behaviors of saturated porous media under different boundary conditions and material features. Particularly, it is shown that the proposed finite element is able to reproduce model sensitivity regarding the gradient characteristic length while assuring mesh objectivity.

CHAPTER 9

Futures developments

The scientific developments carried out in this thesis allows may be continued in the following aspect

a) Extending the scope of the thermodynamically consistent non-local gradient-based theory proposed in this thesis for porous media to simulate the mechanical behavior of young concrete. Thereby the inclusion of both mass transport and temperature are required, as well as the chemical reactions taking place during the set process of the concrete. This allows to simulate the mechanical behavior of young concrete considering the internal heat generation due to the cement set process. The entirely mechanical behavior of concrete from its elaboration to the final deposition taking into account the incidence of pore pressure, temperature and change in the fluid mass due to evaporation may be studied.

b) Regarding to failure prediction, the development of a non-local thermo-chemical-poroplastic theory may allows the study of the transition between ductile and brittle failure in concrete during the set process and establish the corresponding stress states.

c) Furthermore, the extension of the proposed thermodynamically consistent non-local gradient-based theory to multiphase porous media, which incorporates the presence of a gaseous phase and immiscible (or miscible) pollutants, may allows the prediction of failure phenomena in porous media. Therefore, the appropriated environmental damage may be established. On the other hand, an additional scope of the extension of this theory is the non-conventional oil production as well as the reliability evaluation of hydrocarbons transport by pumping.

d) Regarding to the numerical solution of boundary value problems by the finite element method the proposed FE approach developed in this thesis can be easily extended to three-dimensional problems in order to simulate real engineering situations, for example the excavation process of canals and underground tunnels. On the other hand, although the FE formulation proposed in this work was developed for isothermical porous systems its extension to thermo-chemical-coupled phenomena can be done easily as well. In fact, in the proposed FE formulation the non-local effect is restricted to the internal variable, therefore the degree of freedom corresponding to the C1-continuous interpolation function remain unchanged.

e) Finally, from the non-local gradient-based theory for porous media proposed in this thesis a new internal characteristic length regarding to the porous phase is deduced. This characteristic length is directly dependent on both the pore pressure and the saturation degree, through the soil-water characteristic curve. As a further development it may be interesting to experimentally evaluate the limits of this internal length, and its dependence on other factors such as the relative permeability and the grain shape.

APPENDIX A

Gradient plasticity for finite deformation

The present theory was developed under small deformations hypothesis nevertheless it can be easily adapted to finite deformations problems using the concept of corrotational magnitudes [11, 97]. The gradient-plasticity treatment in terms of corrotational magnitudes does not present much complexity since all state variables are objectively described in the corrotational configuration. In contrast, this kind of corrotational-based constitutive models leads to a somewhat awkward in numerical implementation due to the appearance of non-symmetric matrices and deformation-dependent constitutive tensors. However the non-symmetrical part of those constitutive models mainly depends on tangential stress and could be disregarded, in some cases [26].

As we said before, finite deformation problems require an objectivity description of the state variables. Namely, the strain tensor employed should be indifferent under rigid body motions in order to avoid the appearance of unreal stress. The infinitesimal strain tensor ε does not fulfill this postulate and is it mandatory to be replaced by another strain tensor. An appropriated strain measure is the spatial rate of deformation tensor $\mathbf{D}$ which is the symmetric part of the additively decomposition of the spatial velocity gradient $\mathbf{L}$, being its $\mathbf{W}$ the antisymmetric part,

$$\mathbf{L} = \mathbf{D} + \mathbf{W} = \dot{\mathbf{F}} \cdot \mathbf{F}^{-1} = \mathbf{L}^e + \mathbf{F}^e \cdot \mathbf{L}^p \cdot \mathbf{F}^{e^{-1}} \tag{A.1}$$

with $\mathbf{L}^e = \dot{\mathbf{F}}^e \cdot \mathbf{F}^{e^{-1}}$ and $\mathbf{L}^p = \dot{\mathbf{F}}^p \cdot \mathbf{F}^{p^{-1}}$

The basic hypothesis in physical and geometrical non-lineal problem analysis is the multiplicative decomposition of the deformation gradient tensor in its elastic and plastic parts, $\mathbf{F}^e$, $\mathbf{F}^p$, respectively.

$$\mathbf{F} = \mathbf{F}^e \cdot \mathbf{F}^p \tag{A.2}$$

On the other hand, the spatial rate of deformation tensor can be expressed in a convenient form considering the relation between the deformation gradient tensor and the rate of the Green-Lagrange strain tensor, $\dot{\mathbf{E}}$, in the following way

$$\mathbf{D} = \mathbf{F}^{-T} \cdot \dot{\mathbf{E}} \cdot \mathbf{F}^{-1} \tag{A.3}$$

with

$$\dot{\mathbf{E}} = \mathbf{F}^{p^T} \left[\overset{\circ}{\mathbf{E}}{}^e + \frac{1}{2} \left(\mathbf{L}^{pr^T} \cdot \mathbf{C}^e + \mathbf{C}^e \cdot \mathbf{L}^{pr} \right) \right] \mathbf{F}^p \tag{A.4}$$

being $\overset{\circ}{\mathbf{E}}{}^e = \dot{\mathbf{E}}^e - \omega \mathbf{E}^e + \mathbf{E}^e \omega$, $\mathbf{L}^{pr} = \mathbf{L}^p - \omega$, $\mathbf{C}^e = \mathbf{F}^{e^T} \cdot \mathbf{F}^e = \mathbf{I} + 2\mathbf{E}^e$ and $\omega = \dot{\mathbf{R}}\mathbf{R}^T$

Likewise, considering the relationship between the second Piola-Kirchhoff stress tensor $\mathbf{S}$, and the Cauchy stress tensor σ,

$$\mathbf{S} = \bar{\rho}\, \mathbf{F}^{e^{-1}} \cdot \sigma \cdot \mathbf{F}^{e^{-T}} \tag{A.5}$$

it is possible rewrite the Second Principle of the Thermodynamic Eq. (2.55) for isothermal condition

$$\int_\Omega \left[\frac{1}{\bar{\rho}}\, \mathbf{F}^e \cdot \mathbf{S} \cdot \mathbf{F}^{e^T} : \mathbf{F}^{-T} \cdot \dot{\mathbf{E}} \cdot \mathbf{F}^{-1} + p\dot{m} - \dot{\Psi} \right] \mathrm{d}\Omega \geq 0 \tag{A.6}$$

In this gradient plasticity framework, considering corrotational magnitudes, the free energy of Helmholtz can be decomposed in the following way

$$\Psi = \Psi^e \left(\hat{\mathbf{E}}^e, m^e \right) + \Psi^{p,loc} \left(q_\alpha \right) + \Psi^{p,nloc} \left(\hat{\nabla} q_\alpha \right) \tag{A.7}$$

where the operator $\hat{\bullet} = \mathbf{R}^T \cdot \bullet \cdot \mathbf{R}$ implies a configuration change for the magnitude $\bullet$ passing from the reference, $\mathcal{C}$, to the corrotated configuration, $\hat{\mathcal{C}}$. Note that m^e and q_α are considered here as scalar quantities, thus they are indifferent under rigid body motions.

Replacing the rate of the free energy in Eq. (A.6) and considering Eq. (A.4) it is possible to proceed in a similar way to Eq. (3.2), then

$$\begin{aligned} \int_\Omega \Bigg[\left(\frac{1}{\bar{\rho}} \mathbf{S} - \mathbf{R}^T \frac{\partial \Psi}{\partial \hat{\mathbf{E}}^e} \mathbf{R} \right) \overset{\circ}{\mathbf{E}}{}^e + \left(p - \frac{\partial \Psi}{\partial m^e} \right) \dot{m} + \frac{1}{2\bar{\rho}} \mathbf{S} \cdot \Big(\mathbf{L}^{pr^T} \cdot \mathbf{C}^e + \\ \mathbf{C}^e \cdot \mathbf{L}^{pr} \Big) + \frac{\partial \Psi}{\partial m^e} \dot{m}^p + \sum_\alpha \mathbf{Q}_\alpha \dot{q_\alpha} \Bigg] \mathrm{d}\Omega + \int_{\partial\Omega} \sum_\alpha \mathbf{Q}_\alpha^{(b)} \dot{q}_\alpha \, \mathrm{d}\partial\Omega \geq 0 \end{aligned} \tag{A.8}$$

with

$$\mathbf{Q}_\alpha = -\frac{\partial \Psi}{\partial q_\alpha} - \nabla \cdot \left(\mathbf{R}^T \frac{\partial \Psi}{\hat{\nabla} q_\alpha} \right) \qquad \text{in } \Omega \tag{A.9}$$

$$\mathbf{Q}_\alpha^{(b)} = -\mathbf{n} \frac{\partial \Psi}{\hat{\nabla} q_\alpha} \qquad \text{in } \partial\Omega \tag{A.10}$$

Since the inequality (A.8) holds for arbitrary elastic-plastic deformation mechanisms, even when these are purely elastic, all plastic strain variable disappears [97], and inequality (A.8) implies

$$\mathbf{S} = \bar{\rho}\mathbf{R}^T \frac{\partial \Psi}{\partial \hat{\mathbf{E}}^e} \mathbf{R} = \bar{\rho} \frac{\partial \Psi}{\partial \mathbf{E}^e} \tag{A.11}$$

$$p = \frac{\partial \Psi}{\partial m^e} \tag{A.12}$$

Which are the pertinent elasticity laws and the dissipation expression in the domain Ω and on the boundary $\partial\Omega$ are formaly obtained as

$$\mathfrak{D} = \frac{1}{2\bar{\rho}} \mathbf{S} \cdot \left(\mathbf{L}^{pr^T} \cdot \mathbf{C}^e + \mathbf{C}^e \cdot \mathbf{L}^{pr} \right) + p\, \dot{m}^p + \sum_\alpha \mathbf{Q}_\alpha \dot{q}_\alpha \geq 0 \qquad \text{in } \Omega \tag{A.13}$$

$$\mathfrak{D}^{(b)} = \sum_\alpha \mathbf{Q}_\alpha^{(b)} \dot{q}_\alpha \geq 0 \qquad \text{on } \partial\Omega \tag{A.14}$$

APPENDIX B

Matrix expressions of Eqs. (3.45) and (3.46)

The matrix expressions of the gradient-plasticity constitutive relationship of Eq. (3.45) with drained conditions are

$$E^{ep,sd}_{ijkl} = C^{s}_{ijkl} - \frac{C^{s}_{ijmn}\frac{\partial g}{\partial \sigma_{mn}}\frac{\partial f}{\partial \sigma_{pq}}C^{s}_{pqkl}}{h} \tag{B.1}$$

$$E^{ep,pd}_{ij} = -B_{ij} - \frac{C^{s}_{ijkl}\frac{\partial g}{\partial \sigma_{kl}}\left(\frac{\partial f}{\partial p} - \frac{\partial f}{\partial \sigma_{mn}}B_{mn}\right)}{h} \tag{B.2}$$

$$E^{g,spd}_{ij} = \frac{C^{s}_{ijkl}\frac{\partial g}{\partial \sigma_{kl}}}{h} \tag{B.3}$$

$$\dot{f}^{g} = l^{2}_{\alpha}\frac{\partial f}{\partial Q_{\alpha}}\frac{\partial g}{\partial Q_{\alpha}}H^{nloc}_{\alpha\, ij}\dot{\lambda}_{,ij} \tag{B.4}$$

In the same way, the matrix expressions of the gradient-plasticity constitutive relationship of Eq. (3.46) with undrained conditions are presented here as

$$\begin{aligned} E^{ep,su}_{ijkl} = C_{ijkl} - \frac{C_{ijmn}\frac{\partial g}{\partial \sigma_{mn}}\frac{\partial f}{\partial \sigma_{pq}}C_{pqkl}}{h} - \mathrm{M}^{2}\frac{\frac{\partial g}{\partial p}B_{ij}B_{kl}\frac{\partial f}{\partial p}}{h} + \\ \mathrm{M}\left(\frac{C_{ijmn}\frac{\partial g}{\partial \sigma_{mn}}B_{kl}\frac{\partial f}{\partial p}}{h} + \frac{\frac{\partial g}{\partial p}B_{ij}C_{mnkl}\frac{\partial f}{\partial \sigma_{mn}}}{h}\right) \end{aligned} \tag{B.5}$$

$$E_{ij}^{ep,pu} = -\mathrm{M}\left(B_{ij} - \frac{\frac{\partial g}{\partial p}B_{ij}\left(\mathrm{M}\frac{\partial f}{\partial p} - \frac{\partial f}{\partial \sigma_{mn}}B_{mn}\right)}{h}\right) - \frac{C_{ijkl}\frac{\partial g}{\partial \sigma_{kl}}\left(\mathrm{M}\frac{\partial f}{\partial p} - \frac{\partial f}{\partial \sigma_{mn}}B_{mn}\right)}{h} \tag{B.6}$$

$$E_{ij}^{g,spu} = \frac{C_{ijkl}\frac{\partial g}{\partial \sigma_{kl}} - \mathrm{M}B_{ij}\frac{\partial g}{\partial p}}{h} \tag{B.7}$$

$$\dot{f}^g = l_\alpha^2 \frac{\partial f}{\partial Q_\alpha}\frac{\partial g}{\partial Q_\alpha} H_{\alpha\, ij}^{nloc}\dot{\lambda}_{,ij} \tag{B.8}$$

APPENDIX C

Flow rules

In this section the gradients of the material models presented in Chapter 4 as well as the gradient of the proposed plastic potential of each material models are summarized.

C.1 Modified Cam Clay

When associative flow rule is assumed, $f = g$, the gradients of the yield function are:

$$\frac{\partial f(\sigma, \tau, p, Q_\alpha)}{\partial \sigma_{ij}} = \frac{\partial f}{\partial \sigma}\frac{\partial \sigma}{\partial \sigma_{ij}} + \frac{\partial f}{\partial \tau}\frac{\partial \tau}{\partial \sigma_{ij}} \tag{C.1}$$

$$\begin{aligned} \frac{\partial f}{\partial \sigma} &= 2(\sigma - \beta p) - Q_\alpha \\ \frac{\partial \sigma}{\partial \sigma_{ij}} &= \frac{\delta_{ij}}{3} \\ \frac{\partial f}{\partial \tau} &= \frac{2\tau}{M^2} \\ \frac{\partial \tau}{\partial \sigma_{ij}} &= \frac{S_{ij}}{2\tau} \end{aligned} \tag{C.2}$$

$$\frac{\partial f}{\partial \sigma_{ij}} = \frac{\delta_{ij}}{3}(2(\sigma - \beta p) - Q_\alpha) + \frac{S_{ij}}{M^2} \tag{C.3}$$

being $S_{ij} = \sigma_{ij} - \sigma\delta_{ij}$ the deviator stress tensor.

$$\frac{\partial f}{\partial p} = 2\beta(\sigma - \beta p) - \beta Q_\alpha \tag{C.4}$$

$$\frac{\partial f}{\partial Q_\alpha} = -(\sigma - \beta p) \tag{C.5}$$

On the other hand, when non-associative flow rule is considered, $f \neq g$, the gradients of the plastic potential function are:

$$\frac{\partial g\left(\sigma,\tau,p,Q_\alpha\right)}{\partial\sigma_{ij}} = \frac{\partial g}{\partial\sigma}\frac{\partial\sigma}{\partial\sigma_{ij}} + \frac{\partial g}{\partial\tau}\frac{\partial\tau}{\partial\sigma_{ij}} \tag{C.6}$$

$$\begin{aligned} \frac{\partial g}{\partial\sigma} &= \eta\alpha \\ \frac{\partial g}{\partial J_2} &= 1 \end{aligned} \tag{C.7}$$

$$\frac{\partial g}{\partial\sigma_{ij}} = \eta\alpha\frac{\delta_{ij}}{3} + S_{ij} \tag{C.8}$$

being $S_{ij} = \sigma_{ij} - \sigma\delta_{ij}$ the deviator stress tensor.

$$\frac{\partial g}{\partial p} = \eta\alpha\beta \tag{C.9}$$

$$\frac{\partial g}{\partial Q_\alpha} = -1 \tag{C.10}$$

C.2 Parabolic Drucker-Prager

Whether associative flow rule is assumed, $f = g$, the gradients of the yield function are:

$$\frac{\partial f\left(\sigma,J_2,p,Q_\alpha\right)}{\partial\sigma_{ij}} = \frac{\partial f}{\partial\sigma}\frac{\partial\sigma}{\partial\sigma_{ij}} + \frac{\partial f}{\partial J_2}\frac{\partial J_2}{\partial\sigma_{ij}} \tag{C.11}$$

$$\begin{aligned} \frac{\partial f}{\partial\sigma} &= \alpha \\ \frac{\partial\sigma}{\partial\sigma_{ij}} &= \frac{\delta_{ij}}{3} \\ \frac{\partial f}{\partial J_2} &= 1 \\ \frac{\partial J_2}{\partial\sigma_{ij}} &= S_{ij} \end{aligned} \tag{C.12}$$

$$\frac{\partial f}{\partial\sigma_{ij}} = \alpha\frac{\delta_{ij}}{3} + S_{ij} \tag{C.13}$$

being $S_{ij} = \sigma_{ij} - \sigma\delta_{ij}$ the deviator stress tensor.

$$\frac{\partial f}{\partial p} = \alpha\beta \tag{C.14}$$

$$\frac{\partial f}{\partial Q_\alpha} = -1 \tag{C.15}$$

Finally, when non-associative flow rule is considered, $f \neq g$, the gradients of the plastic potential function are:

$$\frac{\partial g\left(\sigma, J_2, p, Q_\alpha\right)}{\partial \sigma_{ij}} = \frac{\partial g}{\partial \sigma}\frac{\partial \sigma}{\partial \sigma_{ij}} + \frac{\partial g}{\partial J_2}\frac{\partial J_2}{\partial \sigma_{ij}} \tag{C.16}$$

$$\begin{aligned} \frac{\partial g}{\partial \sigma} &= \eta\alpha \\ \frac{\partial g}{\partial J_2} &= 1 \end{aligned} \tag{C.17}$$

$$\frac{\partial g}{\partial \sigma_{ij}} = \eta\alpha\frac{\delta_{ij}}{3} + S_{ij} \tag{C.18}$$

being $S_{ij} = \sigma_{ij} - \sigma\delta_{ij}$ the deviator stress tensor.

$$\frac{\partial g}{\partial p} = \eta\alpha\beta \tag{C.19}$$

$$\frac{\partial g}{\partial Q_\alpha} = -1 \tag{C.20}$$

APPENDIX D

Compatibility relationship of Hadamard

The discontinuous bifurcation conditions deduced in Chapter 5 were mostly based on the following fundamental theorems of Hadamard [47].

Given a continuous and differentiable function $\phi(\boldsymbol{x}, t)$ in the whole domain of the discontinuity surface $S(t)$ (see Fig. D.1), which presents any of its first derivative discontinuous. It can be proved that this discontinuity (or jump) is not arbitrary and the existence of the function $g(\boldsymbol{x}, t)$ is required, such that

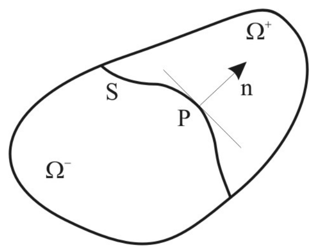

Figure D.1: Discontinuity surface S

a) $[[\phi_{,i}]] = g\, n_i$

b) $\phi(\boldsymbol{x}, t) = -1/c\, [[\dot{\phi}]]$

Firstly, in order to prove the state **a)** the jump operator is defined as:

$$[[\phi_{,i}]] = \phi^+_{,i} - \phi^-_{,i} \tag{D.1}$$

Then, assuming the continuity of the first derivative of $\phi(\boldsymbol{x}, t)$ on the tangential direction to both sides of the surface $S(t)$, the following expression is arrived

$$\frac{\mathrm{d}\phi^+}{\mathrm{d}l} = \phi^+_{,i} t_i \tag{D.2}$$

$$\frac{\mathrm{d}\phi^-}{\mathrm{d}l} = \phi^-_{,i} t_i \tag{D.3}$$

being t_i a unit vector contained in the tangent plane of the surface $S\left(t\right)$.

$$\frac{\mathrm{d}\phi^+}{\mathrm{d}l} - \frac{\mathrm{d}\phi^-}{\mathrm{d}l} = \left[\left[\frac{\mathrm{d}\phi}{\mathrm{d}l}\right]\right] = \left[\left[\phi_{,i}\right]\right] t_i \tag{D.4}$$

However, if the continuity is imposed,

$$\left[\left[\frac{\mathrm{d}\phi}{\mathrm{d}l}\right]\right] = 0 \Rightarrow \left[\left[\phi_{,i}\right]\right] t_i = 0 \tag{D.5}$$

Thereby the condition **a)** is proved given that:

$$\left[\left[\phi_{,i}\right]\right] = g\, n_i \tag{D.6}$$

On the other hand, in order to prove the statement **b)**, for the time instant t it is assumed

$$\phi = \phi\left(\boldsymbol{x}, t\right) \tag{D.7}$$

while for the time instant $t{+}\mathrm{d}t$, the position vector undergoes the following transformation

$$\boldsymbol{x}' = \boldsymbol{x} + \mathrm{d}\boldsymbol{x} = \boldsymbol{x} + c\,\boldsymbol{n}\mathrm{d}t \tag{D.8}$$

where c is propagation velocity of discontinuity,

$$\phi' = \phi\left(\boldsymbol{x}', t + \mathrm{d}t\right) \tag{D.9}$$

$$\phi' = \phi\left(\boldsymbol{x}, t\right) + \phi_{,i}\mathrm{d}x_i + \dot{\phi}\mathrm{d}t \tag{D.10}$$

The continuity of ϕ requires the simultaneously fulfillment of $[[\phi']] = 0$ and $[[\phi]] = 0$, thus

$$\left[\left[\phi\left(\boldsymbol{x}, t\right)\right]\right] + \left[\left[\phi_{,i}\right]\right] \mathrm{d}x_i + [[\dot{\phi}]]\mathrm{d}t = 0 \tag{D.11}$$

$$\left[\left[\phi_{,i}\right]\right] c\, n_i\mathrm{d}t = -[[\dot{\phi}]]\mathrm{d}t \tag{D.12}$$

$$\left[\left[\phi_{,i}\right]\right] = -\frac{1}{c}[[\dot{\phi}]]n_i \tag{D.13}$$

Since $[[\phi_{,i}]] = g\, n_i$ from Eq. (D.6),

$$g\left(\boldsymbol{x}, t\right) = -\frac{1}{c}[[\dot{\phi}]] \tag{D.14}$$

Similarly it is possible to make the same demonstration for higher order functions:

$$[[\phi_{i,j}]] = g_i n_j \tag{D.15}$$

$$g_i = -\frac{1}{c}[[\dot{\phi}_i]]n_i \tag{D.16}$$

APPENDIX E

Stress state domain

Generally, yield surfaces are functions of stress invariants. Therefore, to evaluate the stress state of a generic point on the yield surface it is necessary to obtain a mathematical expression to connect the components of the stress tensor with its invariants (on the yield surface).

Therefore, considering principal stress state for simplicity, the following relationship are used for the first invariant of the stress tensor, I_1, and the second invariant of the deviatoric stress tensor, J_2, [87]

$$I_1 = \sigma_{kk} \quad ; \quad J_2 = \frac{1}{2} S_{ij} S_{ji} \tag{E.1}$$

being $S_{ij} = \sigma_{ij} - \delta_{ij} I_1/3$ the deviatoric stress tensor. When the principal stress state is considered the above expression should be written as

$$\begin{aligned} I_1 &= \sigma_1 + \sigma_2 + \sigma_3 \\ J_2 &= \frac{1}{3} \left[\sigma_1^2 + \sigma_2^2 + \sigma_3^2 - (\sigma_1\sigma_2 + \sigma_2\sigma_3 + \sigma_3\sigma_1) \right] \end{aligned} \tag{E.2}$$

Both invariants are obtained for a specific point of the yield surface. However, the general three-dimensional stress state can not be specified because it has more unknown variables than the amount of equations.

E.1 Plane stress state

For plane stress state the third principal stress is zero,

$$\sigma_3 = 0 \tag{E.3}$$

then, combining Eq. (E.3) with Eq. (E.1) and Eq. (E.2) the remaining principal stress are follows

$$\sigma_1 = \frac{3I_1 + \sqrt{-3I_1^2 + 36J_2}}{6} \tag{E.4}$$

$$\sigma_2 = \frac{3I_1 - \sqrt{-3I_1^2 + 36J_2}}{6} \tag{E.5}$$

From Eq. (E.4) and Eq. (E.5) it can be concluded that the real solutions for σ_1 and σ_2 should satisfy the following expression

$$-3I_1^2 + 36J_2 \geq 0 \tag{E.6}$$

E.2 Plane strain state

In plane strain state the third principal stress is a function of both σ_1 and σ_2,

$$\sigma_3 = \nu\left(\sigma_1 + \sigma_2\right) \tag{E.7}$$

then, combining Eq. (E.7) with Eq. (E.1) and Eq. (E.2) the remaining principal stress are follows

$$\sigma_1 = \frac{I_1}{2\left(1+\nu\right)} + \frac{1}{6\left(1+\nu\right)}\sqrt{-3\left(1-2\nu\right)^2 I_1^2 + 36\left(1+\nu\right)^2 J_2} \tag{E.8}$$

$$\sigma_2 = \frac{I_1}{2\left(1+\nu\right)} - \frac{1}{6\left(1+\nu\right)}\sqrt{-3\left(1-2\nu\right)^2 I_1^2 + 36\left(1+\nu\right)^2 J_2} \tag{E.9}$$

Finally, from Eq. (E.8) and Eq. (E.9) it can be concluded that for plain strain the real solutions of σ_1 and σ_2 should satisfy the following expression

$$-3\left(1-2\nu\right)^2 I_1^2 + 36\left(1+\nu\right)^2 J_2 \geq 0 \tag{E.10}$$

E.3 Domain for a particularized material model

Both limit deduce before, Eq. (E.6) and Eq. (E.10), are generics and therefore are valid for any material model considered, within the hypothesis of plane strain or plane stress. In this regard, the main aim of this section is the definition of the I_1 domain for the modified Cam Clay plasticity model and the parabolic Drucker-Prager criterion.

Modified Cam Clay domain When the Modified Cam Clay plasticity model is considered the second invariant of the deviator stress tensor can be obtained from Eq. (4.1)

$$J_2 = M^2 \left[Q_\alpha (\sigma - \beta p) - (\sigma - \beta p)^2\right] \tag{E.11}$$

for each stress state on the yield surface.

Finally, replacing Eq. (E.11) in the generic domains deduced before, Eq. (E.6) and Eq. (E.10), the following quadratic polynomial expression for the total hydrostatic stress, $\sigma = I_1/3$ are obtained

$$a\sigma^2 + b\sigma + c = 0 \tag{E.12}$$

being, for plane stress,

$$\begin{aligned} a &= -\left(1 + \frac{3}{4M^2}\right) \\ b &= Q_\alpha - 2\beta p \\ c &= Q_\alpha p\beta - (\beta p)^2 \end{aligned} \tag{E.13}$$

and, for plane strain,

$$\begin{aligned} a &= -\left[1 + \frac{3}{4}\left(\frac{1-2\nu}{M(1+\nu)}\right)^2\right] \\ b &= Q_\alpha - 2\beta p \\ c &= Q_\alpha p\beta - (\beta p)^2 \end{aligned} \tag{E.14}$$

Then, the limits of the first invariant of the stress tensor can be obtained by Eq. (E.12) considering Eq. (E.13) for plane stress or Eq. (E.14) for plane strain hypothesis.

Parabolic Drucker-Prager domain Similarly, if the Parabolic Drucker-Prager plasticity model is considered the second invariant of the deviator stress tensor can be obtained from Eq. (4.12)

$$J_2 = Q_\alpha - \alpha(\sigma - \beta p) \tag{E.15}$$

for each stress state on the yield surface.

Then, replacing Eq. (E.15) in Eq. (E.6) and Eq. (E.10), the following quadratic polynomial expression for the first invariant of the stress tensor are obtained

$$aI_1^2 + bI_1 + c = 0 \tag{E.16}$$

being, for plane stress,

$$\begin{aligned} a &= -3 \\ b &= -12\alpha \\ c &= 36\left(Q_\alpha - \alpha\beta p\right) \end{aligned} \tag{E.17}$$

and, for plane strain,

$$\begin{aligned} a &= -3\left(1-2\nu\right)^2 \\ b &= -12\alpha\left(1+\nu\right)^2 \\ c &= 36\left(1+\nu\right)^2\left(Q_\alpha - \alpha\beta p\right) \end{aligned} \tag{E.18}$$

Finally, the limits of the first invariant of the stress tensor can be obtained by Eq. (E.16) considering Eq. (E.17) for plane stress or Eq. (E.18) for plane strain hypothesis.

APPENDIX F

Finite Element Matrix

The matrix expressions of the FE stiffness matrix for gradient-plasticity Eq. (6.21) are

$$\mathbf{K}_{\mathrm{ss}} = \int_\Omega \bar{\mathbf{B}}^T : \mathbf{C}^s : \bar{\mathbf{B}} \; \mathrm{d}\Omega \tag{F.1}$$

$$\mathbf{K}_{\mathrm{pp}} = \int_\Omega \frac{\mathbf{N}_p^T \mathbf{N}_p}{M} \mathrm{d}\Omega \tag{F.2}$$

$$\mathbf{K}_{\lambda\lambda} = \int_\Omega \mathbf{H}^T \left[\mathbf{f}^s : \mathbf{C}^s : \mathbf{g}^s + \bar{H}_\alpha^{loc} \right] \mathbf{H} + l_\alpha^2 \mathbf{H}^T \bar{\mathbf{H}}_\alpha^{nloc} \mathbf{P} \; \mathrm{d}\Omega \tag{F.3}$$

$$\mathbf{H}_{\mathrm{pp}} = \int_\Omega \left(\nabla \mathbf{N}_p \right)^T \cdot \mathbf{k} \cdot \nabla \mathbf{N}_p \mathrm{d}\Omega \tag{F.4}$$

$$\mathbf{Q}_{\mathrm{sp}} = \int_\Omega \bar{\mathbf{B}}^T : \mathbf{B} \mathbf{N}_p \; \mathrm{d}\Omega \tag{F.5}$$

$$\mathbf{Q}_{\mathrm{ps}} = \int_\Omega \mathbf{N}_p^T \mathbf{B} : \bar{\mathbf{B}} \; \mathrm{d}\Omega \tag{F.6}$$

$$\mathbf{Q}_{\mathrm{s}\lambda} = \int_\Omega \bar{\mathbf{B}}^T : \mathbf{C}^s : \mathbf{g}^s \mathbf{H} \; \mathrm{d}\Omega \tag{F.7}$$

$$\mathbf{Q}_{\lambda\mathrm{s}} = \int_\Omega \mathbf{H}^T \mathbf{f}^s : \mathbf{C}^s : \bar{\mathbf{B}} \; \mathrm{d}\Omega \tag{F.8}$$

$$\mathbf{Q}_{\mathrm{p}\lambda} = \int_\Omega \mathbf{N}_p^T \left[\mathrm{g}^p - \mathbf{B} : \mathbf{g}^s \right] \mathbf{H} \; \mathrm{d}\Omega \tag{F.9}$$

$$\mathbf{Q}_{\lambda\mathrm{p}} = \int_\Omega \mathbf{H}^T \left[\mathrm{f}^p - \mathbf{f}^s : \mathbf{B} \right] \mathbf{N}_p \; \mathrm{d}\Omega \tag{F.10}$$

$$\mathbf{F}_{\mathrm{s}}^{\mathrm{int}} = \int_\Omega \bar{\mathbf{B}}^T : \boldsymbol{\sigma}_j \mathrm{d}\Omega \tag{F.11}$$

$$\mathbf{F}_{\mathrm{s}}^{\mathrm{ext}} = \int_{\partial\Omega} \mathbf{N}_u^T \mathbf{t}_{j+1} \mathrm{d}\partial\Omega \tag{F.12}$$

$$\mathbf{F}_{\mathrm{p}} = \Delta t \mathbf{H}_{\mathrm{pp}} \bar{p}_j + \Delta t \int_{\partial\Omega} \mathbf{N}_p^T \mathbf{w}_{j+1} \cdot \mathbf{n} \; \mathrm{d}\partial\Omega \tag{F.13}$$

$$\mathbf{F}_\lambda = \int_\Omega \mathbf{H}^T \; f\left(\boldsymbol{\sigma}_j, p_j, Q_{\alpha_j} \right) \; \mathrm{d}\Omega \tag{F.14}$$

APPENDIX G

Two dimensional hermitian shape functions

In order to derive the hermitian shape functions $\mathbf{H}$ of Eq. (6.14) a natural coordinated system is used (see Fig. 6.1).

This Section presents the Hermitian shape functions of quadrilateral 4-node finite element discussed in Chapter 6. As was outlined in Section 6.2 the plastic multiplier must be interpolated using C_1-continuous shape functions, $\mathbf{H}$, then

$$\mathbf{H} = \bar{\mathbf{H}}\mathbf{K} \tag{G.1}$$

where $\mathbf{H}$ and $\bar{\mathbf{H}}$ are the Hermitian shape functions in global and local coordinate system, respectively, and $\mathbf{K}$ is the coordinate transformation matrix,

$$\mathbf{K} = \begin{bmatrix} 1 & 0 & 0 & 0 \\ 0 & \frac{\partial x}{\partial \xi} & \frac{\partial y}{\partial \xi} & 0 \\ 0 & \frac{\partial x}{\partial \eta} & \frac{\partial y}{\partial \eta} & 0 \\ 0 & 0 & 0 & 1 \end{bmatrix} \tag{G.2}$$

It can be seen that the coordinate transformation matrix $\mathbf{K}$ is formed by elements of the Jacobian matrix, $\mathbf{J}$. Thus, the matrix $\bar{\mathbf{H}}$ corresponding to the j node is

$$\bar{\mathbf{H}} = \begin{Bmatrix} \bar{h}_j \\ \bar{h}_{\xi j} \\ \bar{h}_{\eta j} \\ \bar{h}_{\eta \xi j} \end{Bmatrix} \qquad \text{for node } j = 1, 2, 3, 4 \tag{G.3}$$

with

$$\bar{h}_j(\xi, \eta) = \frac{1}{16}\left[3\xi_j\xi - \xi_j\xi^3 + 2\right]\left[3\eta_j\eta - \eta_j\eta^3 + 2\right] \tag{G.4}$$

$$\bar{h}_{\xi j}(\xi, \eta) = \frac{1}{16}\left[\xi^3 + \xi_j\xi^2 - \xi - \xi_j\right]\left[3\eta_j\eta - \eta_j\eta^3 + 2\right] \tag{G.5}$$

$$\bar{h}_{\eta j}\left(\xi,\eta\right)=\frac{1}{16}\left[3\xi_j\xi-\xi_j\xi^3+2\right]\left[\eta^3+\eta_j\eta^2-\eta-\eta_j\right] \tag{G.6}$$

$$\bar{h}_{\eta\xi j}\left(\xi,\eta\right)=\frac{1}{16}\left[\xi^3+\xi j\xi^2-\xi-\xi j\right]\left[\eta^3+\eta_j\eta^2-\eta-\eta_j\right] \tag{G.7}$$

For better understanding of expressions (G.4) - (G.6) the Hermitian shape function adopted for node 1 are ploted in Fig. G.1.

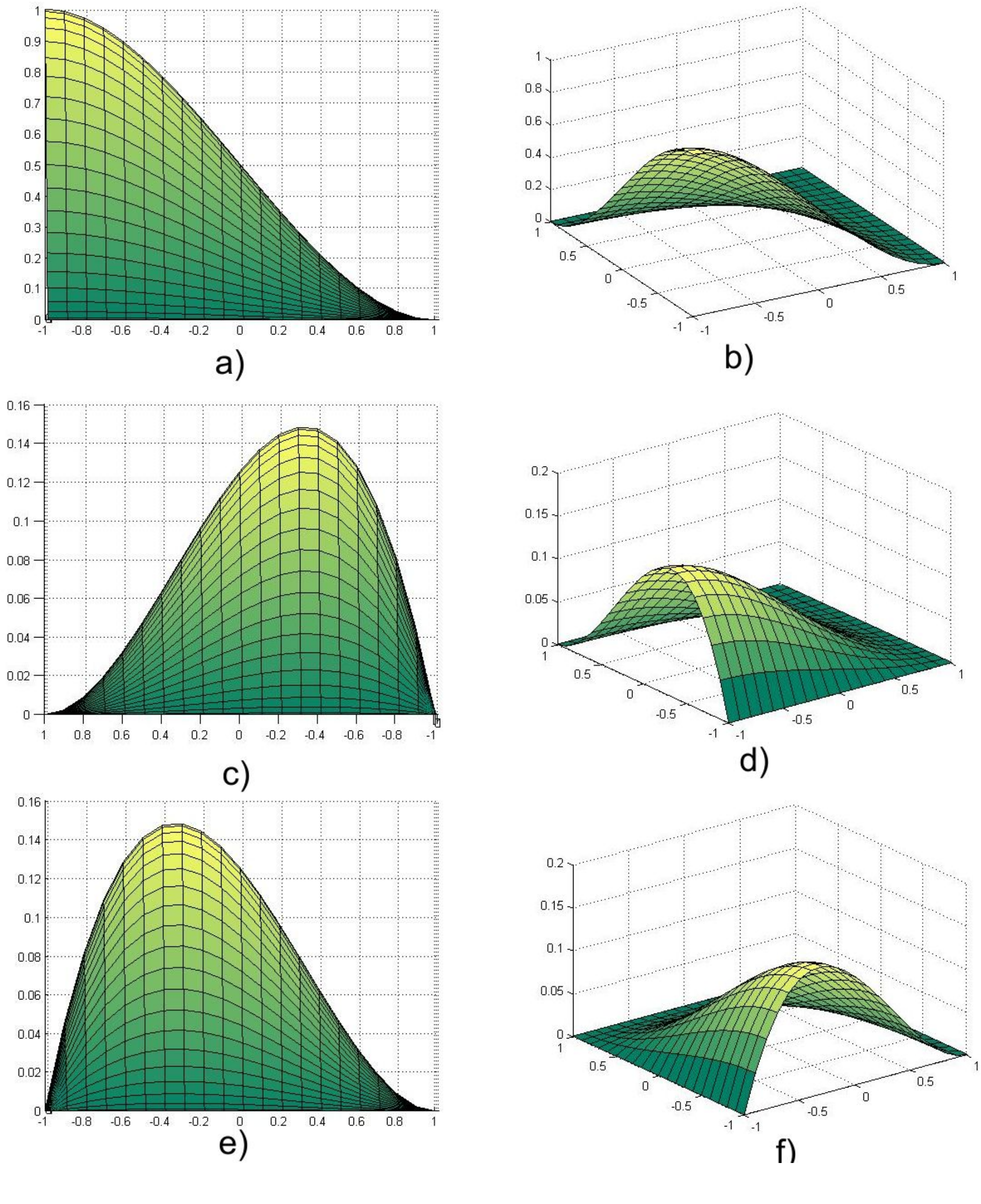

Figure G.1: C_1-continuous shape function for: a) and b) plastic multiplier λ; c) and d) for $\partial\lambda/\partial x$; e) and f) for $\partial\lambda/\partial y$

Bibliography

[1] M.-A. Abellan and R. de Borst. Wave propagation and localisation in a softening two-phase medium. *Comput. Meth. Appl. Mech.*, 195:5011–5019, 2006.

[2] R. K. Abu Al-Rub and G. Z. Voyiadjis. A physically based gradient plasticity theory. *Int. J. Plasticity*, 22(4):654–684, 2006.

[3] R. K. Abu Al-Rub, G. Z. Voyiadjis, and D. J. Bammann. A thermodynamic based higher-order gradient theory for size dependent plasticity. *Int. J. Solids Struct.*, 44(9):2888–2923, 2007.

[4] E. C. Aifantis. On scale invariance in anisotropic plasticity, gradient plasticity and gradient elasticity. *Int. J. Eng. Sci.*, 47(11-12):1089–1099, 2009.

[5] E. E. Alonso, A. Gens, and A. Josa. A constitutive model for partially saturated soils. *Geotechnique*, 40(3):405–430, 1990.

[6] J. L. Auriault and C. Boutin. Deformable porous media with double porosity. Quasi-statics. I: Coupling effects. *Transp. Porous Media*, 7(1):63–82, 1992.

[7] A.R. Balmaceda. *Compacted soils, a theoretical and experimental study (in spanish).* Tesis doctoral, Universidad Politcnica de Catalunya, 1991.

[8] L. Bardella. Some remarks on the strain gradient crystal plasticity modelling, with particular reference to the material length scales involved. *Int. J. Plasticity*, 23(2):296–322, 2007.

[9] L. Bardella. Size effects in phenomenological strain gradient plasticity constitutively involving the plastic spin. *Int. J. Eng. Sci.*, 48(5):550–568, 2010.

[10] B. Bary, J.-P. Bournazel, and E. Bourdarot. Poro-damage approach applied to hydro-fracture analysis of concrete. *J. Eng. Mech.*, 126(9):937–943, 2000.

[11] T. Belytschko, W. K. Liu, and B. Moran. *Nonlinear Finite Elements for Continua and Structures.* John Wiley & Sons, England., 2000.

[12] A. Benallal and C. Comi. Material instabilities in inelastic saturated porous media under dynamic loadings. *Int. J. Solids Struct.*, 39(13-14):3693–3716, 2002.

[13] G. Bolzon, B.A. Schrefler, and O.C. Zienkiewicz. Elastoplastic soil constitutive laws generalized to partially saturated states. *Geotechnique*, 46(2):279–289, 1996.

[14] R. I. Borja. Cam-Clay plasticity. Part V: A mathematical framework for three-phase deformation and strain localization analyses of partially saturated porous media. *Comput. Meth. Appl. Mech.*, 193:5301–5338, 2004.

[15] R. I. Borja and A. Koliji. On the effective stress in unsaturated porous continua with double porosity. *J. Mech. Phys. Solids.*, 57(8):1182–1193, 2009.

[16] A. Carosio, K. Willam, and G. Etse. On the consistency of viscoplastic formulations. *Int. J. Solids Struct.*, 37(48-50):7349–7369, 2000.

[17] C. Comi. Non-local model with tension and compression damage mechanisms. *Eur. J. Mech. A-Solid*, 20(1):1–22, 2001.

[18] O. Coussy. *Mechanics of Porous Continua.* John Wiley & Sons., 1995.

[19] O. Coussy. *Poromechanics.* John Wiley & Sons., 2004.

[20] O. Coussy, L. Dormieux, and E. Detournay. From mixture theory to Biot's approach for porous media. *Int. J. Solids Struct.*, 35(34):4619–4635, 1998.

[21] O. Coussy and P. Monteiro. Unsaturated poroelasticity for crystallization in pores. *Comput. Geotech.*, 34(4):279–290, 2007.

[22] R. de Borst and H. B. Mühlhaus. Gradient-dependent plasticity: Formulation and algorithmic aspects. *Int. J. Numer. Meth. Eng.*, 35:521–539, 1992.

[23] R. de Borst and J. Pamin. Gradient plasticity in numerical simulation of concrete cracking. *Eur. J. Mech. A-Solid*, 15(2):295–320, 1996.

[24] R. de Borst and J. Pamin. Some novel developments in finite element procedures for gradient-dependent plasticity. *Int. J. Numer. Meth. Eng.*, 39(14):2477–2505, 1996.

[25] H. A. Di Rado, P. A. Beneyto, J. L. Mroginski, and A. M. Awruch. Influence of the saturation-suction relationship in the formulation of non-saturated soils consolidation models. *Math. Comput. Model.*, 49(5-6):1058–1070, 2009.

[26] H. A. Di Rado, J. L. Mroginski, P. A. Beneyto, and A. M. Awruch. A symmetric constitutive matrix for the nonlinear analysis of hypoelastic solids based on a formulation leading to a non-symmetric stiffness matrix. *Commun. Numer. Meth. Eng.*, 24(11):1079–1092, 2008.

[27] R. J. Dorgan and G. Z. Voyiadjis. A mixed finite element implementation of a gradient-enhanced coupled damage-plasticity model. *Int. J. Damage Mech.*, 15(3):201–235, 2006.

[28] Robert J. Dorgan. *A nonlocal model for coupled damage-plasticity incorporating gradients of internal state variables at multiscales.* Ph.D. Thesis, Louisiana State University, 2006.

[29] D. C. Drucker and W. Prager. Soil mechanics and plastic analysis of limit design. *Quarterly of Applied Mathematics*, 10:157–165, 1952.

[30] W. Ehlers and P. Blome. A triphasic model for unsaturated soil based on the theory of porous media. *Math. Comput. Model.*, 37:507–513, 2003.

[31] W. Ehlers, T. Graf, and M. Ammann. Deformation and localization analysis of partially saturated soil. *Comput. Meth. Appl. Mech.*, 193(27-29):2885–2910, 2004.

[32] M. Ekh, M. Grymer, K. Runesson, and T Svedberg. Gradient crystal plasticity as part of the computational modelling of polycrystals. *Int. J. Numer. Meth. Eng.*, 72(2):197–220, 2007.

[33] I. Ertürk, J. A. W. van Dommelen, and M. G. D. Geers. Energetic dislocation interactions and thermodynamical aspects of strain gradient crystal plasticity theories. *J. Mech. Phys. Solids.*, 57(11):1801–1814, 2009.

[34] G. Etse, A. Caggiano, and S. Vrech. Multiscale failure analysis of fiber reinforced concrete based on a discrete crack model. *Int. J. Fracture*, page (in press), 2012.

[35] G. Etse and J. L. Mroginski. Thermodynamic consistent gradient-poroplasticity theory for porous media. In *Computational Plasticity XI - Fundamentals and Applications, COMPLAS XI*, pages 342–353, 2011.

[36] G. Etse and S. Vrech. Geometrical method for localization analysis in gradient-dependent J2 plasticity. *J. Appl. Mech.*, 73(6):1026–1030, 2006.

[37] G. Etse, S. M. Vrech, and J. L. Mroginski. Analytical and geometrical localization analysis of the elastoplastic leon-drucker-prager model based on gradient theory and fracture energy. In *Computational Plasticity XI - Fundamentals and Applications, COMPLAS X*, 2009.

[38] G. Etse and K. Willam. Assessment of localized failure in plain concrete. *ZAMM (Zeitschrift fuer angewante Mathemathik und Mechanik)*, pages 234–236, 1994.

[39] G. Etse and K. Willam. Fracture energy formulation for inelastic behavior of plain concrete. *J. Eng. Mech.*, 120(9):1983–2011, 1994.

[40] N. A. Fleck and J. W. Hutchinson. A reformulation of strain gradient plasticity. *J. Mech. Phys. Solids.*, 49(10):2245–2271, 2001.

[41] D. G. Fredlund and A. Xing. Equations for the soil-water characteristic curve. *Can. Geotech. J.*, 31:521–532, 1994.

[42] P. Fredriksson, P. Gudmundson, and L. P. Mikkelsen. Finite element implementation and numerical issues of strain gradient plasticity with application to metal matrix composites. *Int. J. Solids Struct.*, 46(22-23):3977–3987, 2009.

[43] D. Gawin, P. Baggio, and B. A. Schrefler. Coupled heat, water and gas flow in deformable porous media. *Int. J. Numer. Meth. Fl.*, 20:969–987, 1995.

[44] P. Gudmundson. A unified treatment of strain gradient plasticity. *J. Mech. Phys. Solids.*, 52:1379–1406, 2004.

[45] P. Guo. Undrained shear band in water saturated granular media: A critical revisiting with numerical examples. *Int. J. Numer. Anal. Met.*, page (in press) doi: 10.1002/nag.1101, 2011.

[46] M. E. Gurtin and L. Anand. Thermodynamics applied to gradient theories involving the accumulated plastic strain: The theories of aifantis and fleck and hutchinson and their generalization. *J. Mech. Phys. Solids.*, 57(3):405–421, 2009.

[47] J. Hadamard. *Propagation des ondes et les equations d'Hydrodynamique*. New York: Chelsea (reprinted 1949), 1903.

[48] K. Hashiguchi and S. Tsutsumi. Gradient plasticity with the tangential-subloading surface model and the prediction of shear-band thickness of granular materials. *Int. J. Plasticity*, 23(5):767–797, 2007.

[49] S. M. Hassanizadeh and W. G. Gray. General conservation equation for multiphase sistems: 1, averaging procedures. *Adv. Water Resour.*, 2:131–144, 1979.

[50] S. M. Hassanizadeh and W. G. Gray. General conservation equation for multiphase sistems: 2, mass momenta, energy and entropy equations. *Adv. Water Resour.*, 2:191–203, 1979.

[51] S. M. Hassanizadeh and W. G. Gray. General conservation equation for multiphase sistems: 3, constitutive theory for porous media flow. *Adv. Water Resour.*, 3:25–40, 1980.

[52] R. Hill. Acceleration waves in solids. *J. Mech. Phys. Solids.*, 10:1–16, 1962.

[53] C. B. Hirschberger and P. Steinmann. Classification of concepts in thermodynamically consistent generalized plasticity. *J. Eng. Mech.*, 135(3):156–170, 2009.

[54] Y. Huang and Y.-K Zhang. Constitutive relation of unsaturated soil by use of the mixture theory (I) - nonlinear constitutive equations and field equations. *Adv. Appl. Mech.*, 24(2):123–137, 2003.

[55] T. Ito. Effect of pore pressure gradient on fracture initiation in fluid saturated porous media: Rock. *Eng. Fract. Mech.*, 75(7):1753–1762, 2008.

[56] M. Jirsek and S. Rolshoven. Localization properties of strain-softening gradient plasticity models. Part I: Strain-gradient theories. *Int. J. Solids Struct.*, 46(11-12):2225–2238, 2009.

[57] K. Kamrin. Nonlinear elasto-plastic model for dense granular flow. *Int. J. Plasticity*, 26(2):167–188, 2010.

[58] N. Khalili and M. H. Khabbaz. On the theory of three-dimensional consolidation in unsaturated soils. In E.E. Alonso and P. Delage, editors, *First International Conference on Unsaturated Soils - UNSAT'95.*, pages 745–750, 1995.

[59] N. Khalili and B. Loret. An elasto-plastic model for non-isothermal analysis of flow and deformation in unsaturated porous media: formulation. *Int. J. Solids Struct.*, 38(46-47):8305–8330, 2001.

[60] O. Kristensson and A. Ahadi. Numerical study of localization in soil systems. *Comput. Geotech.*, 32(8):600–612, 2005.

[61] M. Kuroda and V. Tvergaard. A finite deformation theory of higher-order gradient crystal plasticity. *J. Mech. Phys. Solids.*, 56(8):2573–2584, 2008.

[62] M. Kuroda and V. Tvergaard. On the formulations of higher-order strain gradient crystal plasticity models. *J. Mech. Phys. Solids.*, 56(4):1591–1608, 2008.

[63] M. Kuroda and V. Tvergaard. An alternative treatment of phenomenological higher-order strain-gradient plasticity theory. *Int. J. Plasticity*, 26(4):507–515, 2010.

[64] L. La Ragione, V. C. Prantil, and I. Sharma. A simplified model for inelastic behavior of an idealized granular material. *Int. J. Plasticity*, 24(1):168–189, 2008.

[65] T. Y. Lai, R. I. Borja, B. G. Duvernay, and R. L. Meehan. Capturing strain localization behind a geosynthetic-reinforced soil wall. *Int. J. Numer. Anal. Met.*, 27:425–451, 2003.

[66] R. W. Lewis and B. A. Schrefler. *The Finite Element Method in the Static and Dynamic Deformation and Consolidation of Porous Media.* John Wiley & Sons., 1998.

[67] T. Liebe, P. Steinmann, and A. Benallal. Theoretical and computational aspects of a thermodynamically consistent framework for geometrically linear gradient damage. *Comput. Meth. Appl. Mech.*, 190:6555–6576, 2001.

[68] X. Liu and A. Scarpas. Numerical modeling of the influence of water suction on the formation of strain localization in saturated sand. *CMES-Comp. Model Eng.*, 9(1):57–74, 2005.

[69] L.E. Malvern. *Introduction to the mechanics of a Continuous Medium.* Prentice Hall. Englewood Cliffs. New York, 1969.

[70] N. J. Mattei, M. M. Mehrabadi, and H. Zhu. A micromechanical constitutive model for the behavior of concrete. *Mech. Mater.*, 39(4):357–379, 2007.

[71] M. Mokni and J. Desrues. Strain localization measurements in undrained plane-strain biaxial tests on hostun RF sand. *Mech. Cohes-Frict. Mat.*, 4:419–441, 1998.

[72] J. L. Mroginski. *Non linear geomechanics applied to environmental problems in partially saturated porous media (in spanish).* Mg. Thesis., Northeast National University, Argentine, 2008.

[73] J. L. Mroginski, H. A. Di Rado, P. A. Beneyto, and A. M. Awruch. A finite element approach for multiphase fluid flow in porous media. *Math. Comput. Simul.*, 81:76–91, 2010.

[74] J. L. Mroginski and G. Etse. Discontinuous bifurcation analysis in thermodynamically consistent gradient poroplastic materials. *Int. J. Solids Struct.*, submitted, 2013.

[75] J. L. Mroginski and G. Etse. A finite element formulation of gradient-based plasticity for porous media with C1 interpolation of internal variables. *Comput. Geotech.*, 49:7–17, 2013.

[76] J. L. Mroginski, G. Etse, and S. M. Vrech. A thermodynamical gradient theory for deformation and strain localization of porous media. *Int. J. Plasticity*, 27:620–634, 2011.

[77] K. K. Muraleetharan, C. Liu, C. Wei, T. C. G. Kibbey, and L. Chen. An elastoplatic framework for coupling hydraulic and mechanical behavior of unsaturated soils. *Int. J. Plasticity*, 25(3):473–490, 2009.

[78] V. D. Murty, C. L. Clay, M. P. Camden, and D. B. Paul. Natural convection around a cylinder buried in a porous medium- non-Darcian effects. *Appl. Math. Modell.*, 18:134–141, 1994.

[79] S. Naili, O. Le Gallo, and D. Geiger. Mechanics of biological porous media. theoretical approach and numerical approximation. *J. Biomech.*, 22(10):1062, 1989.

[80] Q. -S. Nguyen and S. Andrieux. The non-local generalized standard approach: A consistent gradient theory. *Comptes Rendus - Mecanique*, 333(2):139–145, 2005.

[81] F. Nicot and F. Darve. A micro-mechanical investigation of bifurcation in granular materials. *Int. J. Solids Struct.*, 44(20):6630–6652, 2007.

[82] F. Nicot, L. Sibille, and F. Darve. Bifurcation in granular materials: An attempt for a unified framework. *Int. J. Solids Struct.*, 46(22-23):3938–3947, 2009.

[83] N. S. Ottosen and K. Runesson. Properties of discontinuous bifurcation solutions in elasto-plasticity. *Int. J. Solids Struct.*, 27(4):401–421, 1991.

[84] J. Pamin. *Gradient-dependent plasticity in numerical simulation of localization phenomena.* PhD. Thesis., TU-Delft, The Netherlands, 1994.

[85] J. Pamin and A. Stankiewicz. Numerical simulation of instabilities in one- and two-phase soil model based on Cam-clay plasticity. *Technical Transactions*, 20:81–91, 2008. Series Environmental Enginnering 3-S/2008.

[86] Y. Pan, X. Wang, and Z. Li. Analysis of the strain softening size effect for rock specimens based on shear strain gradient plasticity theory. *Int. J. Rock Mech. Min.*, 39(6):801–805, 2002.

[87] J. M. Parns. *Modeling and localized failure analysis in concrete.* Mg. Thesis., National University of Tucuman, Argentine, 2005.

[88] D. M. Pedroso and M. M. Farias. Extended barcelona basic model for unsaturated soils under cyclic loadings. *Comput. Geotech.*, 38(5):731–740, 2011.

[89] R.H.J. Peerlings, R. de Borst, W.A.M. Brekelmans, and M.G.D. Geers. Gradient-enhanced damage modelling of concrete fracture. *Mech. Cohes-Frict. Mat.*, 3(4):323–342, 1998.

[90] D. Perić. *Localized deformation and failure analysis of pressure sensitive granular materials.* PhD. Thesis., University of Colorado, CEAE Dept., Boulder, 1990.

[91] D. Perić and H. A. Rasheed. Localized failure of fibre-reinforced elastic-plastic materials subjected to plane strain loading. *Int. J. Numer. Anal. Met.*, 31(7):893–916, 2007.

[92] F. Pesavento, D. Gawin, and B. A. Schrefler. Modeling cementitious materials as multiphase porous media: Theoretical framework and applications. *Acta Mech.*, 201(1-4):313–339, 2008.

[93] F. Pesavento, B. A. Schrefler, and D. Gawin. Modelling of coupled multifield problems in concrete by means of porous media mechanics. In *Proceedings of the 6th International Conference on Fracture Mechanics of Concrete and Concrete Structures.*, pages 485–493, 2007.

[94] J. Pierre, B. David, H. Petite, and C. Oddou. Mechanics of active porous media: Bone tissue engineering application. *J. Mech. Med. Biol.*, 8(2):281–292, 2008.

[95] C. Polizzotto. Thermodynamics-based gradient plasticity theories with an application to interface models. *Int. J. Solids Struct.*, 45(17):4820–4834, 2008.

[96] C. Polizzotto. A link between the residual-based gradient plasticity theory and the analogous theories based on the virtual work principle. *Int. J. Plasticity*, 25(11):2169–2180, 2009.

[97] C. Polizzotto. A nonlocal strain gradient plasticity theory for finite deformations. *Int. J. Plasticity*, 25(7):1280–1300, 2009.

[98] S. Ramaswamy and N. Aravas. Finite element implementation of gradient plasticity models part I: Gradient-dependent yield functions. *Comput. Meth. Appl. Mech.*, 163(1-4):11–32, 1998.

[99] K.H. Roscoe and J.B. Burland. *On the generalized stress-strain behaviour of wet clay.* In Engineering Plasticity, eds. J. Heyman and F.A. Leckie. Cambridge University Press., 1968.

[100] K.H. Roscoe, A.N. Schofield, and C.P. Wroth. On the yielding of soils. *Geotechnique*, 8:22–53, 1958.

[101] J. Rudnicki and J. Rice. Localization analysis of elastic degradation with application to scalar damage. *J. Eng. Mech.*, 23:371–394, 1975.

[102] K. Runesson, N. S. Ottosen, and P. Dunja. Discontinuous bifurcations of elastic-plastic solutions at plane stress and plane strain. *Int. J. Plasticity*, 7(1-2):99–121, 1991.

[103] K. Runesson, D. Perić, and S. Sture. Effect of pore fluid compressibility on localization in elastic-plastic porous solids under undrained conditions. *Int. J. Solids Struct.*, 33(10):1501–1518, 1996.

[104] P. J. Sabatini and R. J. Finno. Effect of consolidation on strain localization of soft clays. *Comput. Geotech.*, 18(4):311–339, 1996.

[105] R. Schiava and G. Etse. Constitutive modelling and discontinuous bifurcation assessment in unsaturated soils. *J. Appl. Mech.*, 73(6):1039–1044, 2006.

[106] A.N. Schofield and C.P. Wroth. *Critical State Soil Mechanics.* London, England: McGraw-Hill, 1968.

[107] B. A. Schrefler and F. Pesavento. Multiphase flow in deforming porous material. *Comput. Geotech.*, 31:237–250, 2004.

[108] B.A. Schrefler. F.E. in environmental engineering: coupled thermo-hydro-mechanical processes in porous media including pollutant transport. *Archives of Computational Methods in Engineering*, 2(3):1–54, 1995.

[109] L. Schreyer-Bennethum. Theory of flow and deformation of swelling porous materials at the macroscale. *Comput. Geotech.*, 34(4):267–278, 2007.

[110] J. Y. Shu, W. E. King, and N. A. Fleck. Finite elements for materials with strain gradient effects. *Int. J. Numer. Meth. Eng.*, 44(3):373–391, 1999.

[111] J.C. Simo and C. Miehe. Associative coupled thermoplasticity at finite strains: formulation, numerical analysis and implementation. *Comput. Meth. Appl. Mech.*, 98(1):41–104, 1992.

[112] A. Simone, G. N. Wells, and L. J. Sluys. From continuous to discontinuous failure in a gradient-enhanced continuum damage model. *Comput. Meth. Appl. Mech.*, 192(41-42):4581–4607, 2003.

[113] A. Stankiewicz and J. Pamin. Finite element analysis of fluid influence on instabilities in two-phase cam-clay plasticity model. *Computer Assisted Mechanics and Engineering Science*, 13(4):669–682, 2006.

[114] A. Stankiewicz and J. Pamin. Gradient-enhanced cam-clay model in simulation of strain localization in soil. *Foundation of Civil and Environmental Engineering*, 7:293–318, 2006.

[115] J. Sulem. Bifurcation theory and localization phenomena. *European Journal of Environmental and Civil Engineering*, 14(1-10):989–1009, 2010.

[116] T. Svedberg. *On the Modelling and Numerics of Gradient-Regularized Plasticity Coupled to Damage.* PhD. Thesis., Chalmers University of Technology. Gteborg, Sweden, 1999.

[117] T. Svedberg and K. Runesson. A thermodynamically consistent theory of gradient-regularized plasticity coupled to damage. *Int. J. Plasticity*, 13(6-7):669–696, 1997.

[118] T. Svedberg and K. Runesson. An algorithm for gradient-regularized plasticity coupled to damage based on a dual mixed fe-formulation. *Comput. Meth. Appl. Mech.*, 161:49–65, 1998.

[119] S. Swaddiwudhipong, J. Hua, K. K. Tho, and Z. S. Liu. C0 solid elements for materials with strain gradient effects. *Int. J. Numer. Meth. Eng.*, 64(10):1400–1414, 2005.

[120] I. Tsagrakis, A. Konstantinidis, and E.C. Aifantis. Strain gradient and wavelet interpretation of size effects in yield and strength. *Mech. Mater.*, 35:733–745, 2003.

[121] A. Uchaipichat. An elasto-plastic model for cemented soils under unsaturated condition. *European Journal of Scientific Research*, 60(2):213–218, 2012.

[122] F.-J. Ulm, G. Constantinides, and F. H. Heukamp. Is concrete a poromechanics material? - a multiscale investigation of poroelastic properties. *Mater. Struct.*, 37(265):43–58, 2004.

[123] I. Vardoulakis and E. C. Aifantis. A gradient flow theory of plasticity for granular materials. *Acta Mech.*, 87(3-4):197–217, 1991.

[124] G. Z. Voyiadjis, M. I. Alsaleh, and K. A. Alshibli. Evolving internal length scales in plastic strain localization for granular materials. *Int. J. Plasticity*, 21(10):2000–2024, 2005.

[125] G. Z. Voyiadjis and B. Deliktas. Formulation of strain gradient plasticity with interface energy in a consistent thermodynamic framework. *Int. J. Plasticity*, 25(10):1997–2024, 2009.

[126] G. Z. Voyiadjis, G. Pekmezi, and B. Deliktas. Nonlocal gradient-dependent modeling of plasticity with anisotropic hardening. *Int. J. Plasticity*, 26(9):1335–1356, 2010.

[127] S. Vrech and G. Etse. Geometrical localization analysis of gradient-dependent parabolic Drucker-Prager elatoplasticity. *Int. J. Plasticity*, 22(5):943–964, 2005.

[128] S. Vrech and G. Etse. FE approach for thermodynamically consistent gradient-dependent plasticity. *Latin Am. Appl. Res.*, 37:127–132, 2007.

[129] S. M. Vrech. *Computational simulation of localized failure process based on gradient theory (in spanish).* PhD. Thesis., National University of Tucuman, Argentine, 2007.

[130] S. M. Vrech and G. Etse. Gradient and fracture energy-based plasticity theory for quasi-brittle materials like concrete. *Comput. Meth. Appl. Mech.*, 199(1-4):136–147, 2009.

[131] S. M. Vrech and G. Etse. Discontinuous bifurcation analysis in fracture energy-based gradient plasticity for concrete. *Int. J. Solids Struct.*, 49(10):1294–1303, 2012.

[132] Z. M. Wang, X. A. Zhu, C. T. Tsai, C. L. Tham, and J. E. Beraun. Hybrid-conventional finite element for gradient-dependent plasticity. *Finite Elem. Anal. Des.*, 40(15):2085–2100, 2004.

[133] L. I. Xikui and S. Cescotto. Finite element method for gradient plasticity at large strains. *Int. J. Numer. Meth. Eng.*, 39(4):619–633, 1996.

[134] Z. Yin, C. S. Chang, P. Hicher, and M. Karstunen. Micromechanical analysis of kinematic hardening in natural clay. *Int. J. Plasticity*, 25(8):1413–1435, 2009.

[135] H. W. Zhang and B. A. Schrefler. Uniqueness and localization analysis of elastic-plastic saturated porous media. *Int. J. Numer. Anal. Met.*, 25(1):29–48, 2001.

[136] H. W. Zhang and B. A. Schrefler. Analytical and numerical investigation of uniqueness and localization in saturated porous media. *Int. J. Numer. Anal. Met.*, 26(14):1429–1448, 2002.

[137] H. W. Zhang, L. Zhou, and B. A. Schrefler. Material instabilities of anisotropic saturated multiphase porous media. *Eur. J. Mech. A-Solid*, 24(5):713–727, 2005.

[138] Y. Q. Zhang, H. Hao, and M. H. Yu. Effect of porosity on the properties of strain localization in porous media under undrained conditions. *Int. J. Solids Struct.*, 39(7):1817–1831, 2002.

[139] W. Zhen, D. Sun, and Y. Chen. Analytical solution and numerical simulation of shear bands along different stress paths in three-dimensional stress state. *Geotech. Sp.*, 200:192–197, 2010.

[140] Q. Z. Zhu, J. F. Shao, and M. Mainguy. A micromechanics-based elastoplastic damage model for granular materials at low confining pressure. *Int. J. Plasticity*, 26(4):586–602, 2010.